SPECTRAL TUNING OF WINDOW GLASSES FOR IMPROVING ENERGY EFFICIENCY OF BUILDINGS

by

Çağatay Haratoka

B.S., Mechanical Engineering, Özyeğin University, 2018

Submitted to the Institute for Graduate Studies in
Science and Engineering in partial fulfillment of
the requirements for the degree of
Master of Science

Graduate Program in Mechanical Engineering

Boğaziçi University

2021

ACKNOWLEDGEMENTS

Firstly, I would like to express my gratitude to my thesis supervisor Dr. Hakan Ertürk. I always felt his full support during this study. I learned from him how to conduct academic studies and how to approach the problems for overcoming them professionally.

I would like to thank my mother Meral, my father Oktay, and my brother Altay during this journey. They have always supported and encouraged me for completing this thesis in the best way.

I would also like to thank our former graduate, Dr. Refet Ali Yalçın. He voluntarily tried to answer all of my questions that I asked him during this study and helped me as much as he could.

ABSTRACT

SPECTRAL TUNING OF WINDOW GLASSES FOR IMPROVING ENERGY EFFICIENCY OF BUILDINGS

There are significant efforts for improving energy efficiency of residential and office building for reducing total energy consumption and emission of greenhouse gases. Smart windows are one potential technology that can be used for achieving this purpose. In this study, thermo-chromic glazings with VO_2 pigments, promising passive alternatives among smart windows, are studied for obtaining high energy efficiency while considering visual comfort for office buildings. Such systems alter optical properties such as visible and solar transmittance according to their transition temperatures based on environmental conditions. This study considers two different technologies that are VO_2 nano-particle embedded thermo-chromic window and attached thin VO_2 pigmented thermo-chromic film on an ordinary window glass separately. Optical properties of pigmented glazings and coatings depend on design variables such as pigment size, concentration and thickness. The refractive indices are calculated by effective medium theory according to various design variables. Then, radiative transfer equation is solved by four flux method to find optical properties of nano-particle doped thermo-chromic window after scattering and absorption coefficients are determined by Lorenz-Mie theory in the first technology. However, optical properties of whole attached system are determined by transfer matrix method in the second technology. After that, lighting, cooling and heating energy consumption constitute the total energy consumption are determined according to optical properties. Then, optimal thermo-chromic systems are determined by grid search optimization (single or multi variable search) for high energy savings performance for both technologies in various climatic conditions and transition temperatures. Consequently, significant improvement is achieved with both technologies especially in hot climates.

ÖZET

BİNALARIN ENERJİ VERİMLİLİĞİNİN İYİLEŞTİRİLMESİNE YÖNELİK PENCERE CAMLARININ SPEKTRAL AYARI

Toplam enerji tüketimini ve sera gazı emisyonunu azaltmak için konut ve ofis binalarının enerji verimliliğini artırmaya yönelik önemli çabalar vardır. Akıllı pencereler, bu amacın önemli seçeneklerinden biridir. Bu çalışmada, akıllı pencereler arasında pasif bir alternatif olan VO_2 pigmentli termo-kromik sistemler, ofis binalarında görsel konfor göz önünde bulundurularak yüksek enerji verimliliği elde etmek için çalışılmıştır. Bu tür sistemler, çevresel koşullara bağlı olarak geçiş sıcaklıklarına göre görünür ve güneş geçirgenliği gibi optik özellikleri değiştirir. Pigmentli camların ve kaplamaların optik özellikleri; pigment boyutu, konsantrasyon ve kalınlık gibi tasarım değişkenlerine bağlıdır. Bu çalışmada, VO_2 nano-partikül gömülü termo-kromik pencere ve normal bir pencere camına yapıştırılmış ince VO_2 pigmentli termo-kromik film olan iki farklı teknoloji incelenmektedir. Kırılma indisleri, çeşitli tasarım değişkenlerine göre effective medium teorisi ile hesaplanmıştır. Daha sonra, ilk teknoloji için, nano-partikül gömülü termo-kromik pencerenin optik özelliklerini bulmak için ışınım transfer denklemi four flux metodu ile çözülmüştür. Saçılma ve soğurma katsayıları ise Lorenz-Mie teorisi ile belirlenmiştir. Fakat, ikinci teknolojide, tüm birleşik sistemin optik özellikleri transfer matrisi metodu ile belirlenmiştir. Ardından toplam enerji tüketimini oluşturan aydınlatma, soğutma ve ısıtma enerjileri tüketimi optik özelliklere göre belirlenir. Daha sonra, iki teknoloji için de yüksek enerji tasarrufu performansını elde edecek optimum thermo-kromik sistemler çeşitli iklim koşulları ve geçiş sıcaklıklarında optimizasyon (tek veya çok değişkenli arama) çalışması yapılarak belirlenmiştir. Sonuç olarak, iki teknolojide de özellikle sıcak iklimlerde önemli iyileşmeler elde edilmiştir.

TABLE OF CONTENTS

ACKNOWLEDGEMENTS iii
ABSTRACT iv
ÖZET v
LIST OF FIGURES viii
LIST OF TABLES xi
LIST OF SYMBOLS xii
LIST OF ACRONYMS/ABBREVIATIONS xiv
1. INTRODUCTION 1
1.1. Motivation 1
1.2. Literature Survey 3
1.3. Objective of Study 6
2. DETERMINATION OF OPTICAL AND RADIATIVE PROPERTIES . . . 8
2.1. Description of Systems 8
2.1.1. VO_2 Nano-particle Embedded Thermo-chromic Window Technology 8
2.1.2. Attached Thin VO_2 Thermo-chromic Film Technology 9
2.2. Effective Medium Theories 10
2.3. Lorenz-Mie Theory 12
2.4. Four Flux Method 13
2.5. Transfer Matrix Method 15
2.6. Determination of Visible and Solar Transmittance 15
3. METHODOLOGY AND PROBLEM DESCRIPTION 16
3.1. Building Energy Analysis 16
3.2. Simulation Model and Problem Description 17
3.2.1. VO_2 Nano-particle Embedded Thermo-chromic Window Technology 17
3.2.2. Attached Thin VO_2 Thermo-chromic Film Technology 19
3.3. Visual Comfort 20

3.4. Optimization 22
3.5. Validation Studies of Used Methods 23
3.5.1. Validation of Four Flux Method 23
3.5.2. Validation of Transfer Matrix Method 24
3.5.3. Verification of Building Energy Analysis 24
4. RESULTS AND DISCUSSION 25
4.1. Results of VO_2 Nano-particle Embedded Thermo-chromic Window Technology 25
4.1.1. Determination of Concentration Range for Optimization 25
4.1.2. Optimal Particle Concentration 27
4.1.3. Hours in Metallic Phase for Optimum Thermo-chromic Glazing 34
4.1.4. Total Energy Consumption 36
4.1.5. Daylight Illuminance 40
4.2. Results of Attached Thin VO_2 Thermo-chromic Film Technology 41
4.2.1. Optimal Thermo-chromic Coating Thickness and Particle Concentration 41
4.2.2. Hours in Metallic Phase for Optimum Thermo-chromic Coating 49
4.2.3. Total Energy Consumption 50
4.2.4. Daylight Illuminance 53
4.3. Interpretation of Results of Two Distinct Technologies 54
5. CONCLUSION 56
5.1. Conclusions 56
5.2. Recommendations for Future Work 58
REFERENCES 59
APPENDIX A: VERIFICATION RESULTS FOR FOUR FLUX METHOD . 67
APPENDIX B: VERIFICATION RESULTS FOR TRANSFER MATRIX METHOD 68
APPENDIX C: VERIFICATION RESULTS FOR BUILDING ENERGY ANALYSIS 69
APPENDIX D: SAMPLE INPUT FILE OF ENERGYPLUS 70

LIST OF FIGURES

Figure 1.1. Final energy consumption distribution according to sectors. 2

Figure 2.1. Sketch of model of the thermo-chromic glazing. 9

Figure 2.2. Sketch of model of attached thin thermo-chromic coating on an ordinary glass. 10

Figure 3.1. Sketch of office room and thermo-chromic glass configuration. . . . 17

Figure 3.2. Sketch of office room and thin thermo-chromic coating configuration. 20

Figure 4.1. Relationship between pigment diameter and volume fraction: a) $t_{vis,semi}$, b) $t_{vis,met}$, c) $t_{sol,semi}$, d) $t_{sol,met}$, haze alteration for e) semi-conducting and f) metallic phase, modulation of g) visible (Δt_{vis}) and h) solar (Δt_{sol}) energy. 26

Figure 4.2. Change of optical properties with volume fraction value for TC-25 for first technology. 29

Figure 4.3. Change of optical properties with volume fraction value for TC-35 and TC-45 for first technology. 32

Figure 4.4. Hours and annual time rate in metallic phase for all climates according to transition temperature. 35

Figure 4.5. Annual total energy consumption according to transition temperatures and ordinary double glazing for four climates. 37

Figure 4.6. Total energy consumption improvement according to transition temperatures for four climates. 38

Figure 4.7. Lighting energy consumption according to transition temperatures and ordinary double glazing for four climates. 39

Figure 4.8. Annual natural daylight illuminance according to transition temperatures and ordinary double glazing for four climates. 40

Figure 4.9. Energy consumption change according to coating thickness and volume fraction. 43

Figure 4.10. Change of optical properties with volume fraction for second technology. 45

Figure 4.11. Hours and annual time rate in metallic phase for all climates according to transition temperature. 50

Figure 4.12. Annual total energy consumption according to transition temperatures and ordinary double glazing for three climates. 51

Figure 4.13. Total energy consumption improvement according to transition temperatures for three climates. 51

Figure 4.14. Lighting energy consumption according to transition temperatures and ordinary double glazing for three climates. 53

Figure 4.15. Annual natural daylight illuminance according to thermo-chromic coatings and ordinary double glazing for three climates. 54

Figure A.1. Comparison of transmittance results for four flux method verification. 67

Figure B.1. Comparison of transmittance results for transfer matrix method verification. 68

Figure C.1. Comparison of total energy consumption for verification. 69

LIST OF TABLES

Table 4.1. Optimum optical properties for first technology and standard glass. 31

Table 4.2. Optimum optical properties for second technology and standard glass. 44

LIST OF SYMBOLS

A_e	Depolarization factor
a_n, b_n	Mie coefficients
C_{abs}	Absorption cross section [nm^2]
C_{ext}	Extinction cross section [nm^2]
C_{sca}	Scattering cross section [nm^2]
f	Particle volume fraction
f_{max}	Maximum packing fraction
I_c	Collimated forward intensity [W/m^2 $-$ μm $-$ sr]
I_d	Diffuse forward intensity [W/m^2 $-$ μm $-$ sr]
J_c	Collimated backward intensity [W/m^2 $-$ μm $-$ sr]
J_d	Diffuse backward intensity [W/m^2 $-$ μm $-$ sr]
k_e	Extinction index of the VO_2 nano-particle doped matrix
k_m	Extinction index of the medium
m	Relative refractive index
n	Refractive index of VO_2 particles
n_e	Refractive index of the VO_2 nano-particle doped matrix
n_m	Refractive index of the matrix
r	Reflectivity
r_p	Particle radius of VO_2 particles [nm]
r_{sol}	Solar reflectance
r_{vis}	Visible reflectance
t	Transmissivity
T_c	Transition temperature [°C]
t_{sol}	Solar transmittance
t_{vis}	Visible transmittance
V	Particle volume [nm^3]
V_λ	Sensitivity function of light-adapted human eye
x	Size parameter

Δt_{sol}	Solar energy modulation
ϵ_e	Effective dielectric function of coating
ϵ_m	Effective dielectric function of matrix
ϵ_p	Effective dielectric function of doped VO_2 nano-particles
κ	Absorption coefficient [1/m]
λ	Wavelength [nm]
ξ	Average path length parameter
σ_c	Forward scattering ratio for the collimated intensity
σ_d	Forward scattering ratio for the diffuse intensity
σ_s	Scattering coefficients for weakly absorbing medium [1/m]

LIST OF ACRONYMS/ABBREVIATIONS

ASHRAE	American Society of Heating, Refrigerating and Air-Conditioning Engineers
DGI	Daylight Glare Index
DGP	Daylight Glare Probability
IEA	International Energy Agency
NREL	National Renewable Energy Laboratory
TS 825	Thermal Insulation Requirements for Buildings - Turkish Standard
TC-1	Thermo-chromic Coating 1
TC-2	Thermo-chromic Coating 2
TC-3	Thermo-chromic Coating 3
TC-4	Thermo-chromic Coating 4
TC-25	Transition Temperature of 25 °C
TC-35	Transition Temperature of 35 °C
TC-45	Transition Temperature of 45 °C
UDI	Useful Daylight Illuminance

1. INTRODUCTION

1.1. Motivation

Climate change is one of the major problems that must be considered by engineers, scientists and policy makers. There is a tight bond between climate change and greenhouse gas emissions which have been increasing significantly after industrialization, but especially with the growth of population and consumption economy [1]. Although global greenhouse gas emissions of developed countries have decreased by 6.5% from 2000 to 2018, a rise of 43.2% is observed in developing countries from 2000 to 2013 according to report by United Nations [2]. Therefore, major effects of climate change has been observed after mid-20th century and if there are not any actions to prevent these negative effects, its effect could be more significant and irreversible [1].

The main contributor among greenhouse gases that trigger the climate change is CO_2. It is observed that half of the CO_2 emissions since 1750 to 2011, have taken place in the last 40 years [1]. Main reason behind CO_2 emission is due to consumption of fossil fuels and it contributed 78% of the total greenhouse gas emissions between 1970 and 2010 [1]. Although 17.3% of total consumed energy was produced by renewable sources in 2017, utilizing the potential of renewable sources are still at very low levels when compared to fossil fuels [2]. The change of climate affect the lives of people globally in many aspects threatening clean water resources, triggering natural disasters and crop safety. For instance, the second warmest year was 2019 within the warmest decade that is between 2010 and 2020 and this has caused great destruction in nature such as wild fires and droughts [2]. Therefore, it is obvious that rise of greenhouse gas emissions cause more warming and climate change in the future if we do not make any further action.

Greenhouse gas emissions have to drop by 7.6% each year since 2020 and CO_2 emission has to drop by 45% between 2010 and 2030 in order to keep global warming

below 2 °C, which is the determined target agreed upon by the Paris Agreement [2]. Also, one of the major contributor to CO_2 emission, approximately one-third of the total, is the buildings as observed in Figure 1.1 according to data from [3]. Moreover, buildings use more than half of total electricity consumption and it is expected that energy demand rise 50% until 2050 if no action is taken to reduce the energy consumption of buildings [3].

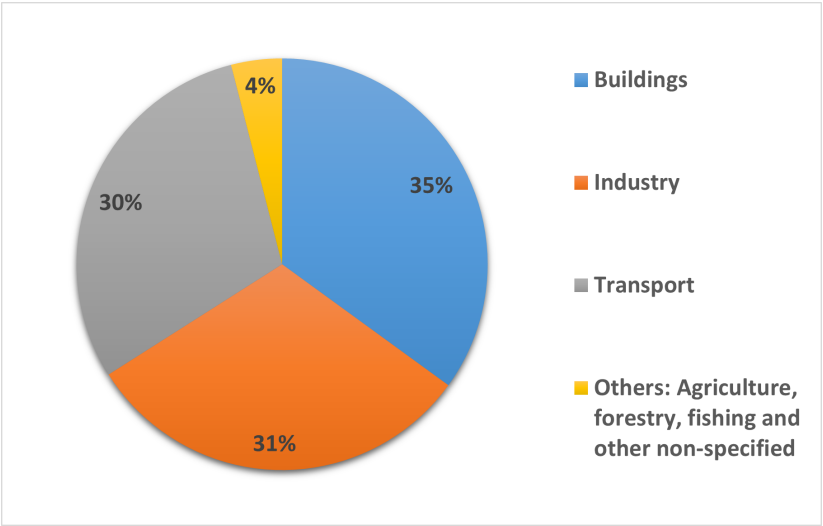


Figure 1.1. Final energy consumption distribution according to sectors.

These facts show that some regulations by policy makers and developments by engineers and scientists are needed for building technologies starting from design especially considering long lifetime of buildings. For instance, improvement on energy standards can cause drop by 14% of electricity energy consumption of building and industry [2]. Moreover, International Energy Agency (IEA) [3] suggests that buildings should harvest solar energy and daylight with high efficiency in order to make this goal real. Also, high performance window glazings and insulation should be used as one of the important primary strategies [3].

Windows play an important role in energy efficiency and reducing greenhouse gas emissions, because optimization for keeping the indoor temperature in desired temperature is a challenge in buildings. For instance, high utilization from solar radiation

is desired in cold weather, but the opposite condition is a need in hot weather [3]. Therefore, windows are considered as a potential area of improvement as together with doors, they are responsible for about 50% of the total energy consumption in buildings and there has been numerous ways of reducing this consumption in regards to window technologies such as reflective and low-emissivity glazing [4], of which altering the optical properties of windows is one of them.

1.2. Literature Survey

Energy efficiency has been considered as a major engineering endeavor, and buildings are responsible for excessive energy consumption, about 40% of the primary energy consumption for the industrialized countries [5]. Moreover, the energy consumption of the buildings in the developing countries are expected to increase to similar levels. For example, energy consumption for buildings in China is expected to reach 35% of total in 2020s [6]. Therefore, in order to decrease energy consumption of buildings, researchers give great importance on coatings, glazings and window technologies.

Chromogenic windows that are also referred as smart glasses are favored for lowering energy consumption in buildings. The properties of the glass can be modified according to the stimuli, which can be electrical voltage, light, gas or heat, to enhance building energy performance. Chromogenic materials are named based on the stimulus, and categorized as electro-chromic, photo-chromic, gaso-chromic or thermo-chromic [7]. Researchers have shown great interest on studying electro-chromic glazing, which is considered as an active technology [8]; whereas, thermo-chromic glazing is considered as a promising passive alternative.

Thermo-chromic features can be observed in many of metal oxides such as Fe_3O_4, $FeSi_2$, Ti_2O_3, V_2O_3 and VO_2, but most encouraging results can be obtained by doping VO_2 [9]. Morin [10] reported that VO_2 phase transition from insulator-to-metal occurs at 68 °C. Monoclinic and tetragonal phases that exist above and below this temperature have different optical properties. The monoclinic structure exhibits transmissive

properties, typical of a semiconducting phase, whereas tetragonal structure has high reflective features of the metallic phase [11].

Production of VO_2 based thermo-chromic films is well established and various methods can be used, such as pulsed laser deposition [12, 13], sputtering [14], e-beam deposition [15–17], sol-gel [18] and chemical vapor deposition [19, 20]. However, there are three major challenges in practical use of thermo-chromic VO_2 films [21]. These are: (a) the solar energy modulation Δt_{sol}, which is the difference of solar transmittance, t_{sol}, between semiconducting and metallic phases, is too low (approximately 10%) for practical use, (b) visible transmittance, t_{vis}, of films is below 40%, which is not often appropriate for building applications, (c) transition temperature of VO_2, T_c, is 68 °C that is quite high when compared to comfort temperature, 25 °C, which makes auto-modulation difficult.

Many researchers have been working to overcome the third challenge, and as a result significant reductions in transition temperature has been observed. It was shown that it is possible to lower the transition temperature to 25 °C preserving the optical quality by doping W into VO_2 [21,22]. Similarly, it is reported that Mg doping into VO_2 can also help to enhance t_{vis} and reduce T_c [23]. Whereas, VO_2 based nano-composites can be used in order to overcome the first two challenges in regards to VO_2 based films. It is shown that both Δt_{sol} and t_{vis} can be enhanced by doping VO_2 nano-particles. Li et al. [24] observed improvement to 20% for Δt_{sol} and 72% and 62% for t_{vis} for semiconducting and metallic phases, respectively.

There are number of methods for producing VO_2 based nano-particles, a comprehensive review of these is presented by Li *et al.* [24]. VO_2 particle size is important in order to prevent haze when using VO_2 nano-particle doped windows. It is reported by Laaksonen *et al.* [25] that VO_2 particle radius should not exceed 20 nm to prevent light scattering to avoid haze. Powder with average particle diameter of 17.8 nm is produced by combination of hydrothermal and sol-gel process by Ji *et al.* [26], where T_c is also decreased to 37 °C by doping W into VO_2. To my knowledge, VO_2 powder

smaller than 17.8 nm has not been reported in the literature. Therefore, this value is considered as minimum size limit of VO_2 powder for smart window applications.

There are also experimental studies on thermo-chromic thin films to reduce the transition temperature and improve the optical properties such as enhanced t_{vis} and Δt_{sol}. Xu *et al.* [27] carried out analyzes on thin VO_2 films with thickness range from 3 to 150 nm, which was produced by radio frequency reactive magnetron sputtering. They observed that when thickness of VO_2 film is less than 50 nm, it has lower transmittance in semiconductor phase than metallic phase and transition temperature drops with decreasing thickness of film [27]. Gagaoudakis *et al.* [28] deposited VO_2 with thickness between 35 nm and 260 nm on commercial SnO_2-coated glass by radio frequency magnetron sputtering and analyzed the change of optical properties with thicknesses. They observed around 6% rise of Δt_{sol} with increasing thickness of the film, but in return, t_{vis} decreased almost 30% [28]. In another study on film thickness, Kolenaty *et al.* [29] prepared VO_2/SiO_2 coatings on soda-lime glass with two different VO_2 thicknesses, 30 and 88 nm, and had similar observations with Gagaoudakis *et al.* [28]; high t_{vis}, and low Δt_{sol} was obtained for thinner VO_2. However, they observed opposite behavior for thicker VO_2 [29]. In addition, Blackman *et al.* [30] examined effect of doping W into VO_2 and thickness of VO_2 film. They achieved a film that has close to silver/blue color and the best optical properties were obtained for film thicknesses between 70 and 90 nm [30].

Use of thermo-chromic windows have been investigated in many studies, where energy performance for buildings are investigated by simulations considering various climates. Saeli *et al.* [31] carried out a study for a simple office room and observed energy savings by using various thermo-chromic glazings especially in warm climates when compared to cold climates. At most, around 40% energy consumption improvement was reported by using a thermo-chromic glass in Rome with a transition temperature of 38.5 °C [31]. Demonstration and simulation of a simple residential room was investigated by Ye *et al.* [32], where depending on the environmental conditions, reduction from 10.2% to 19.9% in cumulative cooling load is achieved by using VO_2 based

thermo-chromic window. They also concluded that absorptivity should be considered as higher energy savings potential can be obtained with significant decrease in t_{sol} with a low increase in solar absorptivity after passing the metallic phase [4]. Hoffmann *et al.* [9] carried out an energy consumption analysis with thermo-chromic windows to identify the effects of assumed optical properties, various window sizes and transition temperatures considering a prototype building. They observed a maximum of 16.7% energy savings for hot climates. Costanzo *et al.* [33] analyzed energy consumption and natural lighting performance of thermo-chromic windows. They reported around 5% and 20% improvements for cold and hot climates, respectively, while preserving suitable natural lighting performance.

Majority of the studies in the literature investigate energy savings performance of thermo-chromic windows based on simulations at various climates not fully considering the daylight performance for visual comfort. However, visual comfort is a critical aspect that must be considered as all these studies focus on applications of thermo-chromic glazings in high occupancy residence or office buildings, where people will be spending long hours. Liang *et al.* [7] made lighting performance analysis with using useful daylight illuminance (UDI) and comparison of thermo-chromic glazings and ordinary window. They found that thermo-chromic glazings provide better daylight performance than ordinary window. Costanzo *et al.* [33] investigated visual comfort for various transition temperatures of thermo-chromic windows in building, considering predefined optical properties in semiconducting and metallic phases of thermo-chromic glazings. They observed that thermochromic glazing gives more uniform illuminance distrubition than reflective and clear ordinary window while all glazing types provide similar daylight illuminance.

1.3. Objective of Study

While there are studies in regards to the effects of using thermo-chromic glazings and coatings on the energy efficiency of buildings, in the existing literature, there are no studies that show the resulting effect of the design parameters such as pigment

size, thickness and volume fraction used in thermo-chromic windows on energy and daylight performance. Therefore, the objective of this study is to investigate VO_2 nano-particle embedded thermo-chromic windows identifying optimal design parameters to achieve energy savings, while considering visual comfort with minimum haze production and adequate natural lighting. For this purpose, this study considers two different technologies and each technology is considered separate parts of this thesis.

Two technologies considered in this study are as follows:

(i) VO_2 nano-particle embedded thermo-chromic window that has identical thickness to an ordinary window glass.
(ii) Attached thin VO_2 thermo-chromic film on an ordinary window glass.

2. DETERMINATION OF OPTICAL AND RADIATIVE PROPERTIES

The optical properties such as reflectance and transmittance of the glazings must be known in order to predict the energy consumption in regards to heating/cooling and lighting. The optical properties of VO_2 nano-particle embedded thermo-chromic glazings depend on pigment size, concentration and glazing thickness and they can be predicted via solution of Maxwell equations. However, for relatively thick windows compared to the visible wavelength and particle size, considering that the particle exhibits both semiconducting and metallic behavior, solution of Maxwell's equations becomes computationally demanding. Instead, solution of radiative transfer equation for this kind of problems would be more adequate [25].

2.1. Description of Systems

2.1.1. VO_2 Nano-particle Embedded Thermo-chromic Window Technology

The illustration of the model for the first technology can be seen in Figure 2.1. The thickness of the thermo-chromic glazing is identical to an ordinary window glass in this technology and the change of other design parameters such as concentration and pigment size of VO_2 nano-particles are analyzed for optimal energy consumption and visual comfort. The optical properties of the glazings are predicted by solution of the radiative transfer equation using the four flux method in conjunction with the Lorenz-Mie theory. The estimated optical behavior of the glazings are used in building energy analysis that is carried out to estimate the heating or cooling and lighting related energy consumption for numerous cities in the USA, which are Phoenix, San Diego, Chicago and Minneapolis.

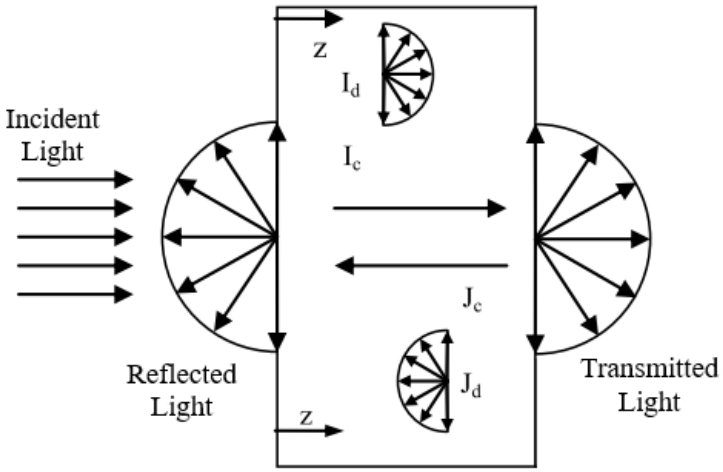


Figure 2.1. Sketch of model of the thermo-chromic glazing.

2.1.2. Attached Thin VO_2 Thermo-chromic Film Technology

Although, relationship of thickness and concentration plays an important role for efficiency performance, there are not any studies that focus on these design parameters of the thermo-chromic coating and energy simulations to get the best energy performance and visual comfort in a single study together. Therefore, in this part of the study, VO_2 nano-particles doped thin thermo-chromic coating with various thicknesses attached on an ordinary glass are focused in order to understand their behaviors and effects. The illustration of the model for the second technology can be seen in Figure 2.2. VO_2 nano-particles doped thin thermo-chromic coating is the matrix and attached ordinary glass is the substrate of this system. Transfer matrix method is utilized for calculating optical properties in this case due to thin thermo-chromic coating attached on an ordinary glass. After estimation of optical properties, energy consumption analysis is made for numerous cities in Turkey, which are Izmir, Istanbul and Ankara.

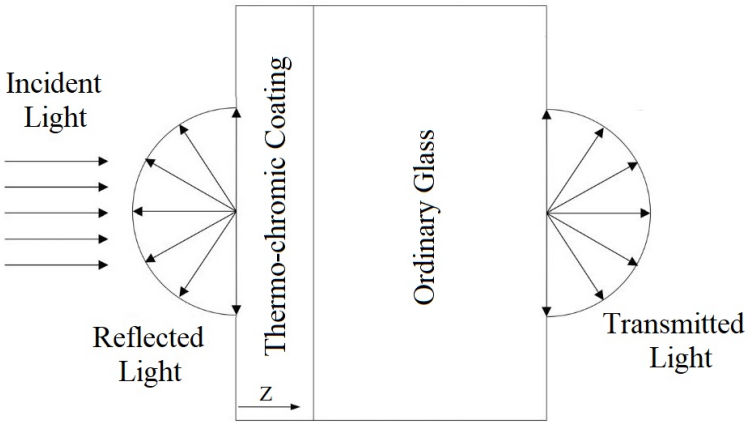


Figure 2.2. Sketch of model of attached thin thermo-chromic coating on an ordinary glass.

2.2. Effective Medium Theories

Effective medium theory in optics is used to estimate refractive index of a medium composed of different materials. Accuracy of this approximation is dependent on various parameters such as concentration ratio, refractive index contrast of the materials and incident wavelength. If size parameter, $x = 2\pi n r_p/\lambda$, which shows the size of particle with respect to wavelength is less than 0.1 [34], EMT is applicable. n and r_p are the refractive index and pigment radius of VO_2 particles, respectively. Most widely used and well-known EMT method is Maxwell-Garnett [35] and Bruggeman [36] theories. The main difference between these theories are the approximation of the structures. Bruggeman is used for aggregate structures, but Maxwell-Garnett theory is used for separated-grain structure [37]. Maxwell-Garnett theory is more suitable for this study due to nano-particle distribution and it gives accurate results when concentration of nano-particles in coating is low [38] and the concentration is quite low due to doping of nano-particles in a thickness of an ordinary glass in the first technology. Therefore, Maxwell-Garnett theory is used for determining the dielectric function of doped glazing in the first technology of this study that is the nano-particle embedded thermo-chromic glazing case as seen in Figure 2.1. The effective dielectric function of nano-particle

doped coating can be determined from the Equation 2.1 [39]:

$$\epsilon_e = \epsilon_r \frac{\epsilon_p + 2\epsilon_m + 2f_v(\epsilon_p - \epsilon_m)}{\epsilon_p + 2\epsilon_m + f_v(\epsilon_p - \epsilon_m)} \tag{2.1}$$

where ϵ_e, ϵ_m and ϵ_p are effective dielectric function of coating, dielectric function of the matrix and doped VO_2 nano-particles, respectively [39]. The effective complex dielectric function, refractive and extinction index of the VO_2 nano-particle doped matrix can be defined by Equation 2.2, 2.3 and 2.4 [39], respectively, as follows:

$$\epsilon_e = \epsilon'_e - i\epsilon''_e\,, \tag{2.2}$$

$$n_e^2 = \frac{1}{2}\left(\epsilon'_e + \sqrt{\epsilon'^2_e + \epsilon''^2_e}\right)\,, \tag{2.3}$$

$$k_e^2 = \frac{1}{2}\left(-\epsilon'_e + \sqrt{\epsilon'^2_e + \epsilon''^2_e}\right) \tag{2.4}$$

where n_e and k_e are the refractive and extinction index of the VO_2 nano-particle doped matrix.

As seen from the sketch of the second technology in Figure 2.2, the design is a multilayer system with a layer of VO_2 nano-particle embedded thin film thermochromic coating attached to an ordinary glass. Since the volume fraction of VO_2 at film deposition exceeds the 10% limit of Maxwell-Garnett theory, Lewis-Nielsen method which can handle high volume fractions is used. Maxwell-Garnett cannot approximate the optical properties accurately for high concentrations as explained before. However, Lewis-Nielsen can handle high volume fractions and give consistent results [38]. Therefore, Lewis-Nielsen method is used in the second technology due to high concentrations of nano-particles in thin coating. The dielectric function of the

doped coating can be calculated by Lewis-Nielsen method as [34],

$$\frac{\epsilon}{\epsilon_m} = \frac{1 + ABf_v}{1 - B\varphi f_v}\,, \tag{2.5}$$

$$A = \frac{1}{A_e} - 1\,, \tag{2.6}$$

$$B = \frac{\epsilon_p/\epsilon_m - 1}{\epsilon_p/\epsilon_m + A}\,, \tag{2.7}$$

$$\varphi = 1 + \frac{1 - f_{max}}{f_{max}^2} f_v \tag{2.8}$$

where ϵ, ϵ_m and ϵ_p are the effective dielectric function of coating, dielectric function of the matrix and doped VO_2 nano-particles as already explained before, respectively [34]. A_e and f_{max} are the depolarization factor and the maximum packing fraction, respectively [34]. Here, A_e is 0.4 for sphere particles and f_{max} is 0.637 for random close packing [34].

2.3. Lorenz-Mie Theory

Solution of radiative transfer equation necessitates radiative properties; scattering and absorption coefficients, which can be determined by Lorenz-Mie theory for dilute particulate systems that are comprised of uniform sized particles. In such systems, each particle scatter light independently and the effective behavior of the medium can be represented in terms of a single particle's behavior, considering the particle concentration.

The scattering, C_{sca}, extinction, C_{ext}, and absorption, C_{abs}, cross sections can be calculated by Lorenz-Mie theory following Equation 2.9, 2.10 and 2.11 [39, 40]:

$$C_{ext} = \frac{2\pi r_p^2}{x^2} \sum_{n=1}^{\infty} (2n+1) Re(a_n + b_n)\,, \tag{2.9}$$

$$C_{sca} = \frac{2\pi r_p^2}{x^2} \sum_{n=1}^{\infty} (2n+1)(|a_n|^2 + |b_n|^2)\,, \tag{2.10}$$

$$C_{abs} = C_{ext} - C_{sca} \tag{2.11}$$

where x is size parameter,

$$x = \frac{2\pi n_m r_p}{\lambda} \tag{2.12}$$

and r_p is the particle radius, n_m is the refractive index of the matrix. Besides, a_n and b_n are Mie coefficients and can be determined by Riccati-Bessel functions as shown in Equation 2.13 and 2.14 as:

$$a_n = \frac{m\psi_n(mx)\psi_n{}'(x) - \psi_n(x)\psi_n{}'(mx)}{m\psi_n(mx)\xi_n{}'(x) - \xi_n(x)\psi_n{}'(mx)}\,, \tag{2.13}$$

$$b_n = \frac{\psi_n(mx)\psi_n{}'(x) - m\psi_n(x)\psi_n{}'(mx)}{\psi_n(mx)\xi_n{}'(x) - m\xi_n(x)\psi_n{}'(mx)} \tag{2.14}$$

where m as observed in Equation 2.15 is the ratio of refractive and extinction indices of particle and refractive index of matrix material,

$$m = \frac{n_p + k_p.i}{n_m}\,. \tag{2.15}$$

2.4. Four Flux Method

Once scattering and absorption coefficients are identified, radiative transfer equation can be solved using four flux method as outlined by Maheu *et al.* [41], approximating the incoming and outgoing intensities in terms of diffuse and collimated components as shown in Figure 2.1. Here: I_c is the collimated forward intensity, J_c is the collimated backward intensity, I_d is the diffuse forward intensity, and J_d is the diffuse backward intensity.

The conversation equations in regards to four intensities in the four flux model

can be defined as:

$$\frac{dI_c}{dz} = -(\sigma_s + \kappa)I_c\,, \tag{2.16}$$

$$\frac{dJ_c}{dz} = (\sigma_s + \kappa)J_c\,, \tag{2.17}$$

$$\frac{dI_d}{dz} = -\xi\kappa I_d - \xi(1-\sigma_d)\sigma_s I_d + \xi(1-\sigma_d)\sigma_s J + \sigma_c\sigma_s I_c + (1-\sigma_c)\sigma_s I_c\,, \tag{2.18}$$

$$\frac{dJ_d}{dz} = \xi\kappa I_d + \xi(1-\sigma_d)\sigma_s J_d - \xi(1-\sigma_d)\sigma_s I_d - \sigma_c\sigma_s J_c - (1-\sigma_c)\sigma_s I_c \tag{2.19}$$

where ξ is average path length parameter that is assumed as 1.6 as suggested by Laaksonen et al [25], σ_c and σ_d are the forward scattering ratio for the collimated and diffuse intensity, respectively. The scattering and absorption coefficients for weakly absorbing medium are defined as:

$$\sigma_s = \frac{fC_{sca}}{V}\,, \tag{2.20}$$

$$\kappa = \frac{fC_{abs}}{V} + \frac{4\pi k_m}{\lambda}\,. \tag{2.21}$$

Here f is the particle volume fraction, V is the particle volume, k_m is the extinction index of the medium. The last term of Equation 2.21 represents the bulk absorption of the medium apart from the embedded particles and applicable only for weak absorbing mediums. [42]. C_{sca} and C_{abs} are scattering and absorption cross sections, respectively. For dilute systems with uniform sized particles, Lorenz-Mie theory can be used to calculate C_{sca} and C_{abs} as mentioned before [39,40]. Then, equations for calculating four intensities of the four flux model as shown in Equation 2.16, 2.17, 2.18 and 2.19 are transformed to collimated-collimated and diffuse for both reflectance and transmittance by Maheu *et al.* [41]. The final forms and intermediate derivations of them are quite long, and available in the literature. Therefore, they are not explicitly presented in this document. However, more information in regards to the derivation and the final forms is available in Maheu *et al.* [41] and Yalcin and Erturk [43].

2.5. Transfer Matrix Method

Transfer matrix method is a well-known solution that is used for determining the transmittance and reflectance of the multilayer planar coatings. This method calculates electric field of the electromagnetic wave through the multilayer structures where each layer is homogenous. Therefore, the method cannot model scattering and can only be used for pigmented coatings if the particles are small enough compared to incident wavelength. Reflectance and transmittance of the thermo-chromic coating which consists of VO_2 nano-layer attached on ordinary glass is calculated using this method after the effective refractive index of deposited coating is calculated by effective medium theory. There are other ways to calculate reflectance and transmittance of multilayer structures such as ray tracing [44]. However, interference is observed for layers whose thickness is in the order of wavelength and ray tracing methods cannot be used since it does not take into account the interference effect. Therefore, ray tracing methods are not considered for this part of the study. Transfer matrix method of Pascoe [45] is used for determining optical properties of combined effect of the multilayer structure in this study. Formulation of transfer matrix method is not given here for brevity but is available in [45].

2.6. Determination of Visible and Solar Transmittance

After radiative transfer equation is solved by explained methods, visible and solar transmittance can be estimated by integrating the spectral properties for visible range, 380-780 nm, for t_{vis} and for solar range, 300-2500 nm, for t_{sol} using standard solar irradiation data presented in ASTM-G173-03 [46] as shown in Equation 2.22 and 2.23:

$$t_{vis} = \frac{\int_{380nm}^{780nm} I_\lambda V_\lambda t_\lambda d\lambda}{\int_{380nm}^{780nm} I_\lambda V_\lambda d\lambda}, \tag{2.22}$$

$$t_{sol} = \frac{\int_{300nm}^{2500nm} I_\lambda t_\lambda d\lambda}{\int_{300nm}^{2500nm} I_\lambda d\lambda} \tag{2.23}$$

where V_λ is the sensitivity function of light-adapted human eye [47].

3. METHODOLOGY AND PROBLEM DESCRIPTION

3.1. Building Energy Analysis

Energy analysis in this study is carried out by EnergyPlus [48], which is an open source software, to evaluate the energy performance of different thermo-chromic glazings in various climates. EnergyPlus is widely used for building simulations and was developed by US Department of Energy. It is capable of analyzing thermal loads by heat balance method iteratively considering input data [49].

Heat and mass balance simulation module of EnergyPlus estimates thermal load considering input data such as defined surface materials, window properties, weather data [49]. Environmental conditions are acquired from weather data that includes various information about location of interest such as temperature, wind conditions, solar irradiation in order to use in heat balance method. Heat balance of outside surfaces, that are exposed to environmental effects, take into consideration of four components; direct and diffuse solar radiation, IR radiation from environment, conduction heat exchange into the external wall of the zone and convective heat exchange with outside ambient air. Besides, heat balance of zone's inside surface has four components for consideration; solar radiation that comes through the window and internal sources such as lights, IR radiation from other surfaces and internal sources such as occupants, conduction heat exchange through internal walls of the zone, convective heat exchange with inside ambient air. Temperature of thermo-chromic glazing is determined by solving heat balance equation. Then, the optical properties of thermo-chromic glazing is used in the simulation assuming the closest temperature of thermo-chromic glazing that was identified [50]. Building systems simulation module considers the systems in the building such as zone equipment, HVAC and electrical system and it estimates contributions to the unit after heat balance simulation is completed [49].

3.2. Simulation Model and Problem Description

3.2.1. VO_2 Nano-particle Embedded Thermo-chromic Window Technology

First case of the study, which is the first technology, is conducted considering thermo-chromic glazings with three different dopings of VO_2 that has transition temperatures, T_c, of 25 °C, 35 °C and 45 °C for four different climates, Phoenix, San Diego, Chicago and Minneapolis. In the same order, their latitudes and longitudes are 33.45° and −111.98°, 32.73° and −117.17°, 41.98° and −87.92°, 44.88° and −93.23°, respectively [51]. Weather data of the cities are taken from [51]. Further on, these thermo-chromic glazings will be referred as TC-25, TC-35 and TC-45 for T_c of 25 °C, 35 °C and 45 °C, respectively. Windows in all cases are always double glazed with air cavity and thermo-chromic glass is always placed in the outside face as shown in the sketch of the configuration in Figure 3.1.

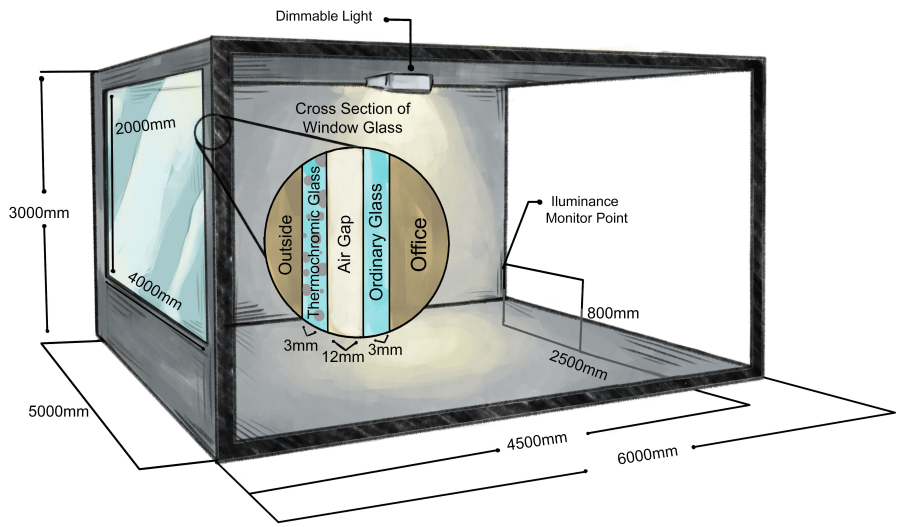


Figure 3.1. Sketch of office room and thermo-chromic glass configuration.

Analysis is performed with modeling a simple office room instead of modeling a whole building, because detailed analyses are carried out in this study to find optimal design parameters of thermo-chromic windows according to transition temperatures and climatic conditions. If whole building were modeled, it would be necessary to focus

on all windows in the building considering all faces and floors individually to identify optimal parameters and this would greatly increase the parameter space considering also various climatic conditions and transition temperatures. Therefore, a simple office room that has dimensions of 6m x 5m x 3m (length x width x height) and has a 4m x 2m window (53.3% window-to-wall ratio) as illustrated in Figure 3.1 is considered for the investigation. It is a mid-floor office room of a multi-story building and placed in northern hemisphere, facing south. Only one wall, the one with the window, is exposed to external conditions. The construction set of ASHRAE Standard 90.1-2010 template for climate zone 3C is used in OpenStudio software, which is a software developed by National Renewable Energy Laboratory (NREL) of the U.S. Department of Energy for building energy analysis [52]. Details of construction materials can be seen in ASHRAE Standard 90.1-2010 [53]. Overall heat transfer coefficient, U, of the external wall for climate zone 3C of the template is specified as 0.70 W/m^2K [52]. In order to examine the effect of thermo-chromic glazing rather than the construction materials on energy efficiency, the construction set for climate zone 3C of the template is used for all climates even if the cities have different construction sets according to their own regulations for their climates.

Internal loads for the study are also defined according to ASHRAE Standard 90.1-2010. Based on that; occupant density is specified as 18.6 m^2/person, lighting loads are 11 W/m^2 and equipment loads are 7 W/m^2. Ventilation rate is set to 0.025 m^3/s. Occupancy schedule of building is defined between 8:00 am and 5:00 pm on weekdays. Illuminance would be less at the back of the room and in order to make sure illuminance is adequate there, illuminance is monitored from 0.8 m above the floor and 4.5 m distance from the window as considered in the various studies in the literature [7, 54]. The illuminance of the room is controlled at this defined point to sustain it at 500 lux at all occupancy hours. Artificial lighting is used when needed based on room natural illuminance to satisfy 500 lux at the specificed point. All internal loads and HVAC system are activated according to this occupancy schedule. Ideal Load Air System that assumes heat is provided with 100% efficiency is considered to avoid issues regarding system and equipment variability in HVAC systems for a straightforward calculation

of heating/cooling energy consumption [50]. Set points of HVAC system are defined as 21 °C for heating and 24 °C for cooling.

3.2.2. Attached Thin VO_2 Thermo-chromic Film Technology

For the second technology considered in the study, attached thin thermo-chromic coatings on an ordinary glass are analyzed for three different transition temperatures, T_c, of 25 °C, 35 °C and 45 °C and they are also referred as TC-25, TC-35 and TC-45. The investigation of the second technology is carried out in Turkey. Therefore, the construction materials have to be selected considering the location of the city according to Turkish Standard, TS 825 [55].

There are defined climate regions according to weather conditions of Turkey in TS 825 and it limits a maximum heat transmission coefficient (U_{max}) according to construction types of the building such as wall, floor or roof constructions [55]. Minimum qualifications that are complied with are defined in order to ensure the energy efficiency of the building according to these climate regions. There are four different climate regions of Turkey according TS 825 published in 2008 [55]. Then, these climate regions increased five climate regions with updated TS 825 in 2013 and some cities in the climate region four are moved to climate region five [56].

3 cities that are all in different climate regions in Turkey are investigated; where Izmir in the first climate region, Istanbul in the second climate region and Ankara in the third climate region. In the same order, their latitudes and longitudes are 38.5° and 27.02°, 40.97° and 28.82°, 40.12° and 32.98°, respectively [51]. These three cities are selected, because 30.5% of Turkey's total population lives in these cities [57]. Moreover, weather data of these three cities from Turkey are available in the weather database of EnergyPlus and are taken from [51].

Identical mid-floor office room that is described in the previous section is also considered with same dimensions for this case as seen in Figure 3.2. Also, windows

are always double glazed with air cavity and VO_2 doped thin film coating is attached on the glass at the outside face of the window. Furthermore, identical used conditions that were described in the first technology such as working hours, internal loads, HVAC system and illuminance controlling system are used in this analyses. However, the construction materials have to be selected considering the location of the city according to Turkish Standard, TS 825 [55] as already mentioned and the construction materials that comply with TS 825 are clearly explained in Dino *et al.* [58]. Construction materials for Istanbul are used for all cities so that the performance investigation focuses on thermo-chromic coating only. Therefore, same construction materials listed for Istanbul in Dino *et al.* [58] is considered, where maximum limit of heat transfer coefficient, U_{max}, as 0.60, 0.40 and 0.60 W/m^{2}K is specified for wall, roof and floor, respectively.

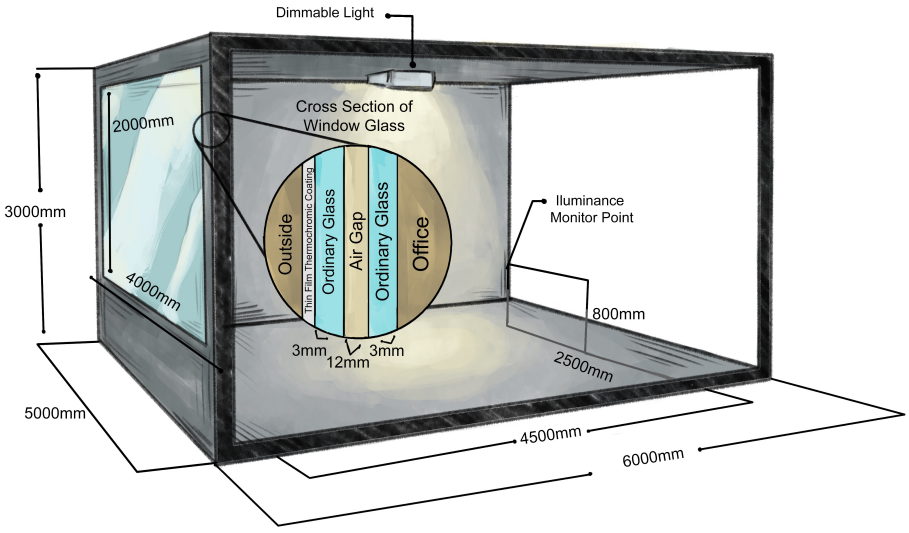


Figure 3.2. Sketch of office room and thin thermo-chromic coating configuration.

3.3. Visual Comfort

Visual comfort must also be taken into consideration by designers of office buildings, as people spend long hours in their offices. Visual comfort can be quantitatively evaluated in terms of illuminance [54] according to regulations for human comfort based

on the purpose of use. 500 lux is recommended as a valid illuminance level to make visual tasks in office rooms according to North America and Europe standards [59,60]. Moreover, Nabil and Mardaljevic developed an approach to quantify the daylight performance that is known as useful daylight illuminance (UDI) [61]. In their method, daylight illuminance is investigated at determined points, considering data of climatic conditions for one year with hourly steps and they defined a range between 100 and 2000 lux of illuminance that is referred as useful daylight illuminance (UDI) [61]. Besides, they [61] listed several important criteria for visual comfort:

(i) Artificial lighting is needed due to low illuminance when daylight illuminance is lower than 500 lux.
(ii) Acceptable illuminance range can be defined as 500 to 2000 lux.
(iii) Visual discomfort may be observed when daylight illuminance is higher than 2000 lux.

Useful daylight performance can be defined and interpreted for an entire year with this method according to amount of hourly determined illuminance satisfies the three criteria listed. Besides, when daylight illuminance is lower than 100 lux, it is insufficient for illumination. Therefore, there should be significant artificial lighting [61]. More recently, Mardaljevic *et al.* [62] updated this criteria and raised the upper limit for beginning of potential discomfort to 3000 lux from 2000 lux [62]. Moreover, in the final form of the criteria, the artificial light is needed between 100 and 300 lux [62]. Besides, there is no need for artificial lighting between 300 and 3000 lux [62].

Although there are various glare indices for examining glare in the buildings, there is no consensus for the best method to evaluate glare [63]. One of the recent methods to quantify the glare is daylight glare probability (DGP), which evaluates the glare from vertical illuminance at eye level [64]. Even though DGP is argued to be more precise, another widely used method, daylight glare index (DGI), is used in this study, due to its high computational efficiency. In DGI method, there is a determined scale that is 22 as upper limit for accepting the glare in suitable condition [54]. This

index is calculated by the formula that regards average luminance of source which is observed from monitored point, solid angle subtended by source and average luminance in the area that can observe the glare source [50, 65].

Consequently, although Mardaljevic *et al.* [62] indicated the range between 100 and 300 lux for artificial lighting, 500 lux was considered as an appropriate illuminance minimum limit in this study due to recommended illuminance level in both North America and Europe standards [59, 60] for visual tasks in offices. Therefore, once illuminance is below 500 lux, artificial lighting is used. Besides, ratio of hours with illuminance higher than 3000 lux and DGI less than 22 to total occupancy hours are also examined for preventing discomfort and quantifying glare occurrence, respectively. Moreover, after optimal properties are determined according to optimization criteria for minimum energy consumption considering visual comfort, comparison for visual comfort of the thermo-chromic systems for both technologies and standard ordinary glass is made by using useful daylight illuminance (UDI) approach in this study.

3.4. Optimization

Visible and solar transmittance of window glasses have significant effect on the energy performance of the buildings, and they can be modified for a nano-particle doped glass by changing particle diameter, volume fraction and thickness of the glass. In this study, technologies of two different thermo-chromic systems are studied as explained before for considering practical applicability of the thermo-chromic windows. Grid search optimization (single or multi variable search) is carried out to find the optimal design parameters such as thickness and particle volume fraction for energy consumption and visual comfort as explained by [54].

Although it is desired to satisfy the visual comfort criteria throughout the occupancy hours without relying on any external means such as using artificial lighting, this is not possible. Therefore, a reasonable or feasible design target in regards to the use of artificial lighting must be defined. Ochoa *et al.* [54] examined various window sizes

in different locations of a room to find optimum window size and location for the best energy performance and visual comfort, and they considered that energy and comfort criteria must be satisfied for at least 50% of the occupancy time without relying on artificial lighting. The same acceptance criteria is used in this study for evaluation of visual comfort as a constraint while minimizing the energy consumption. Therefore, the optimization problem considered can be summarized as: The sum of the yearly energy consumption considering heating, cooling and lighting is minimized; subject to illuminance-based visual comfort constraint so that a minimum of 500 lux at the defined position is satisfied at all times, and the use of artificial lighting not exceeding 50% of total occupancy hours.

3.5. Validation Studies of Used Methods

3.5.1. Validation of Four Flux Method

In order to verify accuracy of optical property calculations by four flux method, a verification study is carried out for comparing the result to those presented in Laaksonen *et al.* [25] and to those that are calculated by Monte-Carlo method for various VO_2 pigment size, concentration and thickness. Laaksonen *et al.* [25] estimated the optical properties of VO_2 coatings using four flux method. Calculations in this study are also performed by using the same method and verified the results by using various pigment size for the same configuration; 10 μm of layer thickness, 0.01 of volume fraction and 5, 20 and 50 nm of three different nanoparticle radii for semiconducting and metallic phases. Average of the total error for semiconducting and metallic phases at different radii is determined to be 1.7% when the transmittance results of our calculation and Laaksonen's are compared [25]. Furthermore, the results are verified by Monte-Carlo method, similarly the error is 2.1% which show the applied method in this study is capable of estimating the optical properties of pigmented coatings. Comparison of these results according to one configuration of Laaksonen *et al.* [25] can be examined in Appendix A.

3.5.2. Validation of Transfer Matrix Method

Optical properties that are predicted by Monte-Carlo method and transfer matrix method for three different thicknesses with particle concentrations are compared to verify the correctness of transfer matrix method. The investigated design parameters are 92 nm and 0.56, 116 nm and 0.51, 134 nm and 0.43 as thicknesses and volume fractions, respectively. Optical properties for attached thin VO_2 thermo-chromic film on an ordinary glass are calculated by transfer matrix method and Monte-Carlo method with these three design parameters. Average of the total error of transmittance for semiconducting and metallic phases for these three design variables are determined to be 2.5%. Therefore, this method is used for the calculations of attached thin VO_2 thermo-chromic film on an ordinary glass due its capability after this comparison. Comparison of these results according to design parameters of 134 nm as thickness and 0.43 as volume fraction can be examined in Appendix B.

3.5.3. Verification of Building Energy Analysis

Building energy analysis is verified by reproducing the results presented by Saeli *et al.* [31]. They examined four different thermo-chromic coatings by modeling a simple office room that has same dimensions of this study, but their window size is different as 1.5m x 2.5m (height x width) and located in the middle of the south wall as seen in [31]. Also, internal loads and construction materials are defined according to their description in their study [31]. Then, total energy consumption is determined according to features of four different thermo-chromic coatings and comparison of total energy consumption is made in four different cities in their study; Milan, Paris, London and Moscow [31]. Similar results are obtained and comparison of these results can be examined in Appendix C. Average of the total error for total energy consumption of all these four thermo-chromic coatings in four cities is determined to be 1.3%. Therefore, it can be deduced from the results of this comparison, accurate calculations are made for building energy analysis.

4. RESULTS AND DISCUSSION

The change in optical properties due to changing design parameters of VO_2 is investigated for two different technologies in order to understand its effect on energy consumption of a simple office room. Effect of different transition temperatures on metallic phase hours, heating/cooling and lighting energy consumption and daylight illuminance are investigated after optimal properties is found. Then the comparison and interpretation of these two different technologies are made in a separate section.

4.1. Results of VO_2 Nano-particle Embedded Thermo-chromic Window Technology

4.1.1. Determination of Concentration Range for Optimization

A parametric study is carried out, estimating visible transmittance, solar transmittance and haze, for a range of pigment diameters and particle volume fractions for a fixed thickness of VO_2 doped window glass so that energy consumption in regards to thermal management and lighting can be investigated. Laaksonen *et al.* [25] indicated that nano-particle radius should be smaller than 20 nm to avoid haze based on their predictions. Zhao *et al.* [66] pointed out that haze of double glazed windows should be smaller than 3%, whereas Laaksonen *et al.* [25] indicated that haze should not exceed 1-2% . Considering these, 2% is specified as the highest haze limit for the optimization carried out in this study. As production of VO_2 pigments with average pigment size below 20 nm is possible [26], pigments as small as diameter of 20 nm or larger is considered in this study.

Variation of optical properties with pigment diameter and volume fraction change are presented in Figure 4.1. The change in visible and solar transmittance can be observed in Figure 4.1. a, b, c and d for semiconducting and metallic phases. Haze is getting smaller with decreasing diameter and volume fraction, and acceptable haze

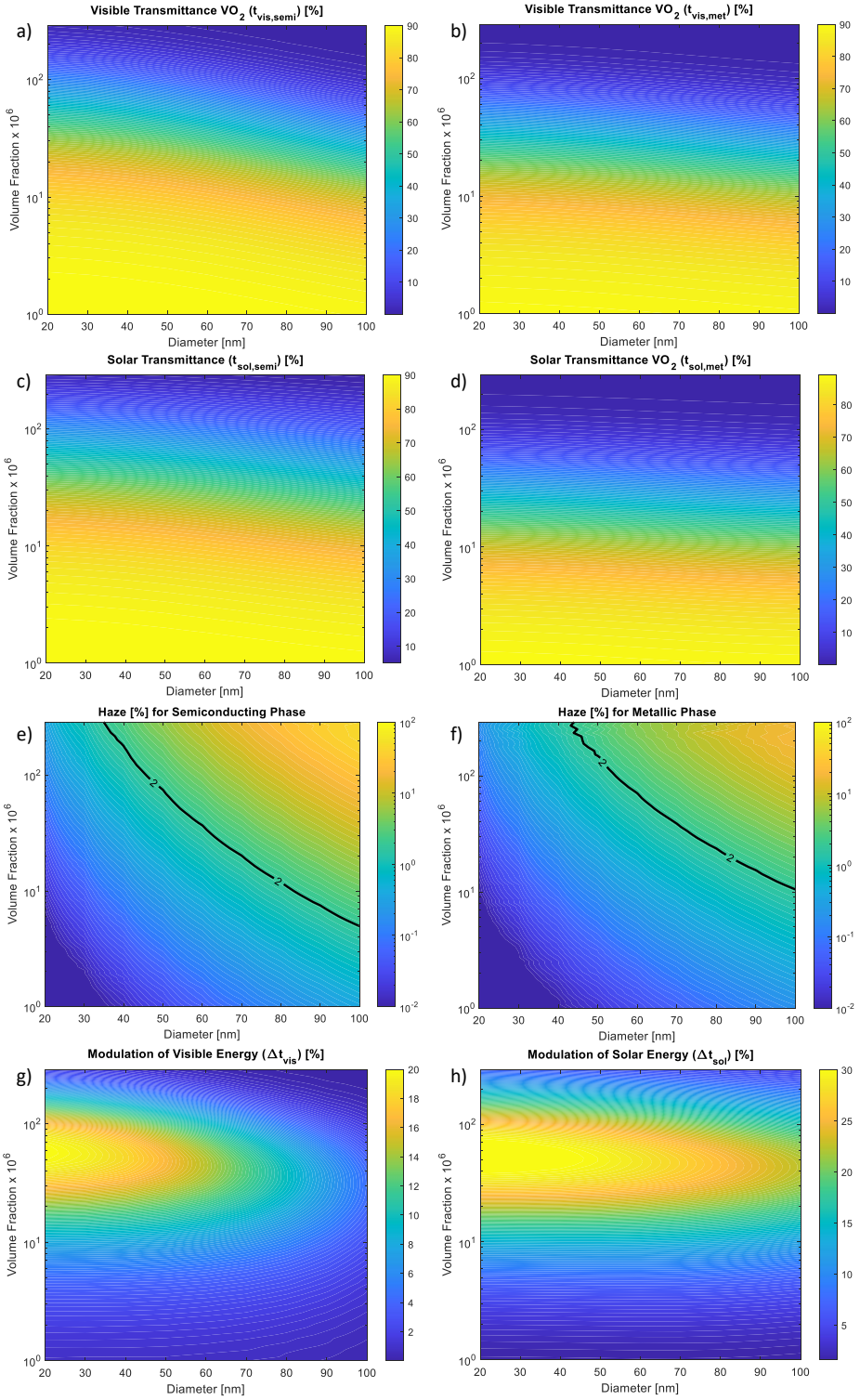


Figure 4.1. Relationship between pigment diameter and volume fraction: a) $t_{vis,semi}$, b) $t_{vis,met}$, c) $t_{sol,semi}$, d) $t_{sol,met}$, haze alteration for e) semiconducting and f) metallic phase, modulation of g) visible (Δt_{vis}) and h) solar (Δt_{sol}) energy.

($< 2\%$) is achieved between 20 nm and 40 nm diameter for volume fractions less than 10^{-4} as seen in Figure 4.1. e and f, for both semiconducting and metallic phases in agreement with [25]. Therefore, volume fraction of interest ranges between 10^{-6} and 10^{-4} considering the upper limit of haze.

Achieving acceptable visible transmittance, t_{vis}, larger than 40% and solar energy modulation, Δt_{sol}, larger than 10% for thermo-chromic VO_2 films are important challenges to achieve for practical applications in buildings as explained before. While t_{vis} limitation can be overcome and it can be observed in Figure 4.1. a and b that acceptable visible transmittance values can be achieved for practical applications with decreasing diameter and volume fraction for both semiconducting and metallic phase. The change of t_{sol} in both phases with volume fraction and diameter can be examined in Figure 4.1. c and d. In addition, high Δt_{sol} values can be achieved for relatively high volume fractions as it could be observed from Figure 4.1. g and h. Thus, based on estimated optical properties and haze analysis and considering production limit, the diameter of nano-particle size is set to 20 nm for visual comfort, considering the parametric analysis presented in Figure 4.1 and carried out energy consumption and daylight performance analysis considering volume fraction changes between 10^{-6} and 10^{-4}, because reducing the pigment diameter from 40 nm to 20 nm yields similar optical properties, with improved haze characteristics.

4.1.2. Optimal Particle Concentration

Grid search optimization is used in this study in order to find the optimum volume fraction. The optimum particle volume fraction is found according to all transition temperatures for four different cities; Phoenix representing extreme hot, San Diego representing hot, Chicago representing cold and Minneapolis representing extreme cold climates. Weather data of the cities are taken from [51].

The optimal concentration can be identified as the particle volume fraction, which has minimum energy consumption among those satisfying illuminance criteria, 500 lux,

for more than 50% of occupancy hours. Considering that the energy consumption decreases monotonically with increasing particle volume fraction, the optimal particle volume fraction becomes the highest particle volume fraction that satisfies the 50% illuminance index criteria. Change of energy consumption and optical properties for TC-25 can be seen in the Figure 4.2. Same procedure is also applied for TC-35 and TC-45 cases. While the optimal particle volume fractions for all cases are presented in Table 4.1, plots for only TC-25 case is presented for all geographic locations. For other two transition temperatures, the results of only extremely hot and cold climates are presented in Figure 4.3 for brevity.

In addition, the ratio of hours when illuminance is higher than 3000 lux and total occupancy hours can be examined in Figure 4.2 and Figure 4.3. A continuous decrease for all climates and transition temperatures with increasing volume fraction is observed and it converges to 0 before optimal particle volume fraction. Therefore, excess illuminance problem is not observed at all regions for optimal particle concentration. Besides, glare is also examined based on DGI as mentioned before and ratio of hours when DGI is in acceptable range, which is less than 22, can be observed in Figure 4.2 and Figure 4.3. In all cases, glare occurrence according to DGI decreases with the rise of volume fraction. However, as observed in Figure 4.2 and Figure 4.3, there is a trade-off between satisfying illuminance and glare criteria. Therefore, during the design of office buildings, one may need to give more importance to one of these criteria according to usage plan of the office.

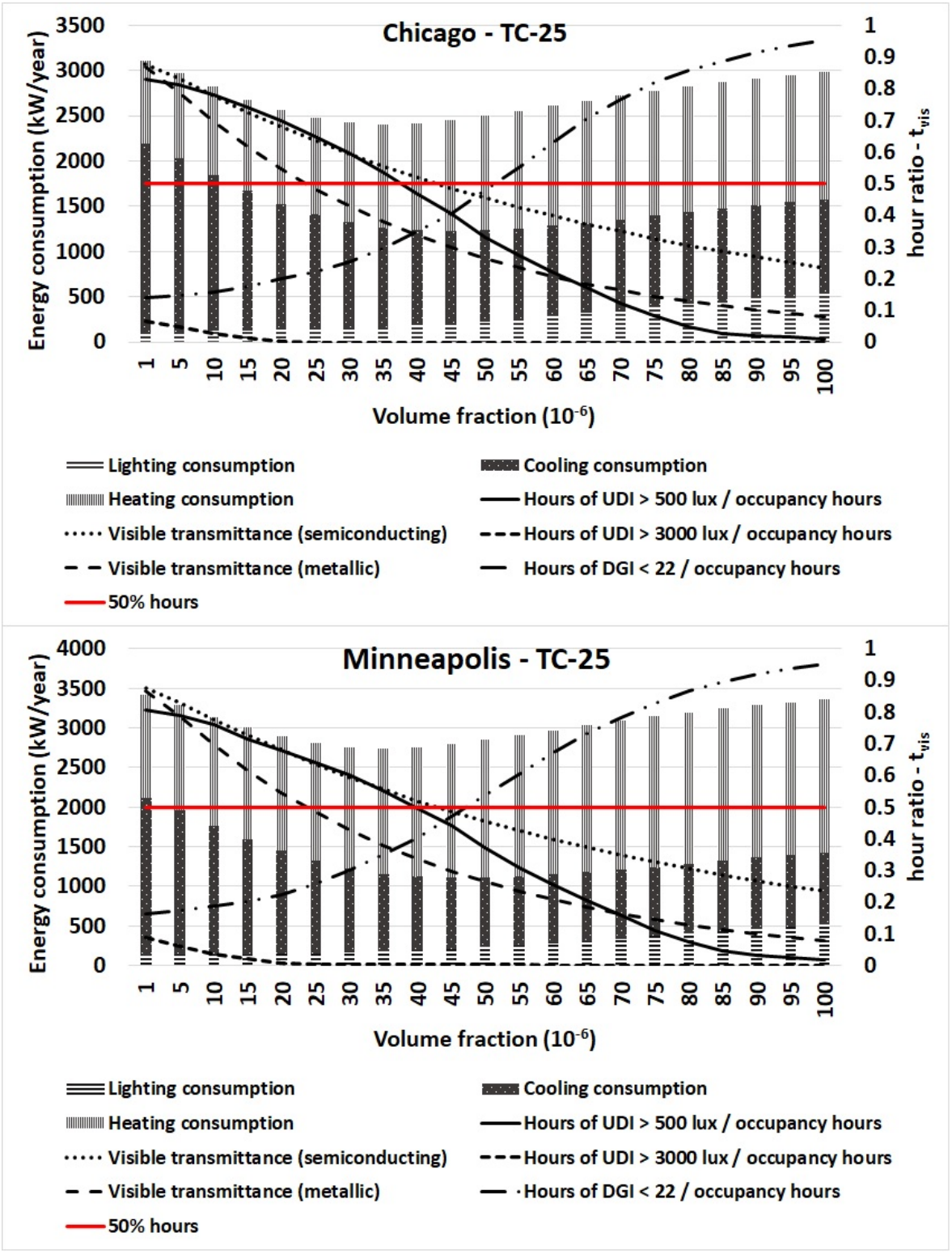


Figure 4.2. Change of optical properties with volume fraction value for TC-25 for first technology.

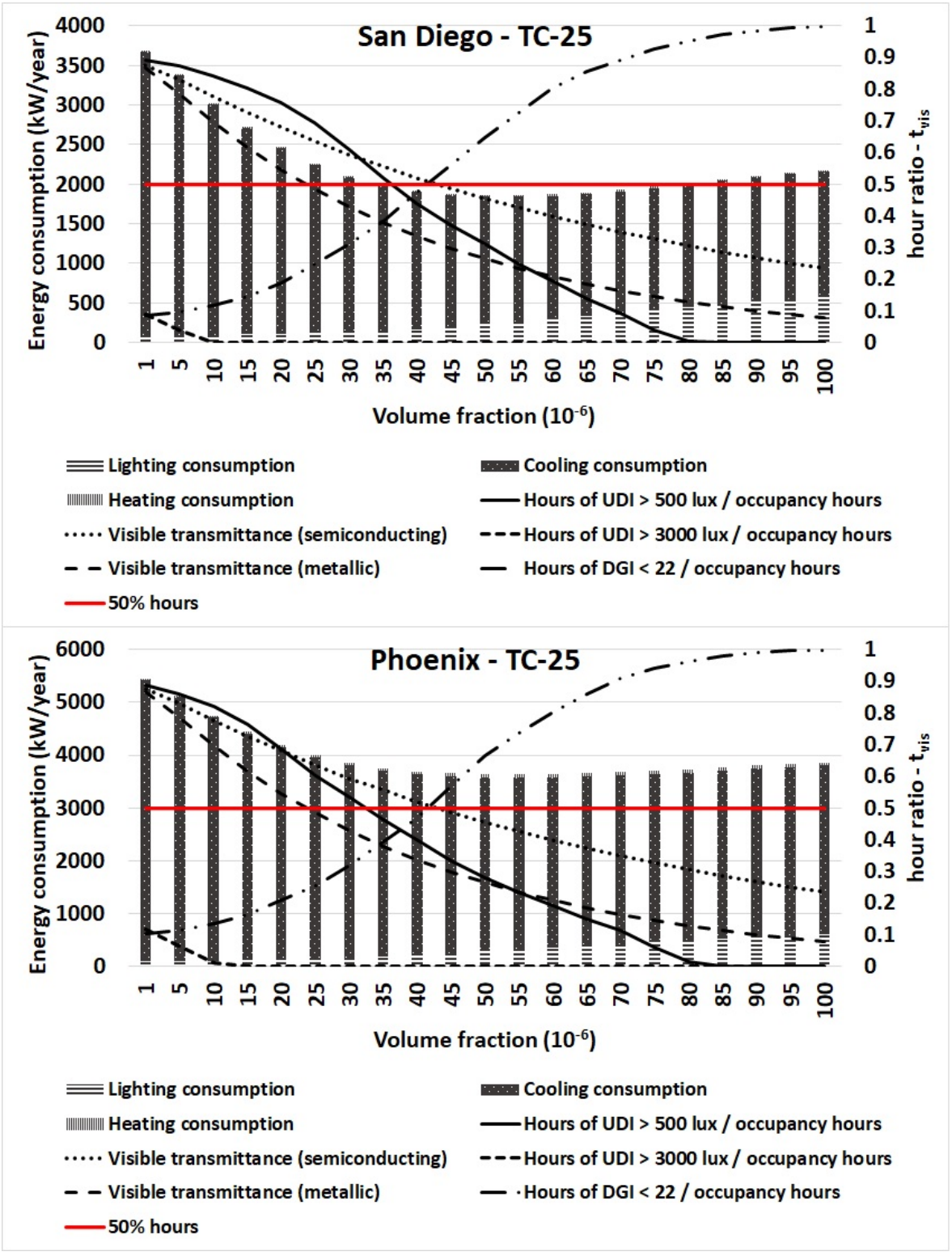


Figure 4.2. Change of optical properties with volume fraction value for TC-25 for first technology (cont.).

Table 4.1. Optimum optical properties for first technology and standard glass.

Cities	T_c	f (10^{-6})	**Phase**	t_{sol}	t_{vis}	r_{sol}	r_{vis}
Chicago	25 °C	35	Semiconducting	0.58	0.56	0.07	0.07
			Metallic	0.29	0.38	0.05	0.05
	35 °C	45	Semiconducting	0.52	0.49	0.07	0.06
			Metallic	0.22	0.30	0.05	0.05
	45 °C	53	Semiconducting	0.47	0.44	0.06	0.06
			Metallic	0.17	0.25	0.04	0.05
Minneapolis	25 °C	35	Semiconducting	0.58	0.56	0.07	0.07
			Metallic	0.29	0.38	0.05	0.05
	35 °C	47	Semiconducting	0.50	0.47	0.07	0.06
			Metallic	0.21	0.28	0.05	0.05
	45 °C	55	Semiconducting	0.46	0.43	0.06	0.06
			Metallic	0.16	0.23	0.04	0.05
San Diego	25 °C	36	Semiconducting	0.57	0.55	0.07	0.07
			Metallic	0.28	0.37	0.05	0.05
	35 °C	48	Semiconducting	0.50	0.47	0.07	0.06
			Metallic	0.20	0.28	0.04	0.05
	45 °C	55	Semiconducting	0.46	0.43	0.06	0.06
			Metallic	0.16	0.23	0.04	0.05
Phoenix	25 °C	33	Semiconducting	0.59	0.57	0.07	0.07
			Metallic	0.31	0.40	0.05	0.05
	35 °C	41	Semiconducting	0.54	0.51	0.07	0.07
			Metallic	0.24	0.33	0.05	0.05
	45 °C	51	Semiconducting	0.48	0.45	0.06	0.06
			Metallic	0.18	0.26	0.04	0.05
Clear glass				0.78	0.88	0.08	0.08

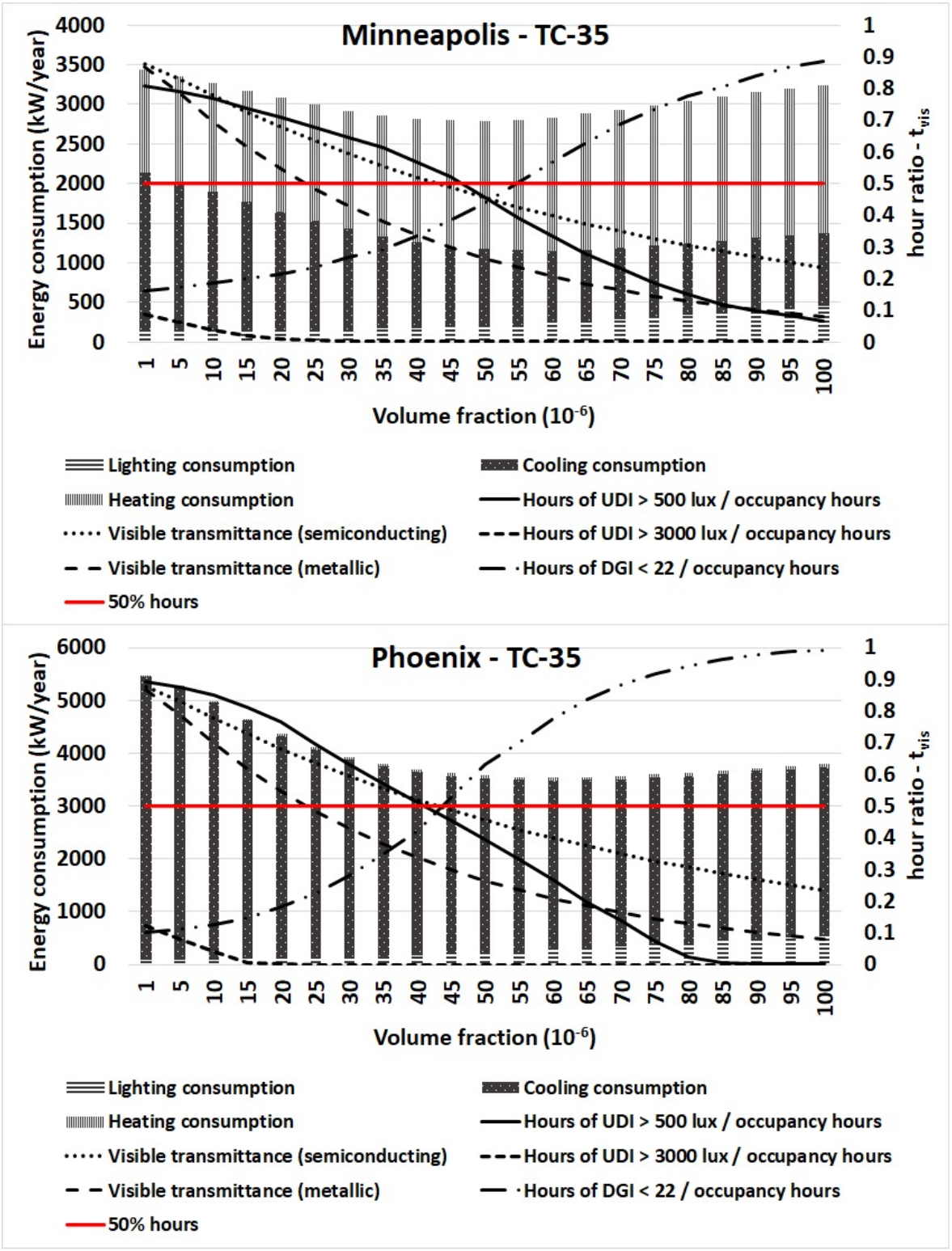


Figure 4.3. Change of optical properties with volume fraction value for TC-35 and TC-45 for first technology.

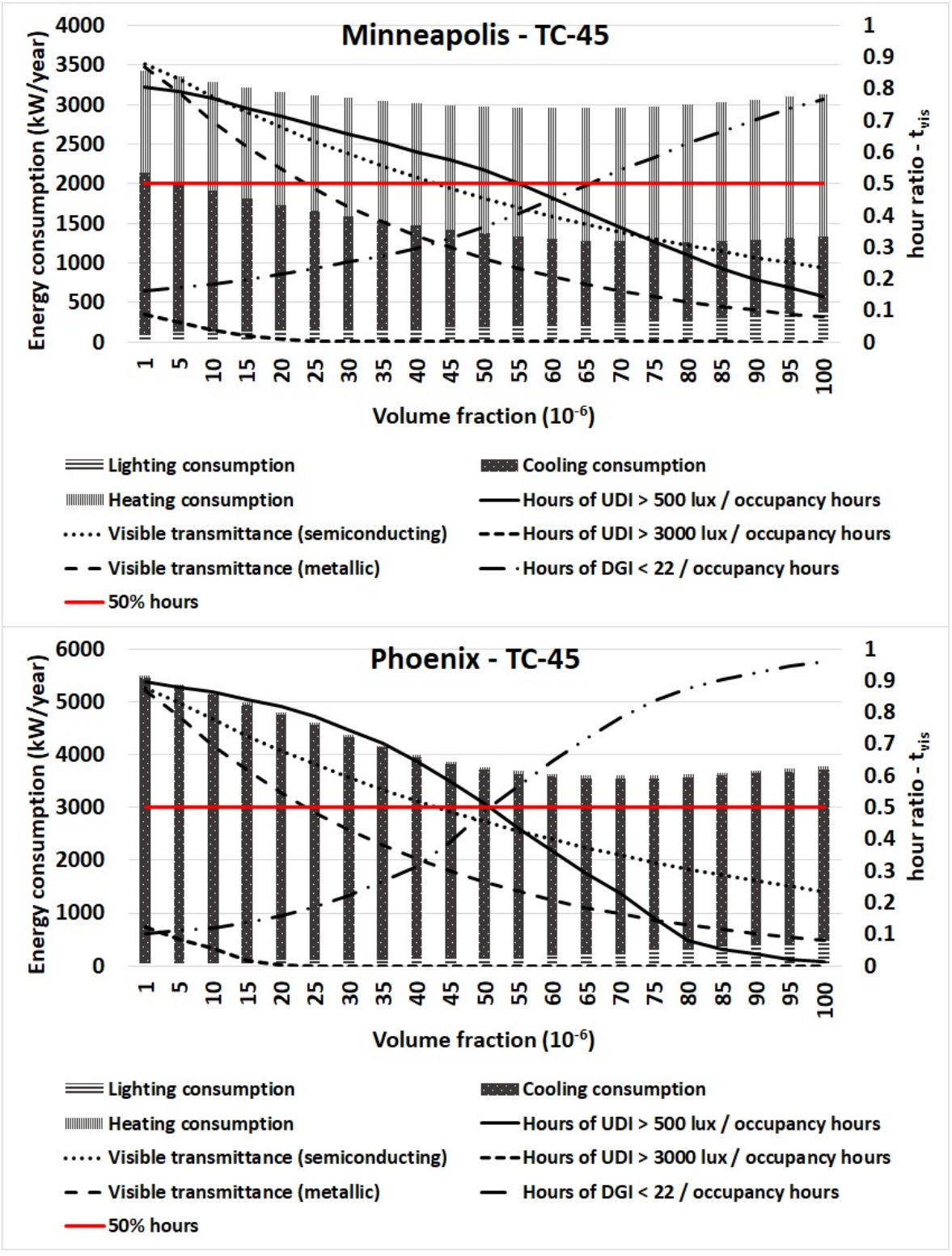


Figure 4.3. Change of optical properties with volume fraction value for TC-35 and TC-45 for first technology (cont.).

In all cases, as the transition temperature of thermo-chromic glass increases, optimum volume fraction tends to increase as well, as seen in Table 4.1. Furthermore, the rise in volume fraction leads to a decline in visible and solar transmittance, necessitating an increase in lighting and heating energy consumption, whereas cooling energy consumption is reduced as shown in Figure 4.2 and Figure 4.3. In hot climates such as Phoenix, the total energy consumption is comprised mostly of cooling energy consumption, about 94% for all transition temperatures. On the other hand, heating energy consumption is more significant in Minneapolis representing cold climates as expected; around 58%, 57% and 55% of total energy consumption for TC-25, TC-35 and TC-45, respectively. Whereas, cooling consumption is around 36%, 36% and 38% in the same order.

When the glass temperature exceeds the transition temperature, VO_2 particles transition from monoclinic structure to tetragonal crystalline structure that leads to a decrease in visible and solar transmittance of the thermo-chromic glass. Decreasing visible and solar transmittance until optimal volume fraction leads to a drop in energy consumption, while reducing illumination. In the cases where transition takes place at higher temperatures, relatively higher particle concentrations satisfy visual comfort criteria as visible and solar transmittance values do not decrease as significantly due to the shift in transition. Therefore, the visual comfort criteria can be satisfied with relatively higher particle volume concentrations for particles with higher transition temperatures as shown also in Figure 4.3.

4.1.3. Hours in Metallic Phase for Optimum Thermo-chromic Glazing

Hours in metallic phase are presented for all cases in Figure 4.4. It must be noted that all internal loads and HVAC system are considered as explained before in order to simulate a realistic use of this system. Each thermo-chromic case in all climates spends hours in metallic phase, but the longest period is spent in Phoenix, representing extreme hot climate case. It can be observed that the particles within optimal thermo-chromic glazings for cities in colder climates such as Chicago and Minneapolis

also spend significant time in metallic phase for lower transition temperatures despite their lower ambient temperatures due to the effect of incident solar radiation. The particles in the thermo-chromic glass can transition to metallic phase when incident solar radiation is high even if outdoor temperature is lower than transition temperature, as also outlined by Liang *et al.* and Hoffmann *et al.* [7, 9].

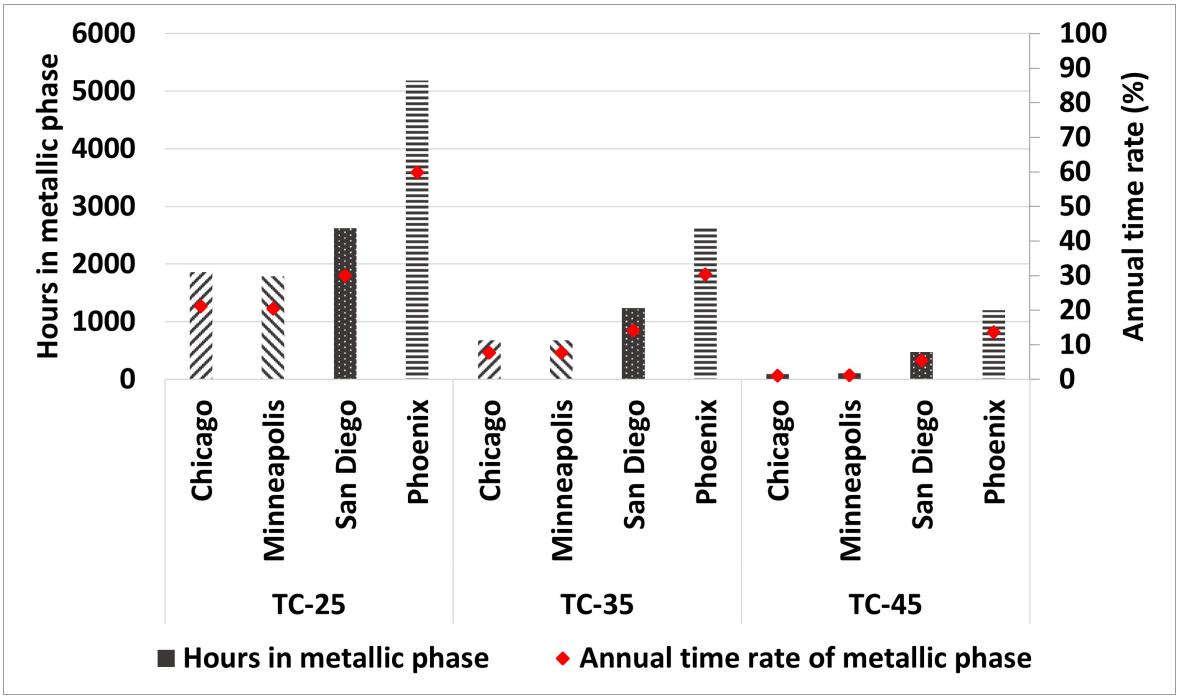


Figure 4.4. Hours and annual time rate in metallic phase for all climates according to transition temperature.

Annual time rate of nanoparticles in metallic phase is estimated as 21.2%, 20.4%, 29.9%, 59.8% for TC-25 as shown in Figure 4.4; whereas, for TC-35, annual time rate in metallic phase decreases to 7.8%, 7.7%, 14.1%, 30.4% for Chicago, Minneapolis, San Diego and Phoenix, respectively. Decrease in annual time rate in metallic phase is more in cold climates than hot climates as transition temperature increases from 25 °C to 35 °C as observed from Figure 4.4. It can also be noticed that hours in metallic phase for TC-45 is negligible for cold climates, but nanoparticles experience 13.7% of annual time in metallic phase for Phoenix.

4.1.4. Total Energy Consumption

Estimated energy consumptions are compared to those for an ordinary double glazing considering different transition temperatures in Figure 4.5 and Figure 4.6. The total energy consumption comprises of lighting, cooling and heating energy consumption, as shown in Figure 4.5. The cooling energy consumption constitutes majority of the consumption in hot climates such as Phoenix and San Diego, whereas cooling and heating consumptions are balanced for colder climates. A general decrease of energy consumption is observed in cold climates with drop of transition temperatures, but a similar general trend cannot be observed for hot climates. The highest energy consumption improvements are observed with TC-35 for San Diego and Phoenix. This is because cooling energy consumption has the highest energy cost in hot climates and it is the lowest in these cities with TC-35 minimizing the overall energy consumption. 46% and 31% drop for cooling energy consumption is observed for TC-35 when compared to ordinary double glazing as the highest in San Diego and Phoenix, respectively. However, San Diego and Phoenix for TC-25 show 45% and 29% decrease in cooling energy consumption, respectively. The results show that TC-35 is the most favorable choice for hot climates since the balance of time passed in semiconducting and metallic phase states is the most suitable among other transition temperatures. Moreover, all thermo-chromic glazings in all climates exhibit improvement with respect to ordinary double glazing. As visible transmittance of thermo-chromic glazing is less than it is for the ordinary glazing, leading to an increase in lighting energy consumption as seen in Figure 4.7.

Although the highest reduction in energy consumption is achieved for Phoenix, the highest improvement rate appears to be in San Diego as shown in Figure 4.6. This is due to the fact that the uttermost reduction in the highest expenditure energy load, which is cooling energy consumption, for hot climates. Therefore, San Diego shows the utmost improvement rates in all transition temperatures. Besides, Phoenix has increased lighting energy consumption in a rate, 95%, 83% and 77%, when compared to that of San Diego, 59%, 62% and 65%, for TC-25, TC-35 and TC-45, respectively.

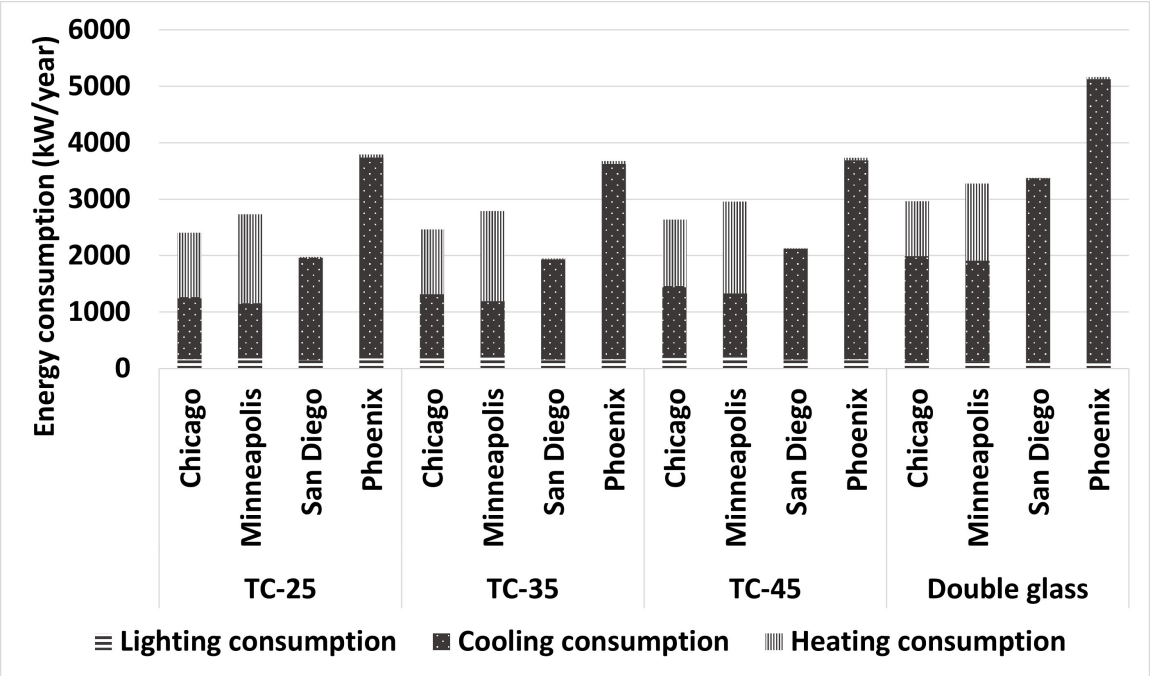


Figure 4.5. Annual total energy consumption according to transition temperatures and ordinary double glazing for four climates.

Whereas, savings in Chicago and Minneapolis, representing cold and extreme cold climates, respectively, are almost identical for all transition temperatures considered. Besides, energy savings in these colder climates are lower than the warmer climates investigated as the hours in metallic phase is less in these climates.

If illuminance at monitoring point is below 500 lux, it is assumed that artificial lighting compensates for the deficiency. Lighting energy consumption increases when visible transmittance decreases in all cases, with clear glazing having the highest visible transmittance, it leads to the lowest lighting energy consumption as seen in Figure 4.7. Lighting energy consumption in San Diego and Phoenix is less than Chicago and Minneapolis due to longer daylight period, except for the case of Phoenix with lowest transition temperature 25 °C. For that case the doped particles are mostly in metallic phase leading to lower visible transmittance that necessitates relatively more need for artificial lighting.

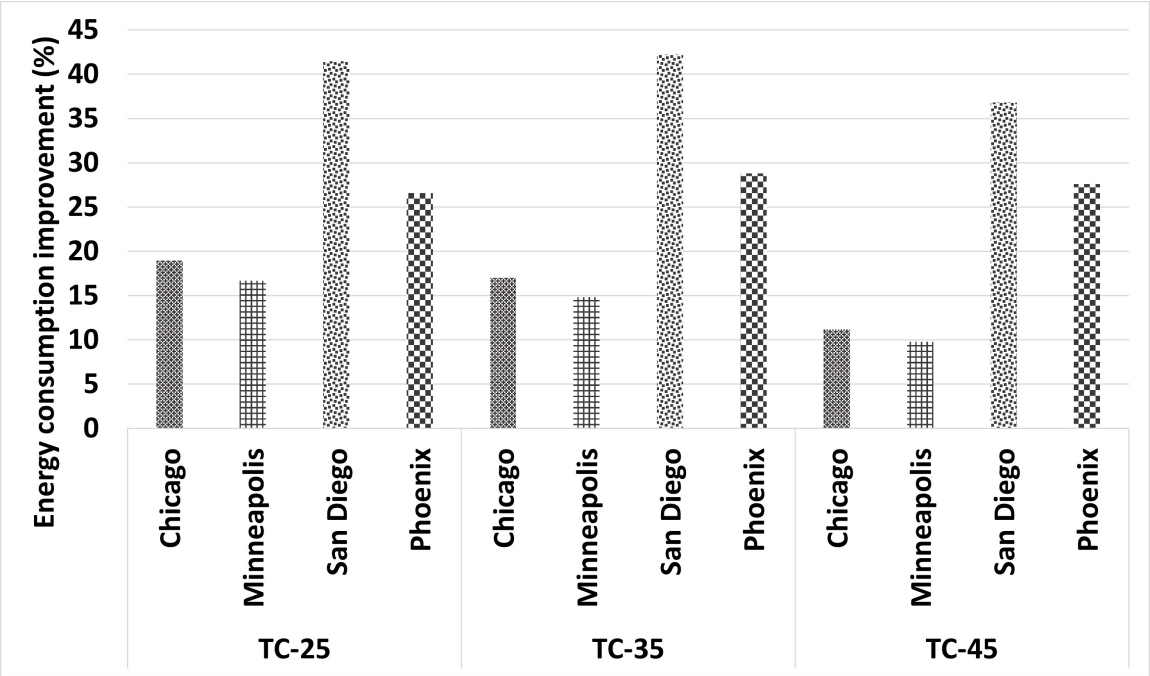


Figure 4.6. Total energy consumption improvement according to transition temperatures for four climates.

Moreover, it is applied the procedure explained so far to a west facing window to examine and document to the position effect of the window. This brief analysis helps the visualizing the position effect of the window in the mind. In this case, optimal conditions subject to visual comfort criteria are satisfied with lower volume fractions, and higher t_{vis} and t_{sol} for all thermo-chromic cases and climates. Besides, when the total energy consumption of west faced window with south faced window is compared, a general increase in total energy consumption in cold and extreme cold climates are observed. Rise of 26%, 25%, 21.3% and 9.7% for Chicago and 28.5%, 27.6%, 23.1% and 11.9% for Minneapolis are observed in total energy consumption for TC-25, TC-35, TC-45 and ordinary double glazing, respectively. However, there is a drop in total energy consumption in extreme hot climate, Phoenix, 4.8%, 4.6%, 6.5% and 21.6% in the same order. Besides, decrease of 8.6% for TC-25, 4.8% for TC-35 and 25.2% for ordinary double glazing is observed in San Diego except insignificant change of TC-45, rise of 0.5%, according to south faced window. These changes are due to rise in heating energy consumption when the window faces west, which leads to an increase in total

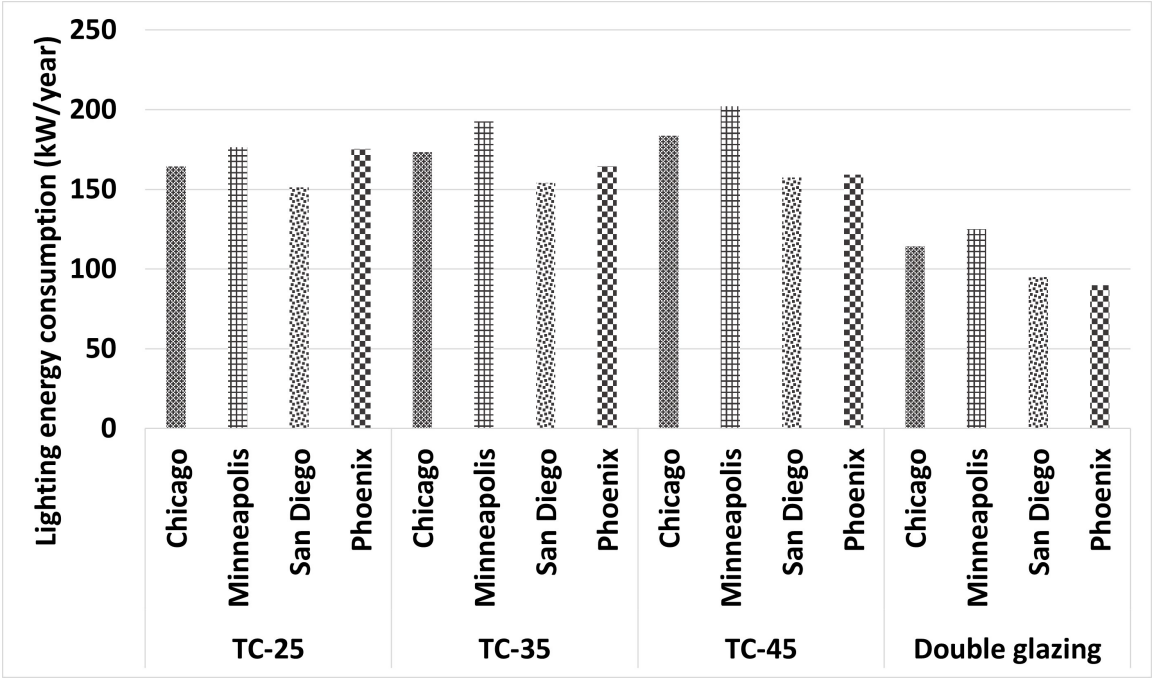


Figure 4.7. Lighting energy consumption according to transition temperatures and ordinary double glazing for four climates.

energy consumption in all cases of cold and extreme cold climates.

Although there are different changes in total energy consumption in hot and cold climates between the cases window facing west and south as explained, similar behavior as seen in Figure 4.6 for energy consumption improvement is observed when the window faces west. However, improvement rates in all cases drop according to south faced window. The highest achieved improvement is observed in San Diego with rates 28% for TC-25, 26% for TC-35, and 15% for TC-45. After San Diego, Phoenix has the highest improvement rate of 11%, 13% and 14% for TC-25, TC-35 and TC-45, respectively. Besides, significant improvement is not observed in cold climates; 7%, 5% and 2% for Chicago and 4%, 3% and 1% for Minneapolis are achieved for TC-25, TC-35 and TC-45, respectively. While it is observed that maximum benefit is achieved for south facing window as expected, this brief analysis for west facing window helps identifying the effect of this technology with changing direction. Also, it was desired to identify the effect on different faces by analyzing south facing window together with

the brief analysis of west facing window so that simple office room is modeled instead a whole building in this study.

4.1.5. Daylight Illuminance

Daylight illuminance is identified by monitoring the illuminance of the point that is 4.5 m from the window as shown in Figure 3.1. The annual percentage of daylight illuminance during occupancy hours is presented according to the updated criteria by Mardaljevic *et al.* [62] for useful daylight illuminance (UDI) approach for thermo-chromic and ordinary double glazing for all climates in Figure 4.8. The acceptable range in daylight illuminance is between 300 and 3000 lux. Artificial lighting is needed when illuminance is lower than 300 lux, whereas illuminance higher than 3000 lux has the possibility of causing discomfort and glare for the occupants.

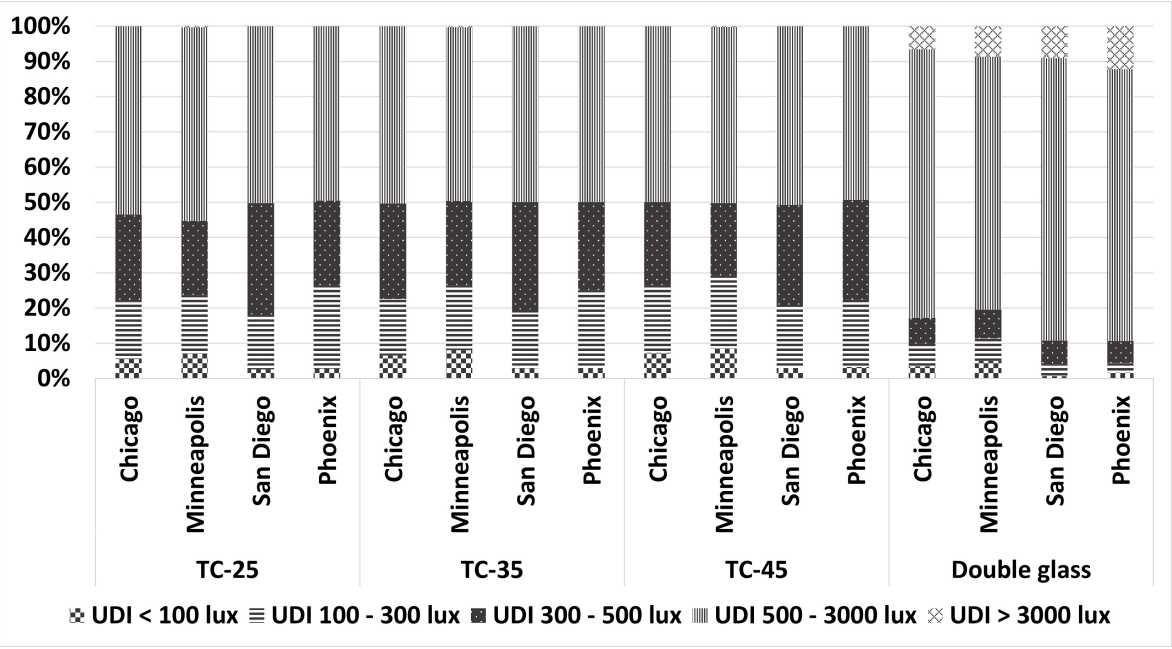


Figure 4.8. Annual natural daylight illuminance according to transition temperatures and ordinary double glazing for four climates.

Optimal thermo-chromic glazing meet the desired visual comfort criteria for daylight illuminance in all cases for all climates. However, in all cases, ordinary double

glazing has still more illuminance between 300 and 3000 lux than thermo-chromic glazings because of having high t_{vis}. This result shows that ordinary double glazing is more advantageous for having more time in the most desired daylight illuminance range, which is between 300 and 3000 lux. Similar outcome is also observed in the visual analysis of Liang *et al.* study [7]. Besides, when ordinary double glazing is examined, it could be observed that its energy consumption due to illumination is the lowest, as seen in Figure 4.8. This is consistent with the results presented in Figure 4.7, shows that ordinary double glazing necessitates the least illumination energy consumption. Therefore, double ordinary glazing is better in saving energy for lighting than thermo-chromic glazings.

In return, as the disadvantage of using ordinary double glazing, it has excess period of time that is higher than 3000 lux and this may cause discomfort with oversupply of daylighting necessitating the use of blinds in office buildings. All thermo-chromic glazing cases show more uniform result with reducing excess of daylight after 300 lux. Costanzo *et al.* [33] also observed the more uniform distribution of illuminance with using thermo-chromic glazing into room as the result of analysis of visual performance in their study. Illuminance higher than 3000 lux can only be observed in extreme cold climate, Minneapolis, and the excess period is negligible as it could be observed from Figure 4.8.

4.2. Results of Attached Thin VO_2 Thermo-chromic Film Technology

4.2.1. Optimal Thermo-chromic Coating Thickness and Particle Concentration

Grid search optimization (single or multi variable search) is utilized in this study for determining optimal thickness and volume fraction according to all transition temperatures. Contour plot analysis of total energy consumption according to thickness and volume fraction change can be observed in Figure 4.9. The line in the Figure 4.9 illustrates the illuminance criteria limit for visual comfort. The coatings with higher

particle volume fraction or thickness with respect to the line, thermo-chromic coating does not satisfy the criteria for visual comfort. The optimal thermo-chromic coating configuration is found according to all transition temperatures for three different cities; Izmir, Istanbul and Ankara.

The optimal point is determined in the region where the illuminance criteria is higher than 500 lux for 50% of occupancy hours for visual comfort that yields minimum energy consumption as explained before. It can be observed in Figure 4.9 that energy consumption increases in the region satisfying visual comfort criteria with decreasing volume fraction and coating thickness in all cities and transition temperatures. However, minimum energy consumption while satisfying visual comfort criteria is located in close proximity of the line with different configuration of concentrations between 0.3 and 0.8 and thicknesses between 50 nm and 150 nm according to climatic conditions of cities and transition temperatures.

The minimum energy consumption is determined while considering visual comfort criteria by performing grid search optimization, and the optimal variables are presented in Table 4.2 where it can be observed that different optimal coating thicknesses and volume fractions yield minimum energy consumption for different climates and transition temperatures. However, in all cases except TC-35 in Izmir, as transition temperature of coating increases, optimal volume fraction increases and optimal coating thickness decreases. Izmir being the hottest city studied, the highest optimal coating thickness obtained at the transition temperature of 35 °C, which is the exceptional case.

Energy consumption variation according to change of VO_2 concentration and specified optimum thickness in Table 4.2 for all cities and transition temperatures can be observed in Figure 4.10 in more detail. In Izmir and Istanbul, it is observed that there is not general behavior for total energy consumption with rise of volume fraction, but total energy consumption increases with rise of volume fraction in Ankara. Cooling energy consumption decreases in all cases while there is an increase on lighting and heating energy consumption with rise of volume fraction as observed in Figure 4.10.

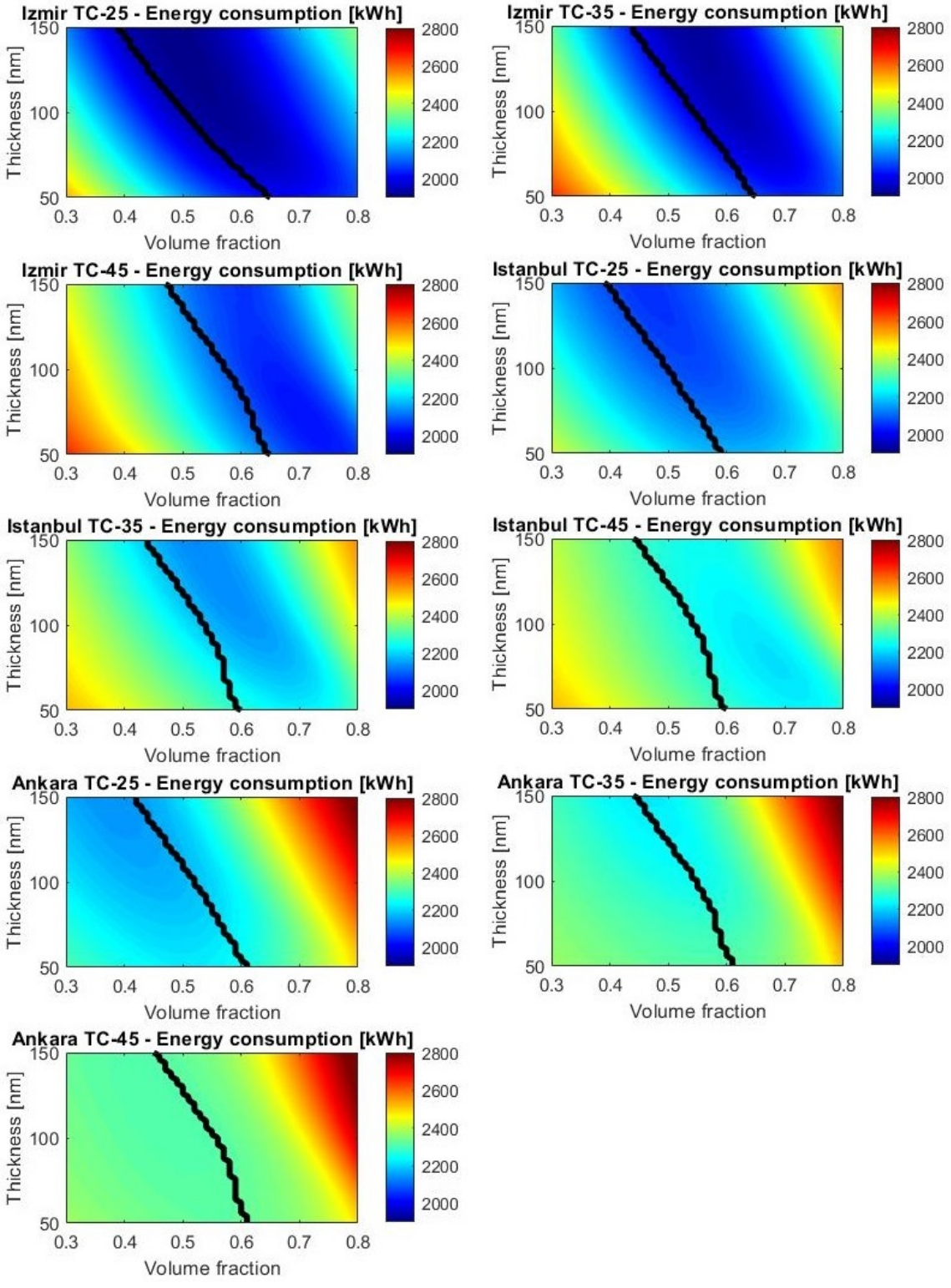


Figure 4.9. Energy consumption change according to coating thickness and volume fraction.

Table 4.2. Optimum optical properties for second technology and standard glass.

Cities	T_c	f	**Thickness [nm]**	**Phase**	t_{sol}	t_{vis}	r_{sol}	r_{vis}
Izmir	25 °C	0.50	102	Semiconducting	0.54	0.60	0.21	0.13
				Metallic	0.37	0.49	0.19	0.11
	35 °C	0.53	108	Semiconducting	0.50	0.56	0.21	0.11
				Metallic	0.32	0.45	0.20	0.11
	45 °C	0.61	82	Semiconducting	0.45	0.49	0.28	0.20
				Metallic	0.32	0.42	0.23	0.18
Istanbul	25 °C	0.43	134	Semiconducting	0.58	0.62	0.17	0.09
				Metallic	0.37	0.50	0.17	0.08
	35 °C	0.51	116	Semiconducting	0.51	0.57	0.20	0.10
				Metallic	0.32	0.45	0.19	0.10
	45 °C	0.56	92	Semiconducting	0.49	0.54	0.24	0.16
				Metallic	0.33	0.45	0.21	0.14
Ankara	25 °C	0.38	150	Semiconducting	0.61	0.64	0.16	0.10
				Metallic	0.40	0.51	0.15	0.08
	35 °C	0.45	148	Semiconducting	0.54	0.55	0.17	0.13
				Metallic	0.32	0.43	0.17	0.09
	45 °C	0.47	116	Semiconducting	0.56	0.61	0.19	0.10
				Metallic	0.36	0.49	0.18	0.09
Clear glass					0.78	0.88	0.08	0.08

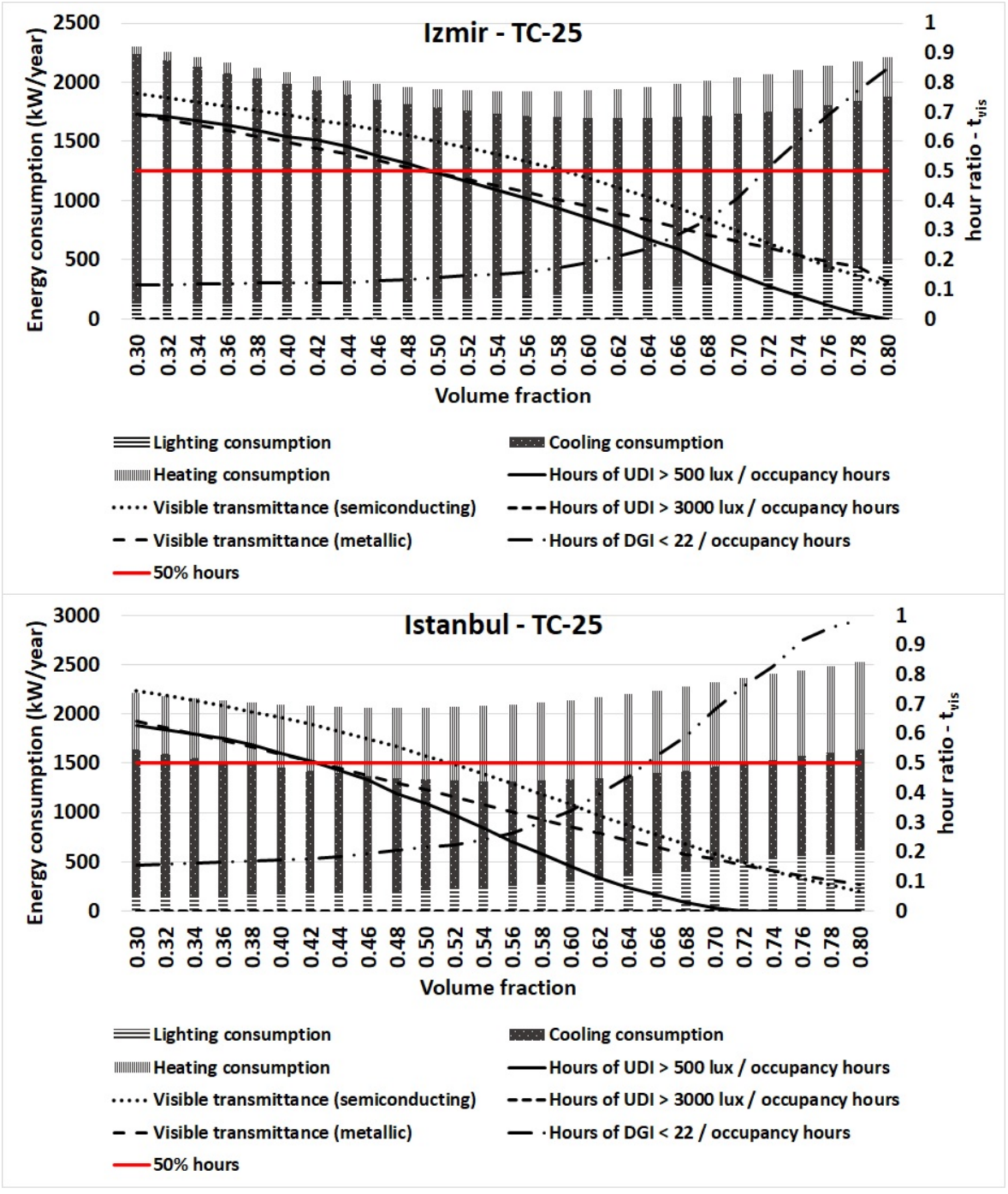


Figure 4.10. Change of optical properties with volume fraction for second technology.

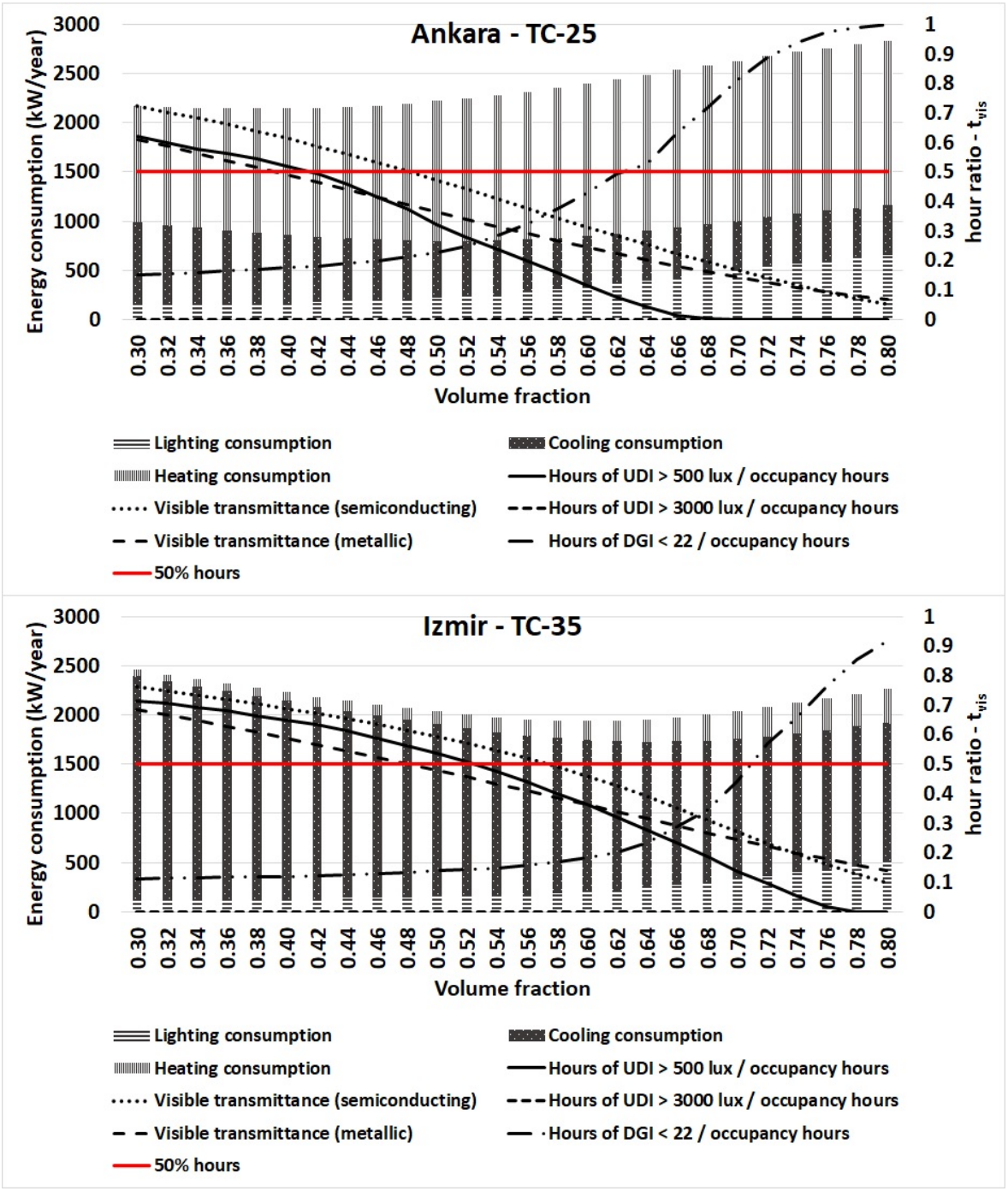


Figure 4.10. Change of optical properties with volume fraction for second technology (cont.).

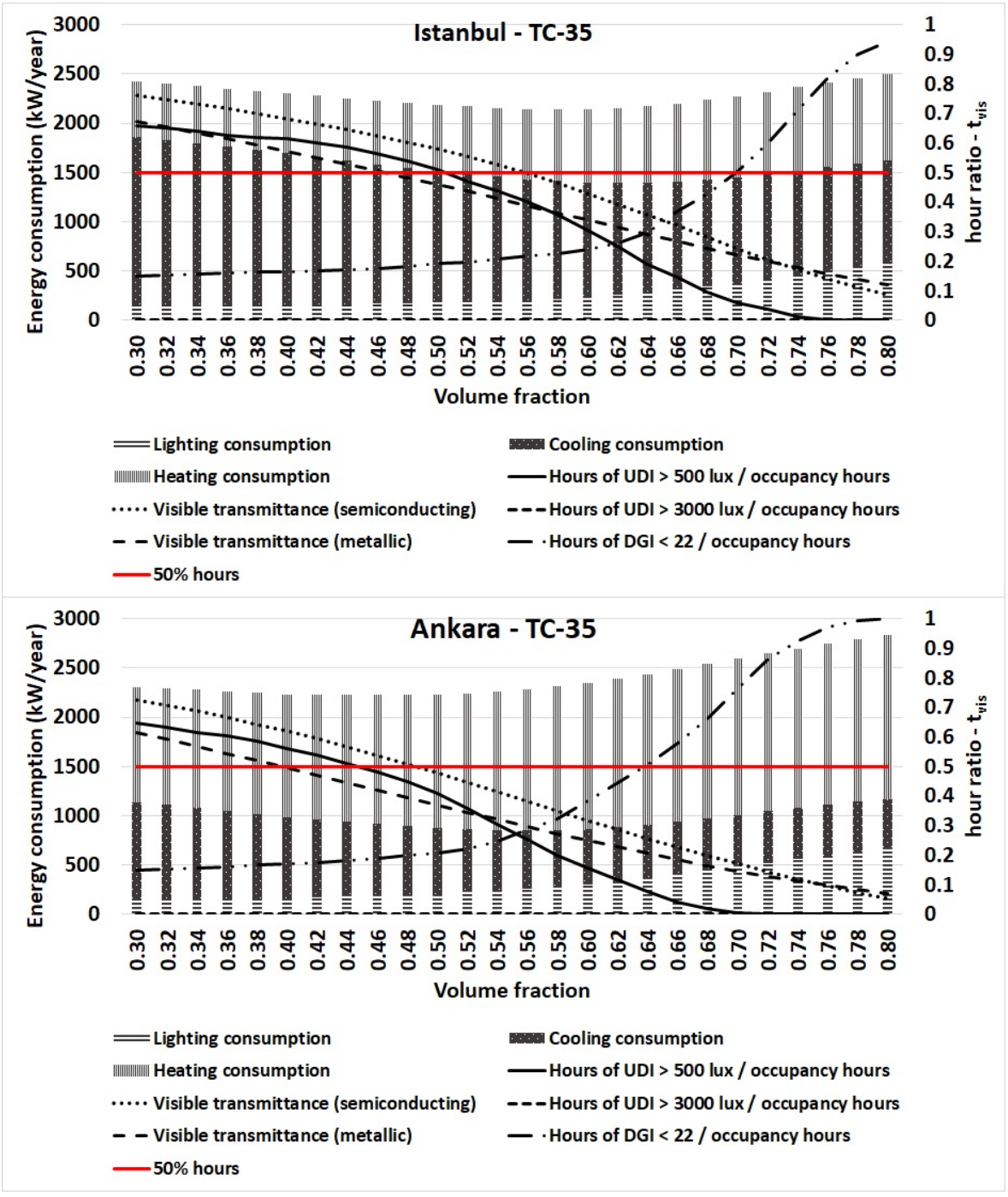


Figure 4.10. Change of optical properties with volume fraction for second technology (cont.).

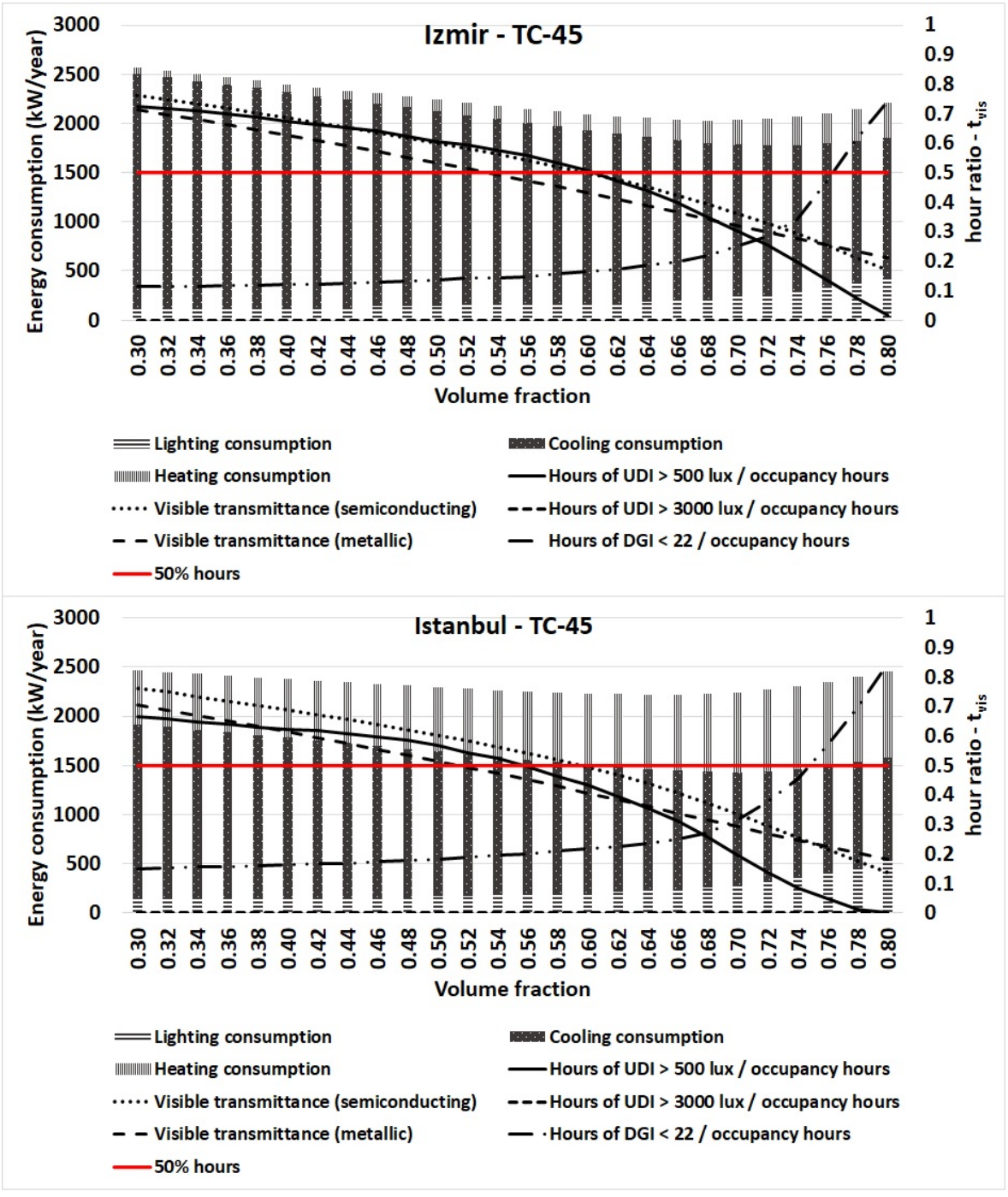


Figure 4.10. Change of optical properties with volume fraction for second technology (cont.).

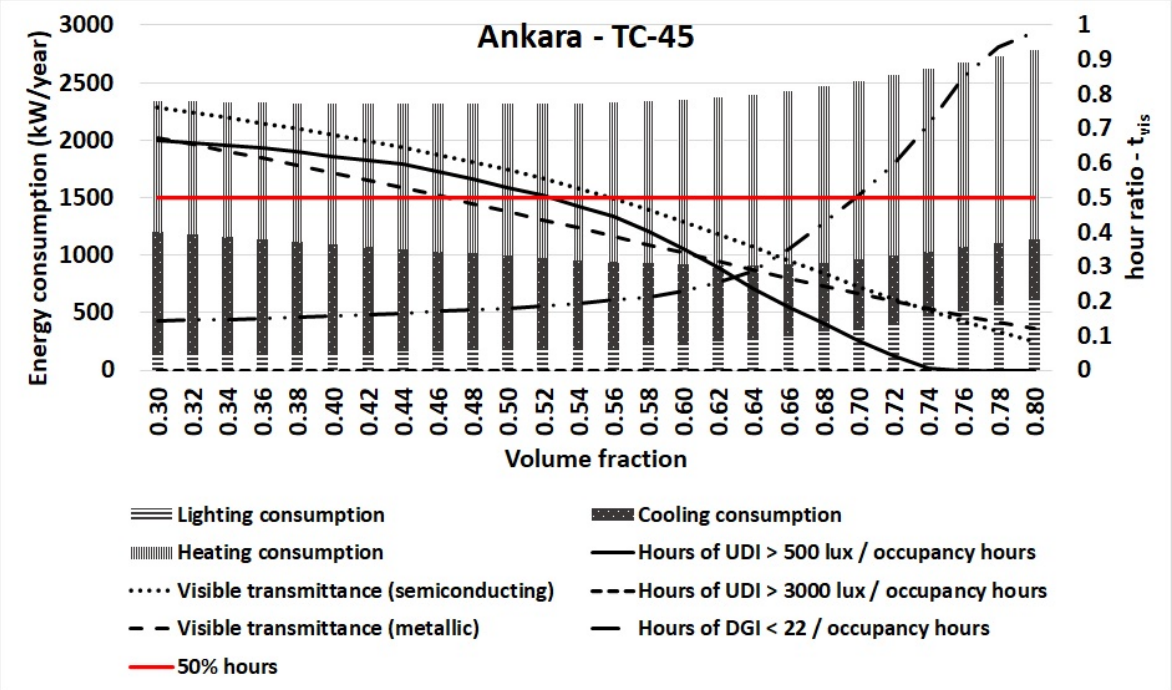


Figure 4.10. Change of optical properties with volume fraction for second technology (cont.).

4.2.2. Hours in Metallic Phase for Optimum Thermo-chromic Coating

The analysis of hours in metallic phase for all climates and transition temperatures can be observed in Figure 4.11. As expected, TC-25 spends the longest time in metallic phases in all climates and the time in metallic phase is correlated with the climates from hot to cold climates. Izmir, representing relatively hot climate, has the highest time rate in metallic phase for TC-25 and TC-35 as 26.5% and 8.0%, respectively. Istanbul, representing temperate climate, and Ankara, representing relatively cold climate, also have significant time rate in metallic phase as 18.9% and 14.8% in TC-25, respectively. Whereas, annual time rate in metallic phase for Istanbul and Ankara drops to 3.8% and 3.7% for TC-35. However, the coating does not transmit its phase to metallic in Istanbul and Ankara for TC-45, whereas hours in metallic phase is negligible in Izmir. Therefore, lower transition temperatures than 45 °C is required for benefiting from phase change materials.

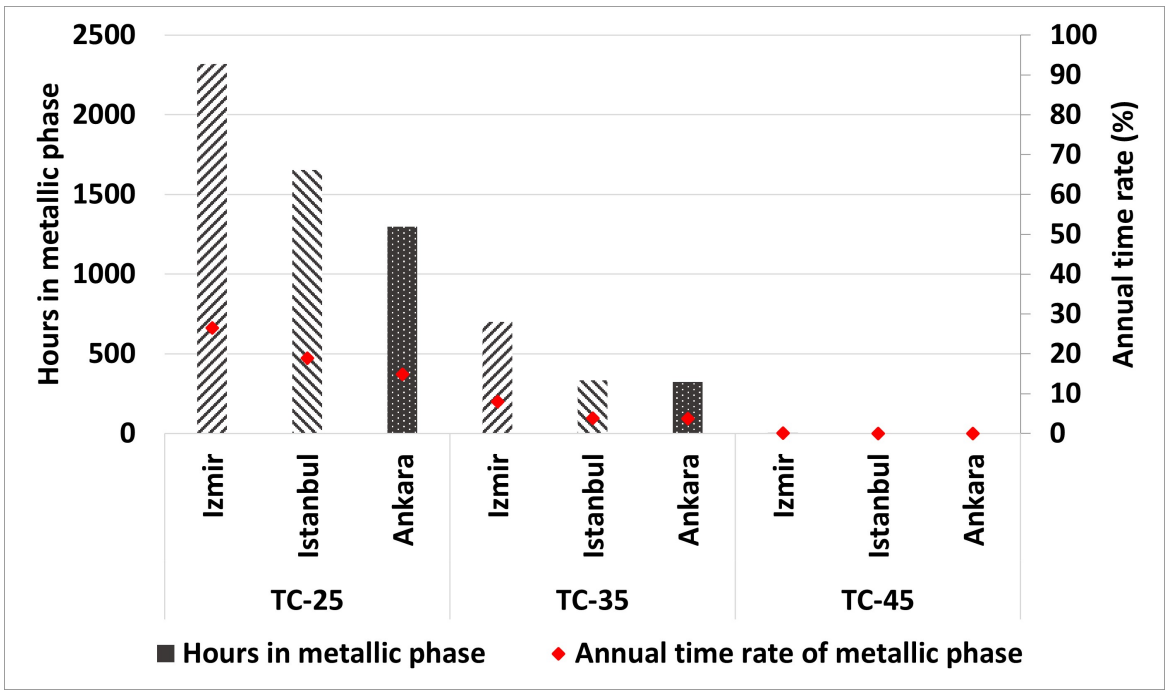


Figure 4.11. Hours and annual time rate in metallic phase for all climates according to transition temperature.

4.2.3. Total Energy Consumption

Lighting, cooling and heating energy consumption constitutes the total energy consumption, as shown in Figure 4.12. The energy consumption improvements of thermo-chromic coating in all cases when they are compared to ordinary double glazing are also shown in Figure 4.13. Decrease in total energy consumption and increase in energy consumption improvement are observed as drop of the transition temperature in all cases.

Heating energy consumption constitutes the majority of total energy consumption in relatively colder climate such as Ankara as shown in Figure 4.12. Furthermore, thermo-chromic coating causes rise of heating energy consumption as 17%, 20% and 19% for TC-25, TC-35 and TC-45, respectively. On the other hand, there is a drop on cooling energy consumption with using thermo-chromic coating as 38%, 36% and 26% with the same transition temperature alignment. These together with lighting energy

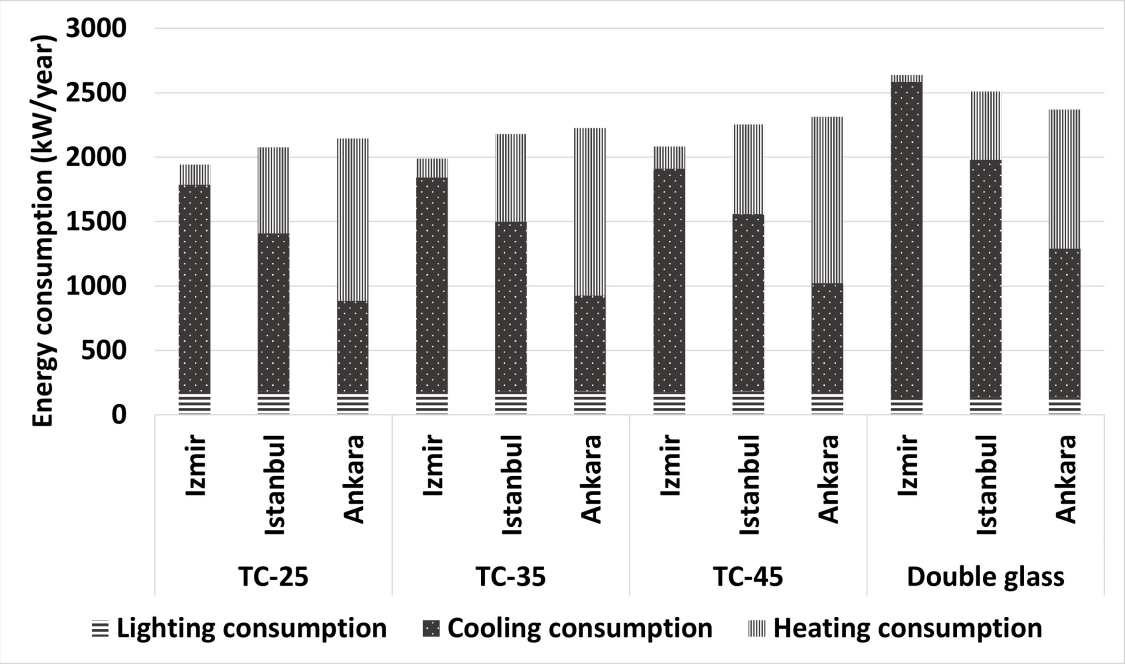


Figure 4.12. Annual total energy consumption according to transition temperatures and ordinary double glazing for three climates.

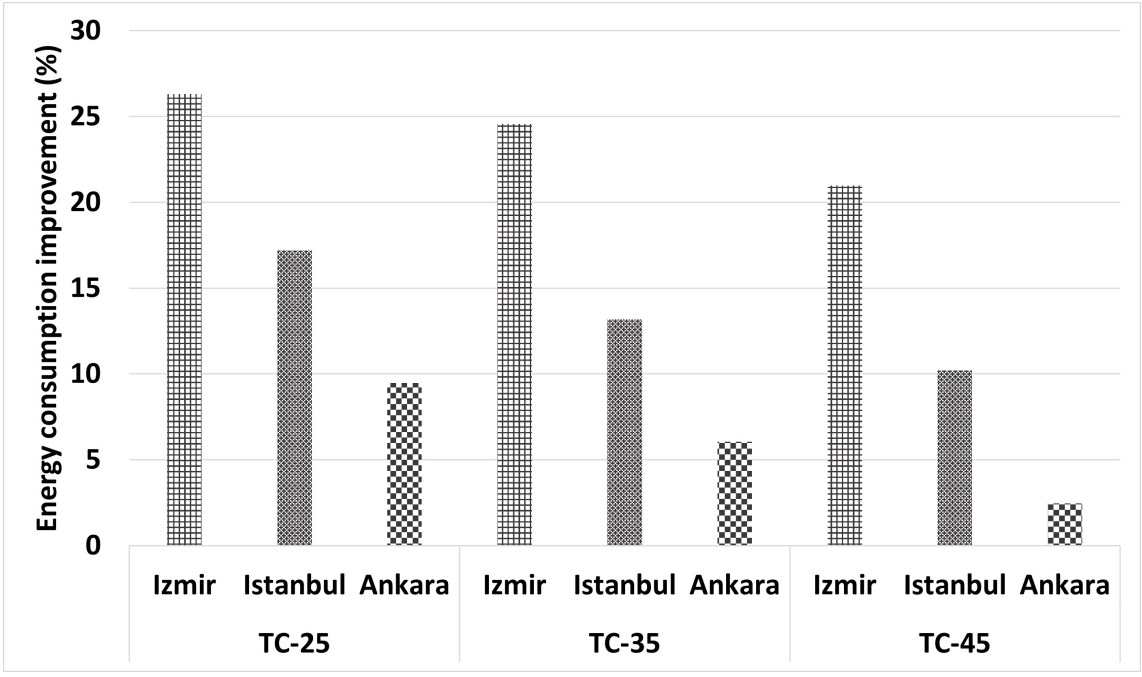


Figure 4.13. Total energy consumption improvement according to transition temperatures for three climates.

consumption cause an overall energy improvement even in relatively cold climate case as 9%, 6% and 2% for TC-25, TC-35 and TC-45, respectively.

In relatively hot and temperate climates, Izmir and Istanbul, cooling energy consumption is the major contributor to total energy consumption, whereas heating energy consumption is relatively lower in these climates. Using thermo-chromic coating leads drop of cooling energy consumption similar to cases in Ankara. Decrease of cooling energy consumption is 34%, 32% and 30% in Izmir and 33%, 29% and 26% in Istanbul for TC-25, TC-35 and TC-45, respectively. However, heating energy consumption in Istanbul is also increased 26%, 28% and 31% for TC-25, TC-35 and TC-45, respectively. Whereas, around twice as much of rise in heating energy consumption with using thermo-chromic coating is observed in Izmir, when it is compared to ordinary double glazing. Nevertheless, heating energy consumption is quite low in these climates when it is compared to cooling energy consumption. Therefore, thermo-chromic coating provides significant energy performance improvement considering all three elements of total energy consumption; which are heating, cooling and lighting, in relatively hot and temperate climates as 26%, 25% and 21% in Izmir and 17%, 13% and 6% in Istanbul for TC-25, TC-35 and TC-45, respectively.

The lighting energy consumption, which contributes the least to the total energy consumption, is shown in Figure 4.14. As previously explained, the illuminance is monitored from a defined point and if the illuminance is below 500 lux, artificial lighting compensates for the required illuminance to reach the minimum limit, 500 lux. Consequently, it is observed that ordinary double glazing has the minimum lighting energy consumption, due to its highest visible transmittance among all cases. Thermochromic coatings in all cities cause more lighting energy consumption. Although the city that has the lowest energy consumption is changing according to transition temperature, Istanbul has the highest lighting energy consumption in all cases. Izmir has the lowest energy consumption in TC-25 and TC-35. However, Izmir has lower visible transmittance than Ankara in TC-45 as the result of optimization for optimal conditions for satisfying visual comfort and this causes higher lighting energy consumption

as a deficiency.

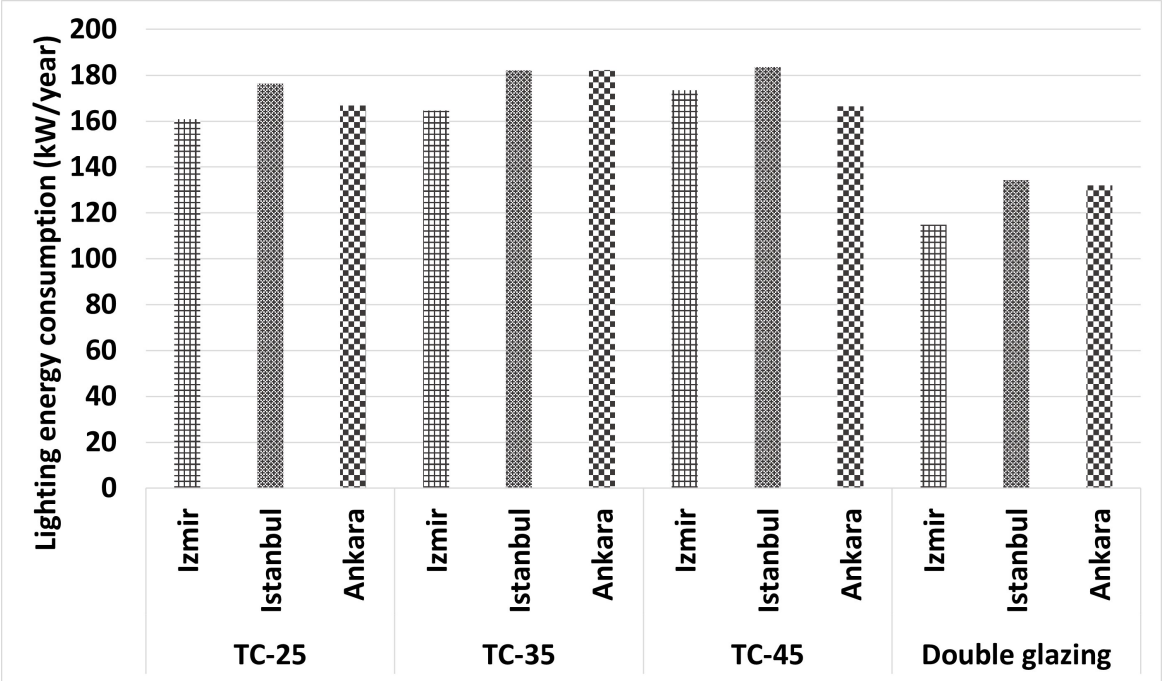


Figure 4.14. Lighting energy consumption according to transition temperatures and ordinary double glazing for three climates.

4.2.4. Daylight Illuminance

Same metric, which is proposed by Mardaljevic *et al.* [62], and monitored point as seen in Figure 3.2 as explained in the first technology is also used for this technology. The UDI method and its three acceptable ranges are explained before; therefore, it is not repeated here. Furthermore, DGI is also analyzed as in the first technology. Illuminance that is higher than 3000 lux is not observed as seen in Figure 4.10 in this second technology. Therefore, there is not discomfort due to excess illuminance according to UDI analysis. Moreover, glare occurrence according to DGI decreases with the rise of volume fraction like observed in the first technology as seen in Figure 4.10. However, there is a more gap for trade-off between satisfying illuminance and glare criteria for the second technology.

Similar outcomes are obtained in this technology as seen in Figure 4.14 like in

the first technology. Using ordinary double glazing leads to a higher time rate where illuminance is between 300 and 3000 lux when compared to rate where illuminance is below 300 lux when compared to thermo-chromic coatings. Therefore, considering UDI, ordinary double glazing is more advantegous than thermo-chromic coatings. This outcome can also seen from results of lighting energy consumption. Moreover, illuminance that is higher than 3000 lux is not observed in this technology just like the first technology.

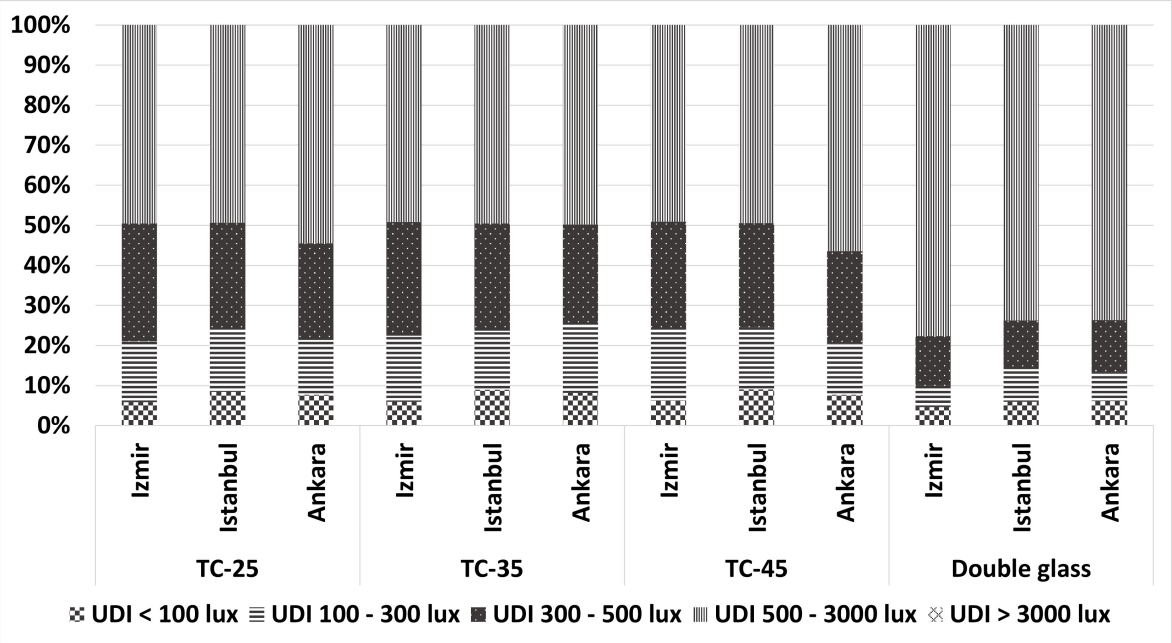


Figure 4.15. Annual natural daylight illuminance according to thermo-chromic coatings and ordinary double glazing for three climates.

4.3. Interpretation of Results of Two Distinct Technologies

Similar behavior is observed for determined optimal design properties in both technologies. High particle concentrations are obtained for decreasing t_{vis} to satisfy visual comfort criteria while T_c of the glazings or coatings increases in all cities. However, second technology, which is the thin film thermo-chromic coating, is generally satisfied the optimization criteria with higher t_{vis} than first technology in all conditions and there is less difference between optimal t_{vis} with change of T_c as seen in Table 4.1 and

Table 4.2. This result shows that using of a thin film coating that has higher t_{vis} is expected if thin film coating is desired to use in an application instead of thermo-chromic glazing.

Change of cooling energy consumption has a great effect on total energy consumption for office buildings especially in the hot climates as observed in the analysis of both technologies. Therefore, although the differences of improvement between TC-25 and TC-35 are quite close, the highest energy consumption improvement is obtained at TC-35 cases due to decrease of cooling energy consumption with the first technology in hot climates. However, this situation is not observed with the second technology and the highest energy consumption improvement is obtained at TC-25. Therefore, although the lowest T_c is the expected T_c for high efficiency before making analysis, this result shows that the most suitable result may be obtained with different T_c due to the interaction of many energy consumption variables in hot climates and it is not required to decrease the T_c to the lowest possible value for thermo-chromic glazing technology.

Resulting t_{vis} values of the optimal designs are lower than t_{vis} of the ordinary glass in both technologies. This caused higher lighting energy consumption with the case of thermo-chromic technologies. Furthermore, ordinary glass spends more time in the most suitable range of UDI as an advantage, but it may spend time in the excess illuminance region of UDI as seen in the first technology and this may cause visual discomfort due to excess illuminance. Blinds can be used to handle excess illuminance, but they are not considered in this study as this complicated the problem. Therefore, ordinary glass and thermo-chromic technologies have different advantages for visual comfort, but both thermo-chromic technologies show the same features within themselves for lighting energy performance and UDI approach. However, there is a difference between two technologies for the trade-off between illuminance and glare. Higher amount of trade-off between illuminance and glare is observed for the second technology as seen in Figure 4.10. Thus, it can be deduced that first technology is more advantageous than the second technology for this aspect.

5. CONCLUSION

5.1. Conclusions

To summarize the merit of this study and outcomes as a whole; there is not a study that examines the main design variables of pigmented thermo-chromic glazings and thin film coatings and their effects for energy consumption and visual comfort analysis in a single study. VO_2 based thermo-chromic glazings that have identical thickness to an ordinary glass as the first technology and attached thin VO_2 thermo-chromic film on an ordinary glass as the second technology are individually optimized for three transition temperatures in this study to maximize energy efficiency, while considering visual comfort for a unit room in an office building in a number of different climate conditions. A radiative transfer model of the pigmented thermo-chromic glazings based on four flux method is used so that optical properties of the glazings can be predicted for design variables in the first technology. However, transfer matrix method is used for determining the optical properties due to the need of analyzing the attached system as a whole in the second technology. These optical properties are then utilized for analysis of annual energy consumption of the unit room considering heating, cooling and lighting energy consumption.

In the first technology, VO_2 based thermo-chromic glazing provides promising improvement for building energy consumption in both hot and cold climates. Thermo-chromic glazing in warmer climates has obviously more advantage than in cold climates since the glazing helps to reduce cooling load by filtering solar energy. In warmer climates, San Diego and Phoenix, it is observed 42% and 29% energy consumption improvement, respectively. The improvement is obtained at the transition temperature of 35 °C which is the middle of chosen three 25 °C, 35 °C, 45 °C. However, in cold climates, Chicago and Minneapolis, the highest energy consumption improvements 19% and 17% respectively, are observed with the transition temperature of 25 °C . Therefore, it is observed that the optimal transition temperature depends on the climate conditions

and increases with decreasing latitude.

In the second technology, VO_2 based thin thermo-chromic coatings have a great potential for energy performance while maintaining visual comfort for occupants in buildings. Overall, energy performance improvement of 26%, 25% and 21% in Izmir and 17%, 13% and 6% in Istanbul is obtained for TC-25, TC-35 and TC-45, respectively. Besides, even if there is a low energy performance improvement of 9%, 6% and 2% in Ankara for TC-25, TC-35 and TC-45, respectively, thermo-chromic coating gives promising result especially for low transition temperatures and hot climates for energy performance. However, coating features such as thickness and concentration should be determined according to transition temperature and climatic condition of the applied environment. In temperate and cold climates, it is observed that thickness of coating should be increased while lowering the transition temperature, but in hot climates, thickness of the coating becomes more important, as thickness does not vary proportionally with transition temperature.

For all cases of transition temperatures and climates that are investigated, the lowest energy consumption is observed at the illuminance constraint criteria region. As a result of decreasing visible transmittance, the both first and second technology consume more lighting energy than ordinary glass in all cases. This is the expected drawback of using thermo-chromic technology instead of ordinary double glazing. However, all thermo-chromic cases show more uniform results as none of the optimal cases results daylight illuminance brighter than 3000 lux for the second technology and negligible for the first technology when compared to double glazing which could eliminate using of window blinds. To conclude, using thermo-chromic systems help to achieve energy efficient buildings by decreasing cooling loads, however; the transition temperature and concentration of used VO_2 should be chosen according to the climate conditions for maximum efficiency.

Consequently, it is observed that adjusting main design variables especially volume fraction according to climatic conditions and transition temperature can increase

the efficiency of thermo-chromic systems. Although lowering the transition temperatures of thermo-chromic glazings improves energy consumption in general, it is observed that this is not the case for all cases investigated. Therefore, individual analyses should be carried out for utilizing thermo-chromic materials with maximum benefit.

5.2. Recommendations for Future Work

Promising outcomes for thermo-chromic glazings and coatings are observed in this theoretical study. As the next step after these promising results, further research should be conducted by producing thermo-chromic glazings and coatings and measuring their properties and effects in similar climatic conditions experimentally.

One of the biggest drawback of thermo-chromic coatings for practical usage is their aesthetic. Although there are great efforts to obtain thermo-chromic coatings that have more pleasant color to human eye, VO_2 nano-particles cause yellowish color in thermo-chromic coatings. Doping W or gold nano-particles into coating can transform the color of thermo-chromic coating to a more pleasant color for some extent, but both these techniques need to be developed and alternative solutions should be sought for improving their aesthetic.

Manufacturing techniques should be focused for both VO_2 nano-particle embedded glazings and thin VO_2 thermo-chromic coatings, because concentration of VO_2 nano-particles and thickness of coating have a direct connection with energy consumption as seen in this study. Therefore, manufacturing techniques that can capable of producing precise VO_2 nano-particle concentrations and thicknesses should be developed for mass production for high efficient thermo-chromic systems. Besides, it should be taken into account that the manufacturing techniques for mass production need to be capable of producing durable thin thermo-chromic coatings with large surface area such as the surface area of an ordinargy glass.

REFERENCES

1. Pachauri, R. K., M. R. Allen, V. R. Barros, J. Broome, W. Cramer, R. Christ, J. A. Church, L. Clarke, Q. Dahe, P. Dasgupta *et al.*, *Climate change 2014: synthesis report. Contribution of Working Groups I, II and III to the fifth assessment report of the Intergovernmental Panel on Climate Change*, Ipcc, 2014.

2. Nations, U., *The Sustainable Development Goals Report 2020*, United Nations, 2020.

3. AA.VV. (IEA), *Transition to Sustainable Buildings*, IEA, 2013, `https://www.iea.org/reports/transition-to-sustainable-buildings`, accessed in May 2021.

4. Ye, H., X. Meng and B. Xu, "Theoretical discussions of perfect window, ideal near infrared solar spectrum regulating window and current thermochromic window", *Energy and Buildings*, Vol. 49, pp. 164 – 172, 2012.

5. Richter, B., D. Goldston, G. Crabtree, L. Glicksman, D. Goldstein, D. Greene, D. Kammen, M. Levine, M. Lubell, M. Savitz, D. Sperling, F. Schlachter, J. Scofield and J. Dawson, "How America can look within to achieve energy security and reduce global warming", *Rev. Mod. Phys.*, Vol. 80, pp. S1–S109, Dec 2008.

6. Chen, H., W. Lee and X. Wang, "Energy assessment of office buildings in China using China building energy codes and LEED 2.2", *Energy and Buildings*, Vol. 86, pp. 514 – 524, 2015.

7. Liang, R., Y. Sun, M. Aburas, R. Wilson and Y. Wu, "Evaluation of the thermal and optical performance of thermochromic windows for office buildings in China", *Energy and Buildings*, Vol. 176, pp. 216 – 231, 2018.

8. Baetens, R., B. P. Jelle and A. Gustavsen, "Properties, requirements and possibil-

ities of smart windows for dynamic daylight and solar energy control in buildings: A state-of-the-art review", *Solar Energy Materials and Solar Cells*, Vol. 94, No. 2, pp. 87–105, 2010.

9. Hoffmann, S., E. S. Lee and C. Clavero, "Examination of the technical potential of near-infrared switching thermochromic windows for commercial building applications", *Solar Energy Materials and Solar Cells*, Vol. 123, pp. 65 – 80, 2014.

10. Morin, F. J., "Oxides Which Show a Metal-to-Insulator Transition at the Neel Temperature", *Phys. Rev. Lett.*, Vol. 3, pp. 34–36, Jul 1959.

11. Liu, M., H. Y. Hwang, H. Tao, A. C. Strikwerda, K. Fan, G. R. Keiser, A. J. Sternbach, K. G. West, S. Kittiwatanakul, J. Lu, S. A. Wolf, F. G. Omenetto, X. Zhang, K. A. Nelson and R. D. Averitt, "Terahertz-field-induced insulator-to-metal transition in vanadium dioxide metamaterial", *Nature*, Vol. 487, No. 7407, pp. 345–348, 2012.

12. Borek, M., F. Qian, V. Nagabushnam and R. K. Singh, "Pulsed laser deposition of oriented VO2 thin films on R-cut sapphire substrates", *Applied Physics Letters*, Vol. 63, No. 24, pp. 3288–3290, 1993.

13. Pauli, S. A., R. Herger, P. R. Willmott, E. U. Donev, J. Y. Suh and R. F. Haglund, "X-ray diffraction studies of the growth of vanadium dioxide nanoparticles", *Journal of Applied Physics*, Vol. 102, No. 7, p. 073527, 2007.

14. Burkhardt, W., T. Christmann, B. Meyer, W. Niessner, D. Schalch and A. Scharmann, "W- and F-doped VO2 films studied by photoelectron spectrometry", *Thin Solid Films*, Vol. 345, No. 2, pp. 229 – 235, 1999.

15. Leroy, J., A. Bessaudou, F. Cosset and A. Crunteanu, "Structural, electrical and optical properties of thermochromic VO2 thin films obtained by reactive electron beam evaporation", *Thin Solid Films*, Vol. 520, No. 14, pp. 4823 – 4825, 2012.

16. Théry, V., A. Boulle, A. Crunteanu, J. C. Orlianges, A. Beaumont, R. Mayet, A. Mennai, F. Cosset, A. Bessaudou and M. Fabert, "Structural and electrical properties of large area epitaxial VO2 films grown by electron beam evaporation", *Journal of Applied Physics*, Vol. 121, No. 5, p. 055303, 2017.

17. Marvel, R., K. Appavoo, B. Choi, J. Nag and R. Haglund, "Electron-beam deposition of vanadium dioxide thin films", *Applied Physics A*, Vol. 111, No. 3, pp. 975–981, 2013.

18. Chae, B.-G., H.-T. Kim, S.-J. Yun, B.-J. Kim, Y.-W. Lee, D.-H. Youn and K.-Y. Kang, "Highly Oriented VO2 Thin Films Prepared by Sol-Gel Deposition", *Electrochemical and Solid-State Letters*, Vol. 9, No. 1, p. C12, 2006.

19. Malarde, D., M. J. Powell, R. Quesada-Cabrera, R. L. Wilson, C. J. Carmalt, G. Sankar, I. P. Parkin and R. G. Palgrave, "Optimized Atmospheric-Pressure Chemical Vapor Deposition Thermochromic VO2 Thin Films for Intelligent Window Applications", *ACS Omega*, Vol. 2, No. 3, pp. 1040–1046, 2017.

20. Parkin, I. P., R. Binions, C. Piccirillo, C. S. Blackman and T. D. Manning, "Thermochromic Coatings for Intelligent Architectural Glazing", *Journal of Nano Research*, Vol. 2, pp. 1–20, 6 2008.

21. Li, S.-Y., G. Niklasson and C. Granqvist, "Thermochromic fenestration with VO2-based materials: Three challenges and how they can be met", *Thin Solid Films*, Vol. 520, No. 10, pp. 3823 – 3828, 2012.

22. Tazawa, M., P. Jin and S. Tanemura, "Optical constants of V1-xWxO2 films", *Appl. Opt.*, Vol. 37, No. 10, pp. 1858–1861, Apr 1998.

23. Mlyuka, N. R., G. A. Niklasson and C. G. Granqvist, "Mg doping of thermochromic VO2 films enhances the optical transmittance and decreases the metal-insulator transition temperature", *Applied Physics Letters*, Vol. 95, No. 17, p. 171909, 2009.

24. Li, S.-Y., G. A. Niklasson and C. G. Granqvist, "Nanothermochromics: Calculations for VO2 nanoparticles in dielectric hosts show much improved luminous transmittance and solar energy transmittance modulation", *Journal of Applied Physics*, Vol. 108, No. 6, p. 063525, 2010.

25. Laaksonen, K., S.-Y. Li, S. Puisto, N. Rostedt, T. Ala-Nissila, C. Granqvist, R. Nieminen and G. Niklasson, "Nanoparticles of TiO2 and VO2 in dielectric media: Conditions for low optical scattering, and comparison between effective medium and four-flux theories", *Solar Energy Materials and Solar Cells*, Vol. 130, pp. 132 – 137, 2014.

26. Ji, S., F. Zhang and P. Jin, "Preparation of high performance pure single phase VO2 nanopowder by hydrothermally reducing the V2O5 gel", *Solar Energy Materials and Solar Cells*, Vol. 95, No. 12, pp. 3520 – 3526, 2011.

27. Xu, G., P. Jin, M. Tazawa and K. Yoshimura, "Thickness dependence of optical properties of VO2 thin films epitaxially grown on sapphire (0001)", *Applied Surface Science*, Vol. 244, No. 1, pp. 449 – 452, 2005.

28. Gagaoudakis, E., E. Aperathitis, G. Michail, M. Panagopoulou, D. Katerinopoulou, V. Binas, Y. Raptis and G. Kiriakidis, "Low-temperature rf sputtered VO2 thin films as thermochromic coatings for smart glazing systems", *Solar Energy*, Vol. 165, pp. 115 – 121, 2018.

29. Kolenaty, D., J. Houska and J. Vlcek, "Improved performance of thermochromic VO2/SiO2 coatings prepared by low-temperature pulsed reactive magnetron sputtering: Prediction and experimental verification", *Journal of Alloys and Compounds*, Vol. 767, pp. 46 – 51, 2018.

30. Blackman, C. S., C. Piccirillo, R. Binions and I. P. Parkin, "Atmospheric pressure chemical vapour deposition of thermochromic tungsten doped vanadium dioxide thin films for use in architectural glazing", *Thin Solid Films*, Vol. 517, No. 16, pp.

4565 – 4570, 2009.

31. Saeli, M., C. Piccirillo, I. P. Parkin, R. Binions and I. Ridley, "Energy modelling studies of thermochromic glazing", *Energy and Buildings*, Vol. 42, No. 10, pp. 1666 – 1673, 2010.

32. Ye, H., L. Long, H. Zhang, B. Xu, Y. Gao, L. Kang and Z. Chen, "The demonstration and simulation of the application performance of the vanadium dioxide single glazing", *Solar Energy Materials and Solar Cells*, Vol. 117, pp. 168 – 173, 2013.

33. Costanzo, V., G. Evola and L. Marletta, "Thermal and visual performance of real and theoretical thermochromic glazing solutions for office buildings", *Solar Energy Materials and Solar Cells*, Vol. 149, pp. 110 – 120, 2016.

34. Nielsen, L. E., "The permittivity of suspensions and two-phase mixtures", *Journal of Physics D: Applied Physics*, Vol. 7, No. 11, pp. 1549–1554, jul 1974.

35. Garnett, J. C. M. and J. Larmor, "XII. Colours in metal glasses and in metallic films", *Philosophical Transactions of the Royal Society of London. Series A, Containing Papers of a Mathematical or Physical Character*, Vol. 203, No. 359-371, pp. 385–420, 1904.

36. Bruggeman, D. A. G., "Berechnung verschiedener physikalischer Konstanten von heterogenen Substanzen. I. Dielektrizitätskonstanten und Leitfähigkeiten der Mischkörper aus isotropen Substanzen", *Annalen der Physik*, Vol. 416, No. 7, pp. 636–664, 1935.

37. Niklasson, G. and C. Granqvist, "Effective Medium Models for the Optical-Properties of Inhomogeneous Materials", *Applied Optics*, Vol. 20, pp. 26–30, 01 1981.

38. Monsalve-Bravo, G. M. and S. K. Bhatia, "Extending effective medium theory to finite size systems: Theory and simulation for permeation in mixed-matrix mem-

branes", *Journal of Membrane Science*, Vol. 531, pp. 148–159, 2017.

39. Yalçın, R. A. and H. Ertürk, "Inverse Design of Spectrally Selective Thickness Sensitive Pigmented Coatings for Solar Thermal Applications", *Journal of Solar Energy Engineering*, Vol. 140, No. 3, 02 2018, 031006.

40. Bohren, C. F. and D. R. Huffman, *Absorption and Scattering of Light by Small Particles*, John Wiley & Sons, 1998.

41. Maheu, B., J. N. Letoulouzan and G. Gouesbet, "Four-flux models to solve the scattering transfer equation in terms of Lorenz-Mie parameters", *Appl. Opt.*, Vol. 23, No. 19, pp. 3353–3362, Oct 1984.

42. Etherden, N., T. Tesfamichael, G. A. Niklasson and E. Wäckelgård, "A theoretical feasibility study of pigments for thickness-sensitive spectrally selective paints", *Journal of Physics D: Applied Physics*, Vol. 37, No. 7, pp. 1115–1122, mar 2004.

43. *Optimization of Pigmented Coatings for Concentrating Solar Thermal Applications*, Vol. Volume 4: Energy Systems Analysis, Thermodynamics and Sustainability; Combustion Science and Engineering; Nanoengineering for Energy, Parts A and B of *ASME International Mechanical Engineering Congress and Exposition*, 11 2011.

44. Howell, J. R., M. P. Mengüç, K. Daun and R. Siegel, *Thermal radiation heat transfer*, CRC press, 2020.

45. Pascoe, K. J., *Reflectivity and transmissivity through layered, lossy media: a user-friendly approach*, Tech. rep., Air Force Institute of Technology Wright-Patterson Air Force Base OH School Of Engineering, 2001.

46. ASTM International, "ASTM Standard Reference Spectra G173-03", *ASTM*, 2012.

47. Wyszecki, G. and W. Stiles, *Color Science: Concepts and Methods, Quantitative*

Data and Formulae, 2nd Edition, Wiley, Jul 2000.

48. Doe, U. D. o. E., *EnergyPlus Energy Simulation Software*, 2013.

49. Crawley, D. B., L. K. Lawrie, F. C. Winkelmann, W. Buhl, Y. Huang, C. O. Pedersen, R. K. Strand, R. J. Liesen, D. E. Fisher, M. J. Witte and J. Glazer, "EnergyPlus: creating a new-generation building energy simulation program", *Energy and Buildings*, Vol. 33, No. 4, pp. 319 – 331, 2001.

50. EnergyPlus, *EnergyPlus-Engineering Reference*, 2016.

51. National Renewable Energy Laboratory (NREL), *EnergyPlus Weather Data*, 2019.

52. U.S. Department of Energy - DOE, *OpenStudio*, 2011.

53. Committee, A. S. *et al.*, *ANSI/ASHRAE/IES Standard 90.1-2010: Energy Standard for Buildings Except Low-rise Residential Buildings*, 2010.

54. Ochoa, C. E., M. B. Aries, E. J. van Loenen and J. L. Hensen, "Considerations on design optimization criteria for windows providing low energy consumption and high visual comfort", *Applied Energy*, Vol. 95, pp. 238 – 245, 2012.

55. Institute, T. S., *Thermal insulation requirements for buildings (TS-825)*, 2008.

56. Institute, T. S., *Thermal insulation requirements for buildings (TS-825)*, 2013.

57. Institute, T. S., *The Results of Address Based Population Registration System, 2020*, Feb. 2021, `https://data.tuik.gov.tr/Bulten/Index?p=The-Results-of-Address-Based-Population-Registration-System-2020-37210`, accessed in May 2021.

58. Dino, I. G. and C. Meral Akgül, "Impact of climate change on the existing residential building stock in Turkey: An analysis on energy use, greenhouse gas emissions

and occupant comfort", *Renewable Energy*, Vol. 141, pp. 828 – 846, 2019.

59. Society, I. E., *American National Standard Practice for Office Lighting (ANSI/IES RP-1-12)*, Illuminating Engineering Society of North America, 2013, `https://webstore.ansi.org/standards/iesna/ansiiesnarp12`.

60. Technical Committee CEN/TC 169 "Light and Lighting", "Light and lighting - Lighting of work places - Part 1 : Indoor work", *European Standard*, 2002.

61. Nabil, A. and J. Mardaljevic, "Useful daylight illuminances: A replacement for daylight factors", *Energy and Buildings*, Vol. 38, No. 7, pp. 905 – 913, 2006.

62. Mardaljevic, J., M. Andersen, N. Roy and J. Christoffersen, "Daylighting metrics: is there a relation between useful daylight illuminance and daylight glare probabilty?", *Proceedings of the building simulation and optimization conference BSO12*, CONF, 2012.

63. Osterhaus, W. K., "Discomfort glare assessment and prevention for daylight applications in office environments", *Solar Energy*, Vol. 79, No. 2, pp. 140–158, 2005.

64. Wienold, J. and J. Christoffersen, "Evaluation methods and development of a new glare prediction model for daylight environments with the use of CCD cameras", *Energy and Buildings*, Vol. 38, No. 7, pp. 743–757, 2006.

65. Hopkinson, R., "Glare from daylighting in buildings", *Applied Ergonomics*, Vol. 3, No. 4, pp. 206–215, 1972.

66. Zhao, L., E. Strobach, B. Bhatia, S. Yang, A. Leroy, L. Zhang and E. N. Wang, "Theoretical and experimental investigation of haze in transparent aerogels", *Opt. Express*, Vol. 27, No. 4, pp. A39–A50, Feb 2019.

APPENDIX A: VERIFICATION RESULTS FOR FOUR FLUX METHOD

Optical properties of thermo-chromic coating are calculated by using the same configurations of Laaksonen *et al.* [25] to verify the accuracy of four flux method. In addition, optical properties are calculated by Monte-Carlo method to be more sure of the accuracy. Transmittance result of one of the configurations that is 5 nm as nano-particle radius, 0.01 as volume fraction and 10 µm as thickness can be observed according to calculations by four flux method and Monte-Carlo method in Figure A.1.

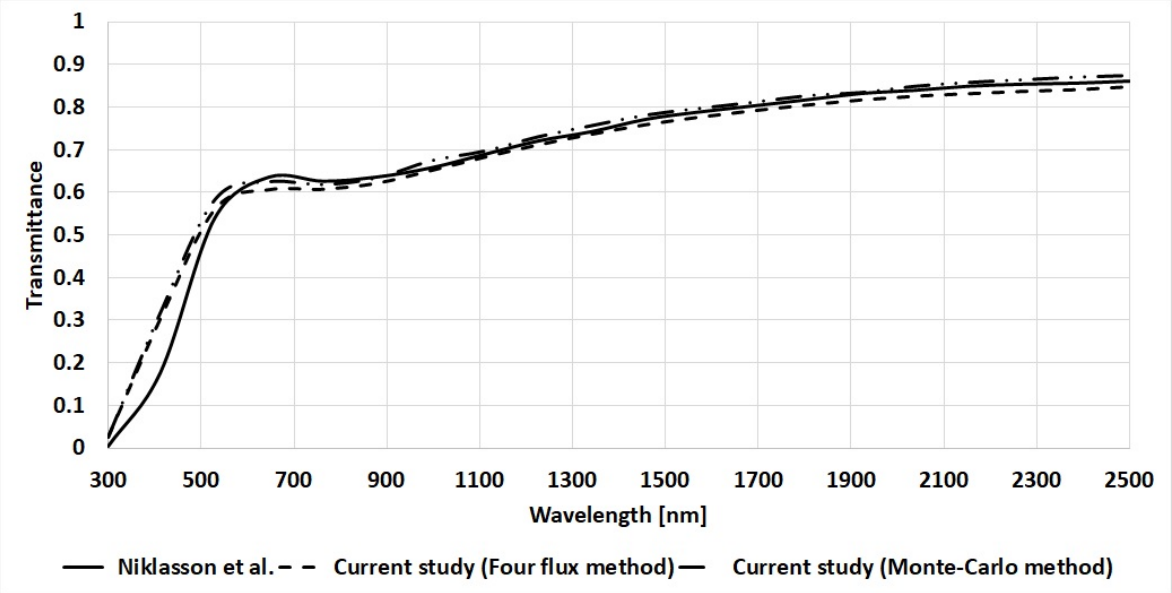


Figure A.1. Comparison of transmittance results for four flux method verification.

APPENDIX B: VERIFICATION RESULTS FOR TRANSFER MATRIX METHOD

Optical properties of thermo-chromic coating are calculated by Monte-Carlo method and transfer matrix method according to three different configurations to verify the correctness of transfer matrix method. Transmittance result of one of the configurations that is 0.43 as volume fraction and 134 nm as thickness can be observed according to calculations by transfer matrix method and Monte-Carlo method in Figure B.1.

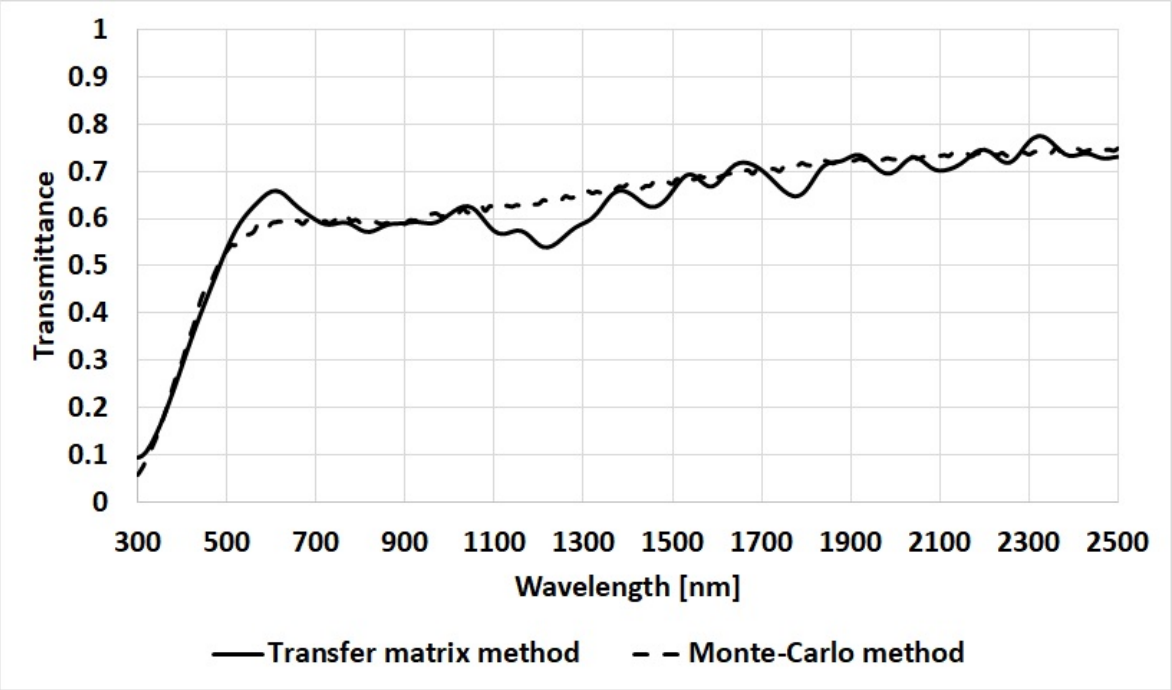


Figure B.1. Comparison of transmittance results for transfer matrix method verification.

APPENDIX C: VERIFICATION RESULTS FOR BUILDING ENERGY ANALYSIS

Saeli *et al.* [31] examined four different thermo-chromic coatings with different properties for energy performance in a simple office room. The total energy consumption that is taken from the study of Saeli *et al.* [31] and the total energy consumption is calculated by using the created model of this study for verification can be observed in Figure C.1. Thermo-chromic coating 1, thermo-chromic coating 2, thermo-chromic coating 3 and thermo-chromic coating 4 of Saeli *et al.* [31] are referred as TC-1, TC-2, TC-3 and TC-4 in this study as seen in Figure C.1.

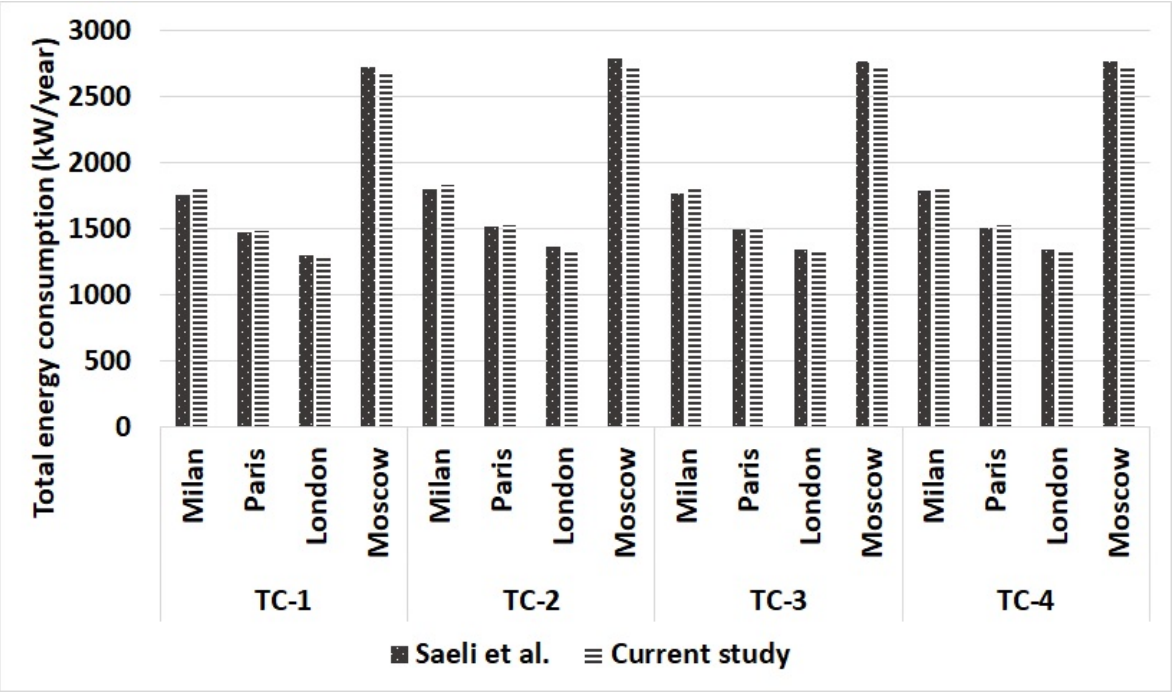


Figure C.1. Comparison of total energy consumption for verification.

APPENDIX D: SAMPLE INPUT FILE OF ENERGYPLUS

Sample input file, which is according to data of optimal optical properties for transition temperature of 35 °C in Chicago, is provided for EnergyPlus.

```
!-Generator IDFEditor 1.51
!-Option OriginalOrderTop UseSpecialFormat

!-NOTE: All comments with '!-' are ignored by the IDFEditor and are generated
automatically.
!-      Use '!' comments if they need to be retained when using the IDFEditor.

Construction,
    thermo_window_1,         !- Name
    thermo_glazing,          !- Outside Layer
    AIR 12MM,                !- Layer 2
    CLEAR 3MM 1;             !- Layer 3

WindowMaterial:Glazing,
    thermochromic_low,       !- Name
    SpectralAverage,         !- Optical Data Type
    ,                        !- Window Glass Spectral Data Set Name
    0.003,                   !- Thickness {m}
    0.516111,                !- Solar Transmittance at Normal Incidence
    0.066712,                !- Front Side Solar Reflectance at Normal Incidence
    0.066712,                !- Back Side Solar Reflectance at Normal Incidence
    0.486417,                !- Visible Transmittance at Normal Incidence
    0.062800,                !- Front Side Visible Reflectance at Normal Incidence
    0.062800,                !- Back Side Visible Reflectance at Normal Incidence
    0,                       !- Infrared Transmittance at Normal Incidence
    0.84,                    !- Front Side Infrared Hemispherical Emissivity
    0.84,                    !- Back Side Infrared Hemispherical Emissivity
    0.6,                     !- Conductivity {W/m-K}
```

```
    1,                      !- Dirt Correction Factor for Solar and Visible
Transmittance
    No;                     !- Solar Diffusing

WindowMaterial:Glazing,
    thermochromic_high,     !- Name
    SpectralAverage,        !- Optical Data Type
    ,                       !- Window Glass Spectral Data Set Name
    0.003,                  !- Thickness {m}
    0.217854,               !- Solar Transmittance at Normal Incidence
    0.045647,               !- Front Side Solar Reflectance at Normal Incidence
    0.045647,               !- Back Side Solar Reflectance at Normal Incidence
    0.298216,               !- Visible Transmittance at Normal Incidence
    0.048615,               !- Front Side Visible Reflectance at Normal Incidence
    0.048615,               !- Back Side Visible Reflectance at Normal Incidence
    0,                      !- Infrared Transmittance at Normal Incidence
    0.84,                   !- Front Side Infrared Hemispherical Emissivity
    0.84,                   !- Back Side Infrared Hemispherical Emissivity
    0.6,                    !- Conductivity {W/m-K}
    1,                      !- Dirt Correction Factor for Solar and Visible
Transmittance
    No;                     !- Solar Diffusing

WindowMaterial:GlazingGroup:Thermochromic,
    thermo_glazing,         !- Name
    34,                     !- Optical Data Temperature 1 {C}
    thermochromic_low,      !- Window Material Glazing Name 1
    35,                     !- Optical Data Temperature 2 {C}
    thermochromic_high;     !- Window Material Glazing Name 2

Output:Variable,Daylighting Reference Point 1 Glare Index,Hourly;
Output:Variable,Daylighting Reference Point 1 Glare Index Setpoint Exceeded Time,
Hourly;
Output:Variable,Site Outdoor Air Drybulb Temperature,Hourly;
Output:Variable,Zone Air System Sensible Cooling Energy,Hourly;
Output:Variable,Zone Air System Sensible Heating Energy,Hourly;
Output:Variable,Zone Air Temperature,Hourly;
```

```
Output:Variable,Daylighting Reference Point 1 Illuminance,Hourly;
Output:Variable,Surface Window Thermochromic Layer Temperature,Hourly;
Output:Variable,Surface Window Thermochromic Layer Property Specification
Temperature,Hourly;
Output:Variable,Surface Window Transmitted Solar Radiation Rate,Hourly;
Output:Variable,Zone Ideal Loads Supply Air Total Cooling Energy,Hourly;
Output:Variable,Zone Ideal Loads Supply Air Sensible Heating Energy,Hourly;
Output:Variable,Lights Electric Energy,Hourly;
Output:Variable,Daylighting Reference Point 2 Glare Index,Hourly;
Output:Variable,Daylighting Reference Point 2 Glare Index Setpoint Exceeded Time,
Hourly;
Output:Variable,Daylighting Reference Point 2 Illuminance,Hourly;
Version,9.3;
Timestep,20;

Building,
    closed office,             !- Name
    ,                         !- North Axis {deg}
    ,                         !- Terrain
    ,                         !- Loads Convergence Tolerance Value {W}
    ,                         !- Temperature Convergence Tolerance Value {deltaC}
    ,                         !- Solar Distribution
    ,                         !- Maximum Number of Warmup Days
    ;                         !- Minimum Number of Warmup Days

Zone,
    Thermal Zone: closed office,  !- Name
    -0,                       !- Direction of Relative North {deg}
    0, 0, 0;                              !- X,Y,Z  {m}

BuildingSurface:Detailed,
    east_wall,                !- Name
    Wall,                     !- Surface Type
    Interior Wall,            !- Construction Name
    Thermal Zone: closed office,  !- Zone Name
    Adiabatic,                !- Outside Boundary Condition
    ,                         !- Outside Boundary Condition Object
```

```
    NoSun,                  !- Sun Exposure
    NoWind,                 !- Wind Exposure
    ,                       !- View Factor to Ground
    ,                       !- Number of Vertices
    5, 0, 3,                        !- X,Y,Z  1 {m}
    5, 0, 0,                        !- X,Y,Z  2 {m}
    5, 6, 0,                        !- X,Y,Z  3 {m}
    5, 6, 3;                        !- X,Y,Z  4 {m}

BuildingSurface:Detailed,
    floor_down,             !- Name
    Floor,                  !- Surface Type
    ExtSlabCarpet 4in ClimateZone 1-8,  !- Construction Name
    Thermal Zone: closed office,  !- Zone Name
    Adiabatic,              !- Outside Boundary Condition
    ,                       !- Outside Boundary Condition Object
    NoSun,                  !- Sun Exposure
    NoWind,                 !- Wind Exposure
    ,                       !- View Factor to Ground
    ,                       !- Number of Vertices
    5, 6, 0,                        !- X,Y,Z  1 {m}
    5, 0, 0,                        !- X,Y,Z  2 {m}
    0, 0, 0,                        !- X,Y,Z  3 {m}
    0, 6, 0;                        !- X,Y,Z  4 {m}

BuildingSurface:Detailed,
    roof_up,                !- Name
    Ceiling,                !- Surface Type
    ASHRAE 90.1-2010 ExtRoof IEAD ClimateZone 2-8,  !- Construction Name
    Thermal Zone: closed office,  !- Zone Name
    Adiabatic,              !- Outside Boundary Condition
    ,                       !- Outside Boundary Condition Object
    NoSun,                  !- Sun Exposure
    NoWind,                 !- Wind Exposure
    ,                       !- View Factor to Ground
    ,                       !- Number of Vertices
    5, 0, 3,                        !- X,Y,Z  1 {m}
```

```
    5, 6, 3,                                !- X,Y,Z  2 {m}
    0, 6, 3,                                !- X,Y,Z  3 {m}
    0, 0, 3;                                !- X,Y,Z  4 {m}

BuildingSurface:Detailed,
    south_wall,             !- Name
    Wall,                   !- Surface Type
    ASHRAE 90.1-2010 ExtWall Mass ClimateZone 3,  !- Construction Name
    Thermal Zone: closed office,  !- Zone Name
    Outdoors,               !- Outside Boundary Condition
    ,                       !- Outside Boundary Condition Object
    SunExposed,             !- Sun Exposure
    WindExposed,            !- Wind Exposure
    ,                       !- View Factor to Ground
    ,                       !- Number of Vertices
    0, 0, 3,                                !- X,Y,Z  1 {m}
    0, 0, 0,                                !- X,Y,Z  2 {m}
    5, 0, 0,                                !- X,Y,Z  3 {m}
    5, 0, 3;                                !- X,Y,Z  4 {m}

FenestrationSurface:Detailed,
    south_window,           !- Name
    Window,                 !- Surface Type
    thermo_window_1,        !- Construction Name
    south_wall,             !- Building Surface Name
    ,                       !- Outside Boundary Condition Object
    ,                       !- View Factor to Ground
    ,                       !- Frame and Divider Name
    ,                       !- Multiplier
    ,                       !- Number of Vertices
    0.5, 0, 2.5,                            !- X,Y,Z  1 {m}
    0.5, 0, 0.5,                            !- X,Y,Z  2 {m}
    4.5, 0, 0.5,                            !- X,Y,Z  3 {m}
    4.5, 0, 2.5;                            !- X,Y,Z  4 {m}

BuildingSurface:Detailed,
    wall_north,             !- Name
```

```
    Wall,                   !- Surface Type
    Interior Wall,          !- Construction Name
    Thermal Zone: closed office,  !- Zone Name
    Adiabatic,              !- Outside Boundary Condition
    ,                       !- Outside Boundary Condition Object
    NoSun,                  !- Sun Exposure
    NoWind,                 !- Wind Exposure
    ,                       !- View Factor to Ground
    ,                       !- Number of Vertices
    5, 6, 3,                          !- X,Y,Z  1 {m}
    5, 6, 0,                          !- X,Y,Z  2 {m}
    0, 6, 0,                          !- X,Y,Z  3 {m}
    0, 6, 3;                          !- X,Y,Z  4 {m}

BuildingSurface:Detailed,
    west_wall,              !- Name
    Wall,                   !- Surface Type
    Interior Wall,          !- Construction Name
    Thermal Zone: closed office,  !- Zone Name
    Adiabatic,              !- Outside Boundary Condition
    ,                       !- Outside Boundary Condition Object
    NoSun,                  !- Sun Exposure
    NoWind,                 !- Wind Exposure
    ,                       !- View Factor to Ground
    ,                       !- Number of Vertices
    0, 6, 3,                          !- X,Y,Z  1 {m}
    0, 6, 0,                          !- X,Y,Z  2 {m}
    0, 0, 0,                          !- X,Y,Z  3 {m}
    0, 0, 3;                          !- X,Y,Z  4 {m}

Daylighting:Controls,
    Thermal Zone: closed office DaylightingControls,  !- Name
    Thermal Zone: closed office,  !- Zone Name
    ,                       !- Daylighting Method
    ,                       !- Availability Schedule Name
    Continuous,             !- Lighting Control Type
    0.1,                    !- Minimum Input Power Fraction for Continuous or
```

```
ContinuousOff Dimming Control
    0.1,                    !- Minimum Light Output Fraction for Continuous or
ContinuousOff Dimming Control
    ,                       !- Number of Stepped Control Steps
    ,                       !- Probability Lighting will be Reset When Needed
in Manual Stepped Control
    Daylighting Control 1,  !- Glare Calculation Daylighting Reference Point Name
    180,                    !- Glare Calculation Azimuth Angle of View Direction
Clockwise from Zone y-Axis {deg}
    22,                     !- Maximum Allowable Discomfort Glare Index
    ,                       !- DElight Gridding Resolution {m2}
    Daylighting Control 1,  !- Daylighting Reference Point 1 Name
    0,                      !- Fraction of Zone Controlled by Reference Point 1
    ,                       !- Illuminance Setpoint at Reference Point 1 {lux}
    Daylighting Control 2,  !- Daylighting Reference Point 2 Name
    1,                      !- Fraction of Zone Controlled by Reference Point 2
    500;                    !- Illuminance Setpoint at Reference Point 2 {lux}

Daylighting:ReferencePoint,
    Daylighting Control 1,  !- Name
    Thermal Zone: closed office,  !- Zone Name
    2.5,                    !- X-Coordinate of Reference Point {m}
    1.5,                    !- Y-Coordinate of Reference Point {m}
    0.8;                    !- Z-Coordinate of Reference Point {m}

Daylighting:ReferencePoint,
    Daylighting Control 2,  !- Name
    Thermal Zone: closed office,  !- Zone Name
    2.5,                    !- X-Coordinate of Reference Point {m}
    4.5,                    !- Y-Coordinate of Reference Point {m}
    0.8;                    !- Z-Coordinate of Reference Point {m}

ZoneControl:Thermostat,
    Thermal Zone: closed office Thermostat,  !- Name
    Thermal Zone: closed office,  !- Zone or ZoneList Name
    Thermal Zone: closed office Thermostat Schedule,  !- Control Type Schedule Name
    ThermostatSetpoint:DualSetpoint,  !- Control 1 Object Type
```

```
    Thermostat Setpoint Dual Setpoint 1;  !- Control 1 Name

Schedule:Compact,
    Thermal Zone: closed office Thermostat Schedule,  !- Name
    Thermal Zone: closed office Thermostat Schedule Type Limits,  !- Schedule Type
Limits Name
    Through: 12/31,          !- Field 1
    For: AllDays,            !- Field 2
    Until: 24:00, 4;         !- Field 4

ScheduleTypeLimits,
    Thermal Zone: closed office Thermostat Schedule Type Limits,  !- Name
    0,                       !- Lower Limit Value
    4,                       !- Upper Limit Value
    DISCRETE;                !- Numeric Type

ThermostatSetpoint:DualSetpoint,
    Thermostat Setpoint Dual Setpoint 1,  !- Name
    Medium Office HtgSetp,   !- Heating Setpoint Temperature Schedule Name
    Medium Office ClgSetp;   !- Cooling Setpoint Temperature Schedule Name

ScheduleTypeLimits,
    Temperature 36,          !- Name
    ,                        !- Lower Limit Value
    ,                        !- Upper Limit Value
    Continuous,              !- Numeric Type
    temperature;             !- Unit Type

Schedule:Day:Interval,
    Medium Office HtgSetp Rule 1 Day Schedule,  !- Name
    Temperature 36,          !- Schedule Type Limits Name
    No,                      !- Interpolate to Timestep
    24:00,                   !- Time 1 {hh:mm}
    0;                       !- Value Until Time 1

Schedule:Day:Interval,
    Medium Office HtgSetp Default Schedule,  !- Name
```

```
    Temperature 36,          !- Schedule Type Limits Name
    No,                      !- Interpolate to Timestep
    08:00,                   !- Time 1 {hh:mm}
    0,                       !- Value Until Time 1
    17:00,                   !- Time 2 {hh:mm}
    21,                      !- Value Until Time 2
    24:00,                   !- Time 3 {hh:mm}
    0;                       !- Value Until Time 3

Schedule:Day:Interval,
    Medium Office HtgSetp Rule 2 Day Schedule,  !- Name
    Temperature 36,          !- Schedule Type Limits Name
    No,                      !- Interpolate to Timestep
    24:00,                   !- Time 1 {hh:mm}
    0;                       !- Value Until Time 1

Schedule:Week:Daily,
    Medium Office HtgSetp Week Rule - Jan1-Dec31,  !- Name
    Medium Office HtgSetp Rule 1 Day Schedule,  !- Sunday Schedule:Day Name
    Medium Office HtgSetp Default Schedule,  !- Monday Schedule:Day Name
    Medium Office HtgSetp Default Schedule,  !- Tuesday Schedule:Day Name
    Medium Office HtgSetp Default Schedule,  !- Wednesday Schedule:Day Name
    Medium Office HtgSetp Default Schedule,  !- Thursday Schedule:Day Name
    Medium Office HtgSetp Default Schedule,  !- Friday Schedule:Day Name
    Medium Office HtgSetp Rule 2 Day Schedule,  !- Saturday Schedule:Day Name
    Medium Office HtgSetp Default Schedule,  !- Holiday Schedule:Day Name
    Medium Office HtgSetp Summer Design Day,  !- SummerDesignDay Schedule:Day Name
    Medium Office HtgSetp Winter Design Day,  !- WinterDesignDay Schedule:Day Name
    Medium Office HtgSetp Default Schedule,  !- CustomDay1 Schedule:Day Name
    Medium Office HtgSetp Default Schedule;  !- CustomDay2 Schedule:Day Name

Schedule:Year,
    Medium Office HtgSetp,   !- Name
    Temperature 36,          !- Schedule Type Limits Name
    Medium Office HtgSetp Week Rule - Jan1-Dec31,  !- Schedule:Week Name 1
    1,                       !- Start Month 1
    1,                       !- Start Day 1
```

```
    12,                       !- End Month 1
    31;                       !- End Day 1

Schedule:Day:Interval,
    Medium Office HtgSetp Summer Design Day,  !- Name
    Temperature 36,           !- Schedule Type Limits Name
    No,                       !- Interpolate to Timestep
    24:00,                    !- Time 1 {hh:mm}
    0;                        !- Value Until Time 1

Schedule:Day:Interval,
    Medium Office HtgSetp Winter Design Day,  !- Name
    Temperature 36,           !- Schedule Type Limits Name
    No,                       !- Interpolate to Timestep
    24:00,                    !- Time 1 {hh:mm}
    21;                       !- Value Until Time 1

ScheduleTypeLimits,
    Temperature 37,           !- Name
    ,                         !- Lower Limit Value
    ,                         !- Upper Limit Value
    Continuous,               !- Numeric Type
    temperature;              !- Unit Type

Schedule:Day:Interval,
    Medium Office ClgSetp Rule 1 Day Schedule,  !- Name
    Temperature 37,           !- Schedule Type Limits Name
    No,                       !- Interpolate to Timestep
    24:00,                    !- Time 1 {hh:mm}
    60;                       !- Value Until Time 1

Schedule:Day:Interval,
    Medium Office ClgSetp Default Schedule,  !- Name
    Temperature 37,           !- Schedule Type Limits Name
    No,                       !- Interpolate to Timestep
    08:00,                    !- Time 1 {hh:mm}
    60,                       !- Value Until Time 1
```

```
    17:00,                  !- Time 2 {hh:mm}
    24,                     !- Value Until Time 2
    24:00,                  !- Time 3 {hh:mm}
    60;                     !- Value Until Time 3

Schedule:Day:Interval,
    Medium Office ClgSetp Rule 2 Day Schedule,  !- Name
    Temperature 37,         !- Schedule Type Limits Name
    No,                     !- Interpolate to Timestep
    24:00,                  !- Time 1 {hh:mm}
    60;                     !- Value Until Time 1

Schedule:Week:Daily,
    Medium Office ClgSetp Week Rule - Jan1-Dec31,  !- Name
    Medium Office ClgSetp Rule 1 Day Schedule,  !- Sunday Schedule:Day Name
    Medium Office ClgSetp Default Schedule,  !- Monday Schedule:Day Name
    Medium Office ClgSetp Default Schedule,  !- Tuesday Schedule:Day Name
    Medium Office ClgSetp Default Schedule,  !- Wednesday Schedule:Day Name
    Medium Office ClgSetp Default Schedule,  !- Thursday Schedule:Day Name
    Medium Office ClgSetp Default Schedule,  !- Friday Schedule:Day Name
    Medium Office ClgSetp Rule 2 Day Schedule,  !- Saturday Schedule:Day Name
    Medium Office ClgSetp Default Schedule,  !- Holiday Schedule:Day Name
    Medium Office ClgSetp Summer Design Day,  !- SummerDesignDay Schedule:Day Name
    Medium Office ClgSetp Winter Design Day,  !- WinterDesignDay Schedule:Day Name
    Medium Office ClgSetp Default Schedule,  !- CustomDay1 Schedule:Day Name
    Medium Office ClgSetp Default Schedule;  !- CustomDay2 Schedule:Day Name

Schedule:Year,
    Medium Office ClgSetp,  !- Name
    Temperature 37,         !- Schedule Type Limits Name
    Medium Office ClgSetp Week Rule - Jan1-Dec31,  !- Schedule:Week Name 1
    1,                      !- Start Month 1
    1,                      !- Start Day 1
    12,                     !- End Month 1
    31;                     !- End Day 1

Schedule:Day:Interval,
```

```
    Medium Office ClgSetp Summer Design Day,  !- Name
    Temperature 37,          !- Schedule Type Limits Name
    No,                      !- Interpolate to Timestep
    08:00,                   !- Time 1 {hh:mm}
    60,                      !- Value Until Time 1
    17:00,                   !- Time 2 {hh:mm}
    24,                      !- Value Until Time 2
    24:00,                   !- Time 3 {hh:mm}
    60;                      !- Value Until Time 3

Schedule:Day:Interval,
    Medium Office ClgSetp Winter Design Day,  !- Name
    Temperature 37,          !- Schedule Type Limits Name
    No,                      !- Interpolate to Timestep
    24:00,                   !- Time 1 {hh:mm}
    60;                      !- Value Until Time 1

!
! HVACTemplate:Zone:IdealLoadsAirSystem,
!     Thermal Zone: closed office,  !- Zone Name
!     ,                         !- Template Thermostat Name
!     ,                         !- System Availability Schedule Name
!     ,                         !- Maximum Heating Supply Air Temperature {C}
!     ,                         !- Minimum Cooling Supply Air Temperature {C}
!     ,                         !- Maximum Heating Supply Air Humidity Ratio
{kgWater/kgDryAir}
!     ,                         !- Minimum Cooling Supply Air Humidity Ratio
{kgWater/kgDryAir}
!     ,                         !- Heating Limit
!     ,                         !- Maximum Heating Air Flow Rate {m3/s}
!     ,                         !- Maximum Sensible Heating Capacity {W}
!     ,                         !- Cooling Limit
!     ,                         !- Maximum Cooling Air Flow Rate {m3/s}
!     ,                         !- Maximum Total Cooling Capacity {W}
!     ,                         !- Heating Availability Schedule Name
!     ,                         !- Cooling Availability Schedule Name
!     ,                         !- Dehumidification Control Type
```

```
!     ,                         !- Cooling Sensible Heat Ratio {dimensionless}
!     ,                         !- Dehumidification Setpoint {percent}
!     ,                         !- Humidification Control Type
!     ,                         !- Humidification Setpoint {percent}
!     ,                         !- Outdoor Air Method
!     ,                         !- Outdoor Air Flow Rate per Person {m3/s}
!     ,                         !- Outdoor Air Flow Rate per Zone Floor Area
{m3/s-m2}
!     ,                         !- Outdoor Air Flow Rate per Zone {m3/s}
!     ,                         !- Design Specification Outdoor Air Object Name
!     ;                         !- Demand Controlled Ventilation Type
Sizing:Zone,
    Thermal Zone: closed office,  !- Zone or ZoneList Name
    SupplyAirTemperature,     !- Zone Cooling Design Supply Air Temperature Input
Method
    12.8,                     !- Zone Cooling Design Supply Air Temperature {C}
    11.11,                    !- Zone Cooling Design Supply Air Temperature
Difference
{deltaC}
    SupplyAirTemperature,     !- Zone Heating Design Supply Air Temperature Input
Method
    32.2,                     !- Zone Heating Design Supply Air Temperature {C}
    11.11,                    !- Zone Heating Design Supply Air Temperature
Difference
{deltaC}
    0.0085,                   !- Zone Cooling Design Supply Air Humidity Ratio
{kgWater/kgDryAir}
    0.008,                    !- Zone Heating Design Supply Air Humidity Ratio
{kgWater/kgDryAir}
    90.1-2010 - Office - ClosedOffice Ventilation,  !- Design Specification Outdoor
Air Object Name
    ,                         !- Zone Heating Sizing Factor
    ,                         !- Zone Cooling Sizing Factor
    DesignDay,                !- Cooling Design Air Flow Method
    0,                        !- Cooling Design Air Flow Rate {m3/s}
    0.000762,                 !- Cooling Minimum Air Flow per Zone Floor Area
{m3/s-m2}
```

```
    0,                        !- Cooling Minimum Air Flow {m3/s}
    0,                        !- Cooling Minimum Air Flow Fraction
    DesignDay,                !- Heating Design Air Flow Method
    0,                        !- Heating Design Air Flow Rate {m3/s}
    0.002032,                 !- Heating Maximum Air Flow per Zone Floor Area
{m3/s-m2}
    0.1415762,                !- Heating Maximum Air Flow {m3/s}
    0.3,                      !- Heating Maximum Air Flow Fraction
    Thermal Zone: closed office Design Spec Zone Air Dist,  !- Design Specification
Zone Air Distribution Object Name
    No,                       !- Account for Dedicated Outdoor Air System
    NeutralSupplyAir,         !- Dedicated Outdoor Air System Control Strategy
    autosize,                 !- Dedicated Outdoor Air Low Setpoint Temperature
for Design {C}
    autosize;                 !- Dedicated Outdoor Air High Setpoint Temperature
for Design {C}

DesignSpecification:ZoneAirDistribution,
    Thermal Zone: closed office Design Spec Zone Air Dist,  !- Name
    1,                        !- Zone Air Distribution Effectiveness in Cooling
Mode {dimensionless}
    1;                        !- Zone Air Distribution Effectiveness in Heating
Mode {dimensionless}

DesignSpecification:OutdoorAir,
    90.1-2010 - Office - ClosedOffice Ventilation,  !- Name
    Sum,                      !- Outdoor Air Method
    0.002359737216,           !- Outdoor Air Flow per Person {m3/s-person}
    0,                        !- Outdoor Air Flow per Zone Floor Area {m3/s-m2}
    0.025,                    !- Outdoor Air Flow per Zone {m3/s}
    0;                        !- Outdoor Air Flow Air Changes per Hour {1/hr}

ZoneVentilation:DesignFlowRate,
    Thermal Zone: closed office Ventilation per Person,  !- Name
    Thermal Zone: closed office,  !- Zone or ZoneList Name
    Medium Office Bldg Occ,  !- Schedule Name
    Flow/Person,              !- Design Flow Rate Calculation Method
```

```
    ,                       !- Design Flow Rate {m3/s}
    ,                       !- Flow Rate per Zone Floor Area {m3/s-m2}
    0.002359737216,         !- Flow Rate per Person {m3/s-person}
    ,                       !- Air Changes per Hour {1/hr}
    ,                       !- Ventilation Type
    ,                       !- Fan Pressure Rise {Pa}
    ,                       !- Fan Total Efficiency
    ,                       !- Constant Term Coefficient
    ,                       !- Temperature Term Coefficient
    ,                       !- Velocity Term Coefficient
    ;                       !- Velocity Squared Term Coefficient

Schedule:Constant,Always_On,,1;

ZoneVentilation:DesignFlowRate,
    Thermal Zone: closed office Ventilation Rate,  !- Name
    Thermal Zone: closed office,  !- Zone or ZoneList Name
    Always_On,              !- Schedule Name
    Flow/Zone,              !- Design Flow Rate Calculation Method
    0.025,                  !- Design Flow Rate {m3/s}
    ,                       !- Flow Rate per Zone Floor Area {m3/s-m2}
    ,                       !- Flow Rate per Person {m3/s-person}
    ,                       !- Air Changes per Hour {1/hr}
    ,                       !- Ventilation Type
    ,                       !- Fan Pressure Rise {Pa}
    ,                       !- Fan Total Efficiency
    ,                       !- Constant Term Coefficient
    ,                       !- Temperature Term Coefficient
    ,                       !- Velocity Term Coefficient
    ;                       !- Velocity Squared Term Coefficient

SimulationControl,
    Yes,                    !- Do Zone Sizing Calculation
    No,                     !- Do System Sizing Calculation
    No,                     !- Do Plant Sizing Calculation
    Yes,                    !- Run Simulation for Sizing Periods
    Yes;                    !- Run Simulation for Weather File Run Periods
```

```
ConvergenceLimits,
    1;                      !- Minimum System Timestep {minutes}

HeatBalanceAlgorithm,ConductionTransferFunction,200;

RunPeriod,
    Run Period 1,           !- Name
    1,                      !- Begin Month
    1,                      !- Begin Day of Month
    2006,                   !- Begin Year
    12,                     !- End Month
    31,                     !- End Day of Month
    2006,                   !- End Year
    Sunday,                 !- Day of Week for Start Day
    No,                     !- Use Weather File Holidays and Special Days
    No,                     !- Use Weather File Daylight Saving Period
    No,                     !- Apply Weekend Holiday Rule
    Yes,                    !- Use Weather File Rain Indicators
    Yes;                    !- Use Weather File Snow Indicators

ShadowCalculation,
    PolygonClipping,        !- Shading Calculation Method
    Periodic,               !- Shading Calculation Update Frequency Method
    7,                      !- Shading Calculation Update Frequency
    15000,                  !- Maximum Figures in Shadow Overlap Calculations
    SutherlandHodgman;      !- Polygon Clipping Algorithm

SurfaceConvectionAlgorithm:Inside,TARP;
SurfaceConvectionAlgorithm:Outside,DOE-2;

Sizing:Parameters,
    1.25,                   !- Heating Sizing Factor
    1.15;                   !- Cooling Sizing Factor

ZoneAirContaminantBalance,No;
ZoneAirHeatBalanceAlgorithm,AnalyticalSolution;
```

```
ZoneCapacitanceMultiplier:ResearchSpecial,Zone Capacitance Multiplier Research
Special,,,,,;

GlobalGeometryRules,
    UpperLeftCorner,         !- Starting Vertex Position
    Counterclockwise,        !- Vertex Entry Direction
    Relative,                !- Coordinate System
    Relative,                !- Daylighting Reference Point Coordinate System
    Relative;                !- Rectangular Surface Coordinate System

Material,
    1/2IN Gypsum,            !- Name
    Smooth,                  !- Roughness
    0.0127,                  !- Thickness {m}
    0.16,                    !- Conductivity {W/m-K}
    784.9,                   !- Density {kg/m3}
    830.000000000001,        !- Specific Heat {J/kg-K}
    0.9,                     !- Thermal Absorptance
    0.4,                     !- Solar Absorptance
    0.4;                     !- Visible Absorptance

Material,
    1IN Stucco,              !- Name
    Smooth,                  !- Roughness
    0.0253,                  !- Thickness {m}
    0.691799999999999,       !- Conductivity {W/m-K}
    1858,                    !- Density {kg/m3}
    836.999999999999,        !- Specific Heat {J/kg-K}
    0.9,                     !- Thermal Absorptance
    0.92,                    !- Solar Absorptance
    0.92;                    !- Visible Absorptance

Material,
    8IN CONCRETE HW RefBldg, !- Name
    Rough,                   !- Roughness
    0.2032,                  !- Thickness {m}
    1.311,                   !- Conductivity {W/m-K}
```

```
    2240,                    !- Density {kg/m3}
    836.800000000001,        !- Specific Heat {J/kg-K}
    0.9,                     !- Thermal Absorptance
    0.7,                     !- Solar Absorptance
    0.7;                     !- Visible Absorptance

Material,
    F16 Acoustic tile,       !- Name
    MediumSmooth,            !- Roughness
    0.0191,                  !- Thickness {m}
    0.06,                    !- Conductivity {W/m-K}
    368,                     !- Density {kg/m3}
    590.000000000002,        !- Specific Heat {J/kg-K}
    0.9,                     !- Thermal Absorptance
    0.3,                     !- Solar Absorptance
    0.3;                     !- Visible Absorptance

Material,
    G01a 19mm gypsum board,  !- Name
    MediumSmooth,            !- Roughness
    0.019,                   !- Thickness {m}
    0.16,                    !- Conductivity {W/m-K}
    800,                     !- Density {kg/m3}
    1090,                    !- Specific Heat {J/kg-K}
    0.9,                     !- Thermal Absorptance
    0.4,                     !- Solar Absorptance
    0.4;                     !- Visible Absorptance

Material,
    IEAD Roof Insulation R-19.72 IP,  !- Name
    MediumRough,             !- Roughness
    0.170137206506431,       !- Thickness {m}
    0.049,                   !- Conductivity {W/m-K}
    265,                     !- Density {kg/m3}
    836.800000000001,        !- Specific Heat {J/kg-K}
    0.9,                     !- Thermal Absorptance
    0.7,                     !- Solar Absorptance
```

```
    0.7;                    !- Visible Absorptance

Material,
    M11 100mm lightweight concrete,  !- Name
    MediumRough,            !- Roughness
    0.1016,                 !- Thickness {m}
    0.53,                   !- Conductivity {W/m-K}
    1280,                   !- Density {kg/m3}
    840.000000000002,       !- Specific Heat {J/kg-K}
    0.9,                    !- Thermal Absorptance
    0.5,                    !- Solar Absorptance
    0.5;                    !- Visible Absorptance

Material,
    Mass Wall Insulation R-5.74 IP,  !- Name
    MediumRough,            !- Roughness
    0.0495465462712,        !- Thickness {m}
    0.049,                  !- Conductivity {W/m-K}
    265,                    !- Density {kg/m3}
    836.800000000001,       !- Specific Heat {J/kg-K}
    0.9,                    !- Thermal Absorptance
    0.7,                    !- Solar Absorptance
    0.7;                    !- Visible Absorptance

Material,
    MAT-CC05 4 HW CONCRETE,  !- Name
    Rough,                  !- Roughness
    0.1016,                 !- Thickness {m}
    1.311,                  !- Conductivity {W/m-K}
    2240,                   !- Density {kg/m3}
    836.800000000001,       !- Specific Heat {J/kg-K}
    0.9,                    !- Thermal Absorptance
    0.85,                   !- Solar Absorptance
    0.85;                   !- Visible Absorptance

Material,
    Metal Decking,          !- Name
```

```
    MediumSmooth,           !- Roughness
    0.0015,                 !- Thickness {m}
    45.006,                 !- Conductivity {W/m-K}
    7680,                   !- Density {kg/m3}
    418.4,                  !- Specific Heat {J/kg-K}
    0.9,                    !- Thermal Absorptance
    0.6,                    !- Solar Absorptance
    0.6;                    !- Visible Absorptance

Material,
    Roof Membrane,          !- Name
    VeryRough,              !- Roughness
    0.0095,                 !- Thickness {m}
    0.16,                   !- Conductivity {W/m-K}
    1121.29,                !- Density {kg/m3}
    1460,                   !- Specific Heat {J/kg-K}
    0.9,                    !- Thermal Absorptance
    0.7,                    !- Solar Absorptance
    0.7;                    !- Visible Absorptance

Material:AirGap,
    F04 Wall air space resistance,  !- Name
    0.15;                   !- Thermal Resistance {m2-K/W}

Material:AirGap,
    F05 Ceiling air space resistance,  !- Name
    0.18;                   !- Thermal Resistance {m2-K/W}

Material:NoMass,
    CP02 CARPET PAD,        !- Name
    Smooth,                 !- Roughness
    0.1,                    !- Thermal Resistance {m2-K/W}
    0.9,                    !- Thermal Absorptance
    0.8,                    !- Solar Absorptance
    0.8;                    !- Visible Absorptance

WindowMaterial:Gas,
```

```
    AIR 12MM,                !- Name
    Air,                     !- Gas Type
    0.012;                   !- Thickness {m}

WindowMaterial:Glazing,
    CLEAR 3MM 1,             !- Name
    SpectralAverage,         !- Optical Data Type
    ,                        !- Window Glass Spectral Data Set Name
    0.003,                   !- Thickness {m}
    0.78,                    !- Solar Transmittance at Normal Incidence
    0.08,                    !- Front Side Solar Reflectance at Normal Incidence
    0.08,                    !- Back Side Solar Reflectance at Normal Incidence
    0.88,                    !- Visible Transmittance at Normal Incidence
    0.081,                   !- Front Side Visible Reflectance at Normal
Incidence
    0.081,                   !- Back Side Visible Reflectance at Normal Incidence
    0,                       !- Infrared Transmittance at Normal Incidence
    0.84,                    !- Front Side Infrared Hemispherical Emissivity
    0.84,                    !- Back Side Infrared Hemispherical Emissivity
    0.9;                     !- Conductivity {W/m-K}

WindowMaterial:SimpleGlazingSystem,
    Fixed Window 3.69/0.25/0.16,  !- Name
    3.69087117172377,        !- U-Factor {W/m2-K}
    0.25,                    !- Solar Heat Gain Coefficient
    0.16;                    !- Visible Transmittance

Construction,
    ASHRAE 90.1-2010 ExtRoof IEAD ClimateZone 2-8,  !- Name
    Roof Membrane,           !- Outside Layer
    IEAD Roof Insulation R-19.72 IP,  !- Layer 2
    Metal Decking;           !- Layer 3

Construction,
    ASHRAE 90.1-2010 ExtWall Mass ClimateZone 3,  !- Name
    1IN Stucco,              !- Outside Layer
    8IN CONCRETE HW RefBldg, !- Layer 2
```

```
    Mass Wall Insulation R-5.74 IP,  !- Layer 3
    1/2IN Gypsum;            !- Layer 4

Construction,
    ASHRAE 90.1-2010 ExtWindow Metal ClimateZone 3,  !- Name
    Fixed Window 3.69/0.25/0.16;  !- Outside Layer

Construction,
    Dbl Clr 3mm/12mm Air,    !- Name
    CLEAR 3MM 1,             !- Outside Layer
    AIR 12MM,                !- Layer 2
    CLEAR 3MM 1;             !- Layer 3

Construction,
    ExtSlabCarpet 4in ClimateZone 1-8,  !- Name
    MAT-CC05 4 HW CONCRETE,  !- Outside Layer
    CP02 CARPET PAD;         !- Layer 2

Construction,
    Interior Ceiling,        !- Name
    M11 100mm lightweight concrete,  !- Outside Layer
    F05 Ceiling air space resistance,  !- Layer 2
    F16 Acoustic tile;       !- Layer 3

Construction,
    Interior Floor,          !- Name
    F16 Acoustic tile,       !- Outside Layer
    F05 Ceiling air space resistance,  !- Layer 2
    M11 100mm lightweight concrete;  !- Layer 3

Construction,
    Interior Wall,           !- Name
    G01a 19mm gypsum board,  !- Outside Layer
    F04 Wall air space resistance,  !- Layer 2
    G01a 19mm gypsum board;  !- Layer 3

ScheduleTypeLimits,
```

```
    ActivityLevel 13,        !- Name
    0,                       !- Lower Limit Value
    ,                        !- Upper Limit Value
    Continuous,              !- Numeric Type
    activitylevel;           !- Unit Type

ScheduleTypeLimits,
    Always On Discrete Limits,  !- Name
    0,                       !- Lower Limit Value
    1,                       !- Upper Limit Value
    Discrete,                !- Numeric Type
    availability;            !- Unit Type

ScheduleTypeLimits,
    Fraction,                !- Name
    0,                       !- Lower Limit Value
    1,                       !- Upper Limit Value
    CONTINUOUS;              !- Numeric Type

Schedule:Constant,Always On Discrete,Always On Discrete Limits,1;

Schedule:Day:Interval,
    Medium Office Activity Default Schedule,  !- Name
    ActivityLevel 13,        !- Schedule Type Limits Name
    No,                      !- Interpolate to Timestep
    24:00,                   !- Time 1 {hh:mm}
    120;                     !- Value Until Time 1

Schedule:Day:Interval,
    Medium Office Activity Summer Design Day,  !- Name
    ActivityLevel 13,        !- Schedule Type Limits Name
    No,                      !- Interpolate to Timestep
    24:00,                   !- Time 1 {hh:mm}
    120;                     !- Value Until Time 1

Schedule:Day:Interval,
    Medium Office Activity Winter Design Day,  !- Name
```

```
    ActivityLevel 13,        !- Schedule Type Limits Name
    No,                      !- Interpolate to Timestep
    24:00,                   !- Time 1 {hh:mm}
    120;                     !- Value Until Time 1

Schedule:Day:Interval,
    Medium Office Bldg Equip Default Schedule,  !- Name
    Fraction,                !- Schedule Type Limits Name
    No,                      !- Interpolate to Timestep
    08:00,                   !- Time 1 {hh:mm}
    0,                       !- Value Until Time 1
    12:00,                   !- Time 2 {hh:mm}
    0.899999976158142,       !- Value Until Time 2
    13:00,                   !- Time 3 {hh:mm}
    0.800000011920929,       !- Value Until Time 3
    17:00,                   !- Time 4 {hh:mm}
    0.899999976158142,       !- Value Until Time 4
    24:00,                   !- Time 5 {hh:mm}
    0;                       !- Value Until Time 5

Schedule:Day:Interval,
    Medium Office Bldg Equip Rule 1 Day Schedule,  !- Name
    Fraction,                !- Schedule Type Limits Name
    No,                      !- Interpolate to Timestep
    24:00,                   !- Time 1 {hh:mm}
    0;                       !- Value Until Time 1

Schedule:Day:Interval,
    Medium Office Bldg Equip Rule 2 Day Schedule,  !- Name
    Fraction,                !- Schedule Type Limits Name
    No,                      !- Interpolate to Timestep
    24:00,                   !- Time 1 {hh:mm}
    0;                       !- Value Until Time 1

Schedule:Day:Interval,
    Medium Office Bldg Equip Summer Design Day,  !- Name
    Fraction,                !- Schedule Type Limits Name
```

```
    No,                       !- Interpolate to Timestep
    24:00,                    !- Time 1 {hh:mm}
    1;                        !- Value Until Time 1

Schedule:Day:Interval,
    Medium Office Bldg Equip Winter Design Day,  !- Name
    Fraction,                 !- Schedule Type Limits Name
    No,                       !- Interpolate to Timestep
    24:00,                    !- Time 1 {hh:mm}
    0;                        !- Value Until Time 1

Schedule:Day:Interval,
    Medium Office Bldg Occ Default Schedule,  !- Name
    Fraction,                 !- Schedule Type Limits Name
    No,                       !- Interpolate to Timestep
    08:00,                    !- Time 1 {hh:mm}
    0,                        !- Value Until Time 1
    12:00,                    !- Time 2 {hh:mm}
    1,                        !- Value Until Time 2
    13:00,                    !- Time 3 {hh:mm}
    0.5,                      !- Value Until Time 3
    17:00,                    !- Time 4 {hh:mm}
    1,                        !- Value Until Time 4
    24:00,                    !- Time 5 {hh:mm}
    0;                        !- Value Until Time 5

Schedule:Day:Interval,
    Medium Office Bldg Occ Rule 1 Day Schedule,  !- Name
    Fraction,                 !- Schedule Type Limits Name
    No,                       !- Interpolate to Timestep
    24:00,                    !- Time 1 {hh:mm}
    0;                        !- Value Until Time 1

Schedule:Day:Interval,
    Medium Office Bldg Occ Rule 2 Day Schedule,  !- Name
    Fraction,                 !- Schedule Type Limits Name
    No,                       !- Interpolate to Timestep
```

```
    24:00,                  !- Time 1 {hh:mm}
    0;                      !- Value Until Time 1

Schedule:Day:Interval,
    Medium Office Bldg Occ Summer Design Day,  !- Name
    Fraction,               !- Schedule Type Limits Name
    No,                     !- Interpolate to Timestep
    08:00,                  !- Time 1 {hh:mm}
    0,                      !- Value Until Time 1
    17:00,                  !- Time 2 {hh:mm}
    1,                      !- Value Until Time 2
    24:00,                  !- Time 3 {hh:mm}
    0.0500000007450581;     !- Value Until Time 3

Schedule:Day:Interval,
    Medium Office Bldg Occ Winter Design Day,  !- Name
    Fraction,               !- Schedule Type Limits Name
    No,                     !- Interpolate to Timestep
    24:00,                  !- Time 1 {hh:mm}
    0;                      !- Value Until Time 1

Schedule:Day:Interval,
    Medium Office Infil Quarter On Default Schedule,  !- Name
    Fraction,               !- Schedule Type Limits Name
    No,                     !- Interpolate to Timestep
    08:00,                  !- Time 1 {hh:mm}
    1,                      !- Value Until Time 1
    17:00,                  !- Time 2 {hh:mm}
    0.25,                   !- Value Until Time 2
    24:00,                  !- Time 3 {hh:mm}
    1;                      !- Value Until Time 3

Schedule:Day:Interval,
    Medium Office Infil Quarter On Rule 1 Day Schedule,  !- Name
    Fraction,               !- Schedule Type Limits Name
    No,                     !- Interpolate to Timestep
    24:00,                  !- Time 1 {hh:mm}
```

```
    1;                        !- Value Until Time 1

Schedule:Day:Interval,
    Medium Office Infil Quarter On Rule 2 Day Schedule,  !- Name
    Fraction,                 !- Schedule Type Limits Name
    No,                       !- Interpolate to Timestep
    24:00,                    !- Time 1 {hh:mm}
    1;                        !- Value Until Time 1

Schedule:Day:Interval,
    Medium Office Infil Quarter On Summer Design Day,  !- Name
    Fraction,                 !- Schedule Type Limits Name
    No,                       !- Interpolate to Timestep
    08:00,                    !- Time 1 {hh:mm}
    1,                        !- Value Until Time 1
    17:00,                    !- Time 2 {hh:mm}
    0.25,                     !- Value Until Time 2
    24:00,                    !- Time 3 {hh:mm}
    1;                        !- Value Until Time 3

Schedule:Day:Interval,
    Medium Office Infil Quarter On Winter Design Day,  !- Name
    Fraction,                 !- Schedule Type Limits Name
    No,                       !- Interpolate to Timestep
    08:00,                    !- Time 1 {hh:mm}
    1,                        !- Value Until Time 1
    17:00,                    !- Time 2 {hh:mm}
    0.25,                     !- Value Until Time 2
    24:00,                    !- Time 3 {hh:mm}
    1;                        !- Value Until Time 3

Schedule:Day:Interval,
    Office Bldg Light Default Schedule,  !- Name
    Fraction,                 !- Schedule Type Limits Name
    No,                       !- Interpolate to Timestep
    08:00,                    !- Time 1 {hh:mm}
    0,                        !- Value Until Time 1
```

```
    17:00,                  !- Time 2 {hh:mm}
    1,                      !- Value Until Time 2
    24:00,                  !- Time 3 {hh:mm}
    0;                      !- Value Until Time 3

Schedule:Day:Interval,
    Office Bldg Light Rule 1 Day Schedule,  !- Name
    Fraction,               !- Schedule Type Limits Name
    No,                     !- Interpolate to Timestep
    24:00,                  !- Time 1 {hh:mm}
    0;                      !- Value Until Time 1

Schedule:Day:Interval,
    Office Bldg Light Rule 2 Day Schedule,  !- Name
    Fraction,               !- Schedule Type Limits Name
    No,                     !- Interpolate to Timestep
    24:00,                  !- Time 1 {hh:mm}
    0;                      !- Value Until Time 1

Schedule:Day:Interval,
    Office Bldg Light Summer Design Day,  !- Name
    Fraction,               !- Schedule Type Limits Name
    No,                     !- Interpolate to Timestep
    24:00,                  !- Time 1 {hh:mm}
    1;                      !- Value Until Time 1

Schedule:Day:Interval,
    Office Bldg Light Winter Design Day,  !- Name
    Fraction,               !- Schedule Type Limits Name
    No,                     !- Interpolate to Timestep
    24:00,                  !- Time 1 {hh:mm}
    0;                      !- Value Until Time 1

Schedule:Week:Daily,
    Medium Office Activity Week Rule - Jan1-Dec31,  !- Name
    Medium Office Activity Default Schedule,  !- Sunday Schedule:Day Name
    Medium Office Activity Default Schedule,  !- Monday Schedule:Day Name
```

```
    Medium Office Activity Default Schedule,  !- Tuesday Schedule:Day Name
    Medium Office Activity Default Schedule,  !- Wednesday Schedule:Day Name
    Medium Office Activity Default Schedule,  !- Thursday Schedule:Day Name
    Medium Office Activity Default Schedule,  !- Friday Schedule:Day Name
    Medium Office Activity Default Schedule,  !- Saturday Schedule:Day Name
    Medium Office Activity Default Schedule,  !- Holiday Schedule:Day Name
    Medium Office Activity Summer Design Day,  !- SummerDesignDay Schedule:Day
Name
    Medium Office Activity Winter Design Day,  !- WinterDesignDay Schedule:Day
Name
    Medium Office Activity Default Schedule,  !- CustomDay1 Schedule:Day Name
    Medium Office Activity Default Schedule;  !- CustomDay2 Schedule:Day Name

Schedule:Year,
    Medium Office Activity,  !- Name
    ActivityLevel 13,        !- Schedule Type Limits Name
    Medium Office Activity Week Rule - Jan1-Dec31,  !- Schedule:Week Name 1
    1,                       !- Start Month 1
    1,                       !- Start Day 1
    12,                      !- End Month 1
    31;                      !- End Day 1

Schedule:Week:Daily,
    Medium Office Bldg Equip Week Rule - Jan1-Dec31,  !- Name
    Medium Office Bldg Equip Rule 1 Day Schedule,  !- Sunday Schedule:Day Name
    Medium Office Bldg Equip Default Schedule,  !- Monday Schedule:Day Name
    Medium Office Bldg Equip Default Schedule,  !- Tuesday Schedule:Day Name
    Medium Office Bldg Equip Default Schedule,  !- Wednesday Schedule:Day Name
    Medium Office Bldg Equip Default Schedule,  !- Thursday Schedule:Day Name
    Medium Office Bldg Equip Default Schedule,  !- Friday Schedule:Day Name
    Medium Office Bldg Equip Rule 2 Day Schedule,  !- Saturday Schedule:Day Name
    Medium Office Bldg Equip Default Schedule,  !- Holiday Schedule:Day Name
    Medium Office Bldg Equip Summer Design Day,  !- SummerDesignDay Schedule:Day
Name
    Medium Office Bldg Equip Winter Design Day,  !- WinterDesignDay Schedule:Day
Name
    Medium Office Bldg Equip Default Schedule,  !- CustomDay1 Schedule:Day Name
```

```
    Medium Office Bldg Equip Default Schedule;  !- CustomDay2 Schedule:Day Name

Schedule:Year,
    Medium Office Bldg Equip,!- Name
    Fraction,                !- Schedule Type Limits Name
    Medium Office Bldg Equip Week Rule - Jan1-Dec31,  !- Schedule:Week Name 1
    1,                       !- Start Month 1
    1,                       !- Start Day 1
    12,                      !- End Month 1
    31;                      !- End Day 1

Schedule:Week:Daily,
    Medium Office Bldg Occ Week Rule - Jan1-Dec31,  !- Name
    Medium Office Bldg Occ Rule 1 Day Schedule,  !- Sunday Schedule:Day Name
    Medium Office Bldg Occ Default Schedule,  !- Monday Schedule:Day Name
    Medium Office Bldg Occ Default Schedule,  !- Tuesday Schedule:Day Name
    Medium Office Bldg Occ Default Schedule,  !- Wednesday Schedule:Day Name
    Medium Office Bldg Occ Default Schedule,  !- Thursday Schedule:Day Name
    Medium Office Bldg Occ Default Schedule,  !- Friday Schedule:Day Name
    Medium Office Bldg Occ Rule 2 Day Schedule,  !- Saturday Schedule:Day Name
    Medium Office Bldg Occ Default Schedule,  !- Holiday Schedule:Day Name
    Medium Office Bldg Occ Summer Design Day,  !- SummerDesignDay Schedule:Day
Name
    Medium Office Bldg Occ Winter Design Day,  !- WinterDesignDay Schedule:Day
Name
    Medium Office Bldg Occ Default Schedule,  !- CustomDay1 Schedule:Day Name
    Medium Office Bldg Occ Default Schedule;  !- CustomDay2 Schedule:Day Name

Schedule:Year,
    Medium Office Bldg Occ,  !- Name
    Fraction,                !- Schedule Type Limits Name
    Medium Office Bldg Occ Week Rule - Jan1-Dec31,  !- Schedule:Week Name 1
    1,                       !- Start Month 1
    1,                       !- Start Day 1
    12,                      !- End Month 1
    31;                      !- End Day 1
```

```
Schedule:Week:Daily,
    Medium Office Infil Quarter On Week Rule - Jan1-Dec31,  !- Name
    Medium Office Infil Quarter On Rule 1 Day Schedule,  !- Sunday Schedule:Day
Name
    Medium Office Infil Quarter On Default Schedule,  !- Monday Schedule:Day
Name
    Medium Office Infil Quarter On Default Schedule,  !- Tuesday Schedule:Day
Name
    Medium Office Infil Quarter On Default Schedule,  !- Wednesday Schedule:Day
Name
    Medium Office Infil Quarter On Default Schedule,  !- Thursday Schedule:Day
Name
    Medium Office Infil Quarter On Default Schedule,  !- Friday Schedule:Day Name
    Medium Office Infil Quarter On Rule 2 Day Schedule,  !- Saturday Schedule:Day
Name
    Medium Office Infil Quarter On Default Schedule,  !- Holiday Schedule:Day Name
    Medium Office Infil Quarter On Summer Design Day,  !- SummerDesignDay Schedule:
Day Name
    Medium Office Infil Quarter On Winter Design Day,  !- WinterDesignDay Schedule:
Day Name
    Medium Office Infil Quarter On Default Schedule,  !- CustomDay1 Schedule:Day
Name
    Medium Office Infil Quarter On Default Schedule;  !- CustomDay2 Schedule:Day
Name

Schedule:Year,
    Medium Office Infil Quarter On,  !- Name
    Fraction,                !- Schedule Type Limits Name
    Medium Office Infil Quarter On Week Rule - Jan1-Dec31,  !- Schedule:Week
Name 1
    1,                       !- Start Month 1
    1,                       !- Start Day 1
    12,                      !- End Month 1
    31;                      !- End Day 1

Schedule:Week:Daily,
    Office Bldg Light Week Rule - Jan1-Dec31,  !- Name
```

```
    Office Bldg Light Rule 1 Day Schedule,  !- Sunday Schedule:Day Name
    Office Bldg Light Default Schedule,  !- Monday Schedule:Day Name
    Office Bldg Light Default Schedule,  !- Tuesday Schedule:Day Name
    Office Bldg Light Default Schedule,  !- Wednesday Schedule:Day Name
    Office Bldg Light Default Schedule,  !- Thursday Schedule:Day Name
    Office Bldg Light Default Schedule,  !- Friday Schedule:Day Name
    Office Bldg Light Rule 2 Day Schedule,  !- Saturday Schedule:Day Name
    Office Bldg Light Default Schedule,  !- Holiday Schedule:Day Name
    Office Bldg Light Summer Design Day,  !- SummerDesignDay Schedule:Day Name
    Office Bldg Light Winter Design Day,  !- WinterDesignDay Schedule:Day Name
    Office Bldg Light Default Schedule,  !- CustomDay1 Schedule:Day Name
    Office Bldg Light Default Schedule;  !- CustomDay2 Schedule:Day Name

Schedule:Year,
    Office Bldg Light,       !- Name
    Fraction,                !- Schedule Type Limits Name
    Office Bldg Light Week Rule - Jan1-Dec31,  !- Schedule:Week Name 1
    1,                       !- Start Month 1
    1,                       !- Start Day 1
    12,                      !- End Month 1
    31;                      !- End Day 1

Schedule:Constant,Always Off Discrete,,0;
Schedule:Constant,Always On Continuous,,1;

OutdoorAir:Node,
    Model Outdoor Air Node;  !- Name

RunPeriodControl:DaylightSavingTime,
    2nd Sunday in March,     !- Start Date
    1st Sunday in November;  !- End Date

OutputControl:ReportingTolerances,
    0.2,                     !- Tolerance for Time Heating Setpoint Not Met
{deltaC}
    0.2;                     !- Tolerance for Time Cooling Setpoint Not Met
{deltaC}
```

```
Site:Location,
    Chicago Ohare Intl Ap,   !- Name
    41.98,                   !- Latitude {deg}
    -87.92,                  !- Longitude {deg}
    -6,                      !- Time Zone {hr}
    201;                     !- Elevation {m}

SizingPeriod:DesignDay,
    Chicago Ohare Intl Ap Ann Clg .4% Condns DB=>MWB,  !- Name
    7,                       !- Month
    21,                      !- Day of Month
    SummerDesignDay,         !- Day Type
    33.3,                    !- Maximum Dry-Bulb Temperature {C}
    10.5,                    !- Daily Dry-Bulb Temperature Range {deltaC}
    DefaultMultipliers,      !- Dry-Bulb Temperature Range Modifier Type
    ,                        !- Dry-Bulb Temperature Range Modifier Day Schedule
Name
    Wetbulb,                 !- Humidity Condition Type
    23.7,                    !- Wetbulb or DewPoint at Maximum Dry-Bulb {C}
    ,                        !- Humidity Condition Day Schedule Name
    ,                        !- Humidity Ratio at Maximum Dry-Bulb
{kgWater/kgDryAir}
    ,                        !- Enthalpy at Maximum Dry-Bulb {J/kg}
    ,                        !- Daily Wet-Bulb Temperature Range {deltaC}
    98934,                   !- Barometric Pressure {Pa}
    5.2,                     !- Wind Speed {m/s}
    230,                     !- Wind Direction {deg}
    No,                      !- Rain Indicator
    No,                      !- Snow Indicator
    No,                      !- Daylight Saving Time Indicator
    ASHRAETau,               !- Solar Model Indicator
    ,                        !- Beam Solar Day Schedule Name
    ,                        !- Diffuse Solar Day Schedule Name
    0.455,                   !- ASHRAE Clear Sky Optical Depth for Beam Irradiance
taub {dimensionless}
    2.05;                    !- ASHRAE Clear Sky Optical Depth for Diffuse
```

```
Irradiance taud {dimensionless}

SizingPeriod:DesignDay,
    Chicago Ohare Intl Ap Ann Clg .4% Condns DP=>MDB,  !- Name
    7,                        !- Month
    21,                       !- Day of Month
    SummerDesignDay,          !- Day Type
    28.9,                     !- Maximum Dry-Bulb Temperature {C}
    10.5,                     !- Daily Dry-Bulb Temperature Range {deltaC}
    DefaultMultipliers,       !- Dry-Bulb Temperature Range Modifier Type
    ,                         !- Dry-Bulb Temperature Range Modifier Day Schedule
Name
    Dewpoint,                 !- Humidity Condition Type
    23.8,                     !- Wetbulb or DewPoint at Maximum Dry-Bulb {C}
    ,                         !- Humidity Condition Day Schedule Name
    ,                         !- Humidity Ratio at Maximum Dry-Bulb
{kgWater/kgDryAir}
    ,                         !- Enthalpy at Maximum Dry-Bulb {J/kg}
    ,                         !- Daily Wet-Bulb Temperature Range {deltaC}
    98934,                    !- Barometric Pressure {Pa}
    5.2,                      !- Wind Speed {m/s}
    230,                      !- Wind Direction {deg}
    No,                       !- Rain Indicator
    No,                       !- Snow Indicator
    No,                       !- Daylight Saving Time Indicator
    ASHRAETau,                !- Solar Model Indicator
    ,                         !- Beam Solar Day Schedule Name
    ,                         !- Diffuse Solar Day Schedule Name
    0.455,                    !- ASHRAE Clear Sky Optical Depth for Beam Irradiance
taub {dimensionless}
    2.05;                     !- ASHRAE Clear Sky Optical Depth for Diffuse
Irradiance taud {dimensionless}

SizingPeriod:DesignDay,
    Chicago Ohare Intl Ap Ann Clg .4% Condns Enth=>MDB,  !- Name
    7,                        !- Month
    21,                       !- Day of Month
```

```
    SummerDesignDay,          !- Day Type
    31.4,                     !- Maximum Dry-Bulb Temperature {C}
    10.5,                     !- Daily Dry-Bulb Temperature Range {deltaC}
    DefaultMultipliers,       !- Dry-Bulb Temperature Range Modifier Type
    ,                         !- Dry-Bulb Temperature Range Modifier Day Schedule
Name
    Enthalpy,                 !- Humidity Condition Type
    ,                         !- Wetbulb or DewPoint at Maximum Dry-Bulb {C}
    ,                         !- Humidity Condition Day Schedule Name
    ,                         !- Humidity Ratio at Maximum Dry-Bulb
{kgWater/kgDryAir}
    79200,                    !- Enthalpy at Maximum Dry-Bulb {J/kg}
    ,                         !- Daily Wet-Bulb Temperature Range {deltaC}
    98934,                    !- Barometric Pressure {Pa}
    5.2,                      !- Wind Speed {m/s}
    230,                      !- Wind Direction {deg}
    No,                       !- Rain Indicator
    No,                       !- Snow Indicator
    No,                       !- Daylight Saving Time Indicator
    ASHRAETau,                !- Solar Model Indicator
    ,                         !- Beam Solar Day Schedule Name
    ,                         !- Diffuse Solar Day Schedule Name
    0.455,                    !- ASHRAE Clear Sky Optical Depth for Beam Irradiance
taub {dimensionless}
    2.05;                     !- ASHRAE Clear Sky Optical Depth for Diffuse
Irradiance taud {dimensionless}

SizingPeriod:DesignDay,
    Chicago Ohare Intl Ap Ann Clg .4% Condns WB=>MDB,  !- Name
    7,                        !- Month
    21,                       !- Day of Month
    SummerDesignDay,          !- Day Type
    31.2,                     !- Maximum Dry-Bulb Temperature {C}
    10.5,                     !- Daily Dry-Bulb Temperature Range {deltaC}
    DefaultMultipliers,       !- Dry-Bulb Temperature Range Modifier Type
    ,                         !- Dry-Bulb Temperature Range Modifier Day Schedule
Name
```

```
    Wetbulb,                !- Humidity Condition Type
    25.5,                   !- Wetbulb or DewPoint at Maximum Dry-Bulb {C}
    ,                       !- Humidity Condition Day Schedule Name
    ,                       !- Humidity Ratio at Maximum Dry-Bulb
{kgWater/kgDryAir}
    ,                       !- Enthalpy at Maximum Dry-Bulb {J/kg}
    ,                       !- Daily Wet-Bulb Temperature Range {deltaC}
    98934,                  !- Barometric Pressure {Pa}
    5.2,                    !- Wind Speed {m/s}
    230,                    !- Wind Direction {deg}
    No,                     !- Rain Indicator
    No,                     !- Snow Indicator
    No,                     !- Daylight Saving Time Indicator
    ASHRAETau,              !- Solar Model Indicator
    ,                       !- Beam Solar Day Schedule Name
    ,                       !- Diffuse Solar Day Schedule Name
    0.455,                  !- ASHRAE Clear Sky Optical Depth for Beam Irradiance
taub {dimensionless}
    2.05;                   !- ASHRAE Clear Sky Optical Depth for Diffuse
Irradiance taud {dimensionless}

SizingPeriod:DesignDay,
    Chicago Ohare Intl Ap Ann Htg 99.6% Condns DB,  !- Name
    1,                      !- Month
    21,                     !- Day of Month
    WinterDesignDay,        !- Day Type
    -20,                    !- Maximum Dry-Bulb Temperature {C}
    0,                      !- Daily Dry-Bulb Temperature Range {deltaC}
    DefaultMultipliers,     !- Dry-Bulb Temperature Range Modifier Type
    ,                       !- Dry-Bulb Temperature Range Modifier Day Schedule
Name
    Wetbulb,                !- Humidity Condition Type
    -20,                    !- Wetbulb or DewPoint at Maximum Dry-Bulb {C}
    ,                       !- Humidity Condition Day Schedule Name
    ,                       !- Humidity Ratio at Maximum Dry-Bulb
{kgWater/kgDryAir}
    ,                       !- Enthalpy at Maximum Dry-Bulb {J/kg}
```

```
    ,                       !- Daily Wet-Bulb Temperature Range {deltaC}
    98934,                  !- Barometric Pressure {Pa}
    4.9,                    !- Wind Speed {m/s}
    270,                    !- Wind Direction {deg}
    No,                     !- Rain Indicator
    No,                     !- Snow Indicator
    No,                     !- Daylight Saving Time Indicator
    ASHRAEClearSky,         !- Solar Model Indicator
    ,                       !- Beam Solar Day Schedule Name
    ,                       !- Diffuse Solar Day Schedule Name
    ,                       !- ASHRAE Clear Sky Optical Depth for Beam
Irradiance taub {dimensionless}
    ,                       !- ASHRAE Clear Sky Optical Depth for Diffuse
Irradiance taud {dimensionless}
    0;                      !- Sky Clearness

SizingPeriod:DesignDay,
    Chicago Ohare Intl Ap Ann Htg Wind 99.6% Condns WS=>MCDB,  !- Name
    1,                      !- Month
    21,                     !- Day of Month
    WinterDesignDay,        !- Day Type
    -3.5,                   !- Maximum Dry-Bulb Temperature {C}
    0,                      !- Daily Dry-Bulb Temperature Range {deltaC}
    DefaultMultipliers,     !- Dry-Bulb Temperature Range Modifier Type
    ,                       !- Dry-Bulb Temperature Range Modifier Day Schedule
Name
    Wetbulb,                !- Humidity Condition Type
    -3.5,                   !- Wetbulb or DewPoint at Maximum Dry-Bulb {C}
    ,                       !- Humidity Condition Day Schedule Name
    ,                       !- Humidity Ratio at Maximum Dry-Bulb
{kgWater/kgDryAir}
    ,                       !- Enthalpy at Maximum Dry-Bulb {J/kg}
    ,                       !- Daily Wet-Bulb Temperature Range {deltaC}
    98934,                  !- Barometric Pressure {Pa}
    12.4,                   !- Wind Speed {m/s}
    270,                    !- Wind Direction {deg}
    No,                     !- Rain Indicator
```

```
    No,                       !- Snow Indicator
    No,                       !- Daylight Saving Time Indicator
    ASHRAEClearSky,           !- Solar Model Indicator
    ,                         !- Beam Solar Day Schedule Name
    ,                         !- Diffuse Solar Day Schedule Name
    ,                         !- ASHRAE Clear Sky Optical Depth for Beam Irradiance
taub {dimensionless}
    ,                         !- ASHRAE Clear Sky Optical Depth for Diffuse
Irradiance taud {dimensionless}
    0;                        !- Sky Clearness

SizingPeriod:DesignDay,
    Chicago Ohare Intl Ap Ann Hum_n 99.6% Condns DP=>MCDB,  !- Name
    1,                        !- Month
    21,                       !- Day of Month
    WinterDesignDay,          !- Day Type
    -19.2,                    !- Maximum Dry-Bulb Temperature {C}
    0,                        !- Daily Dry-Bulb Temperature Range {deltaC}
    DefaultMultipliers,       !- Dry-Bulb Temperature Range Modifier Type
    ,                         !- Dry-Bulb Temperature Range Modifier Day Schedule
Name
    Dewpoint,                 !- Humidity Condition Type
    -25.7,                    !- Wetbulb or DewPoint at Maximum Dry-Bulb {C}
    ,                         !- Humidity Condition Day Schedule Name
    ,                         !- Humidity Ratio at Maximum Dry-Bulb
{kgWater/kgDryAir}
    ,                         !- Enthalpy at Maximum Dry-Bulb {J/kg}
    ,                         !- Daily Wet-Bulb Temperature Range {deltaC}
    98934,                    !- Barometric Pressure {Pa}
    4.9,                      !- Wind Speed {m/s}
    270,                      !- Wind Direction {deg}
    No,                       !- Rain Indicator
    No,                       !- Snow Indicator
    No,                       !- Daylight Saving Time Indicator
    ASHRAEClearSky,           !- Solar Model Indicator
    ,                         !- Beam Solar Day Schedule Name
    ,                         !- Diffuse Solar Day Schedule Name
```

```
    ,                       !- ASHRAE Clear Sky Optical Depth for Beam Irradiance
taub {dimensionless}
    ,                       !- ASHRAE Clear Sky Optical Depth for Diffuse
Irradiance taud {dimensionless}
    0;                      !- Sky Clearness

ZoneList,
    90.1-2010 - Office - ClosedOffice,  !- Name
    Thermal Zone: closed office;  !- Zone 1 Name

Lights,
    90.1-2010 - Office - ClosedOffice Lights,  !- Name
    90.1-2010 - Office - ClosedOffice,  !- Zone or ZoneList Name
    Office Bldg Light,      !- Schedule Name
    Watts/Area,             !- Design Level Calculation Method
    ,                       !- Lighting Level {W}
    11,                     !- Watts per Zone Floor Area {W/m2}
    ,                       !- Watts per Person {W/person}
    ,                       !- Return Air Fraction
    ,                       !- Fraction Radiant
    ,                       !- Fraction Visible
    ;                       !- Fraction Replaceable

People,
    90.1-2010 - Office - ClosedOffice People,  !- Name
    90.1-2010 - Office - ClosedOffice,  !- Zone or ZoneList Name
    Medium Office Bldg Occ,  !- Number of People Schedule Name
    Area/Person,            !- Number of People Calculation Method
    ,                       !- Number of People
    ,                       !- People per Zone Floor Area {person/m2}
    18.6,                   !- Zone Floor Area per Person {m2/person}
    0.3,                    !- Fraction Radiant
    ,                       !- Sensible Heat Fraction
    Medium Office Activity;  !- Activity Level Schedule Name

ElectricEquipment,
    90.1-2010 - Office - ClosedOffice Electric Equipment,  !- Name
```

```
    90.1-2010 - Office - ClosedOffice,  !- Zone or ZoneList Name
    Medium Office Bldg Equip,!- Schedule Name
    Watts/Area,              !- Design Level Calculation Method
    ,                        !- Design Level {W}
    7,                       !- Watts per Zone Floor Area {W/m2}
    ,                        !- Watts per Person {W/person}
    ,                        !- Fraction Latent
    ,                        !- Fraction Radiant
    ;                        !- Fraction Lost

ZoneInfiltration:DesignFlowRate,
    90.1-2010 - Office - ClosedOffice Infiltration,  !- Name
    90.1-2010 - Office - ClosedOffice,  !- Zone or ZoneList Name
    Medium Office Infil Quarter On,  !- Schedule Name
    Flow/ExteriorArea,       !- Design Flow Rate Calculation Method
    ,                        !- Design Flow Rate {m3/s}
    ,                        !- Flow per Zone Floor Area {m3/s-m2}
    0.000226568,             !- Flow per Exterior Surface Area {m3/s-m2}
    ,                        !- Air Changes per Hour {1/hr}
    ,                        !- Constant Term Coefficient
    ,                        !- Temperature Term Coefficient
    ,                        !- Velocity Term Coefficient
    ;                        !- Velocity Squared Term Coefficient

OutputControl:Table:Style,
    CommaAndHTML,            !- Column Separator
    JtoKWH;                  !- Unit Conversion

Output:Table:SummaryReports,
    AllSummary,              !- Report 1 Name
    EnvelopeSummary;         !- Report 2 Name

Output:VariableDictionary,IDF,Unsorted;

Output:SQLite,
    SimpleAndTabular;        !- Option Type
```

```
!
! ------------------------------------------------------------
! New objects created from ExpandObjects
! ------------------------------------------------------------
!
ZoneHVAC:EquipmentConnections,
    Thermal Zone: closed office,  !- Zone Name
    Thermal Zone: closed office Equipment,  !- Zone Conditioning Equipment List
Name
    Thermal Zone: closed office Ideal Loads Supply Inlet,  !- Zone Air Inlet Node
or NodeList Name
    ,                        !- Zone Air Exhaust Node or NodeList Name
    Thermal Zone: closed office Zone Air Node,  !- Zone Air Node Name
    Thermal Zone: closed office Return Outlet;  !- Zone Return Air Node or NodeList
Name

ZoneHVAC:EquipmentList,
    Thermal Zone: closed office Equipment,  !- Name
    SequentialLoad,          !- Load Distribution Scheme
    ZoneHVAC:IdealLoadsAirSystem,  !- Zone Equipment 1 Object Type
    Thermal Zone: closed office Ideal Loads Air System,  !- Zone Equipment 1 Name
    1,                       !- Zone Equipment 1 Cooling Sequence
    1,                       !- Zone Equipment 1 Heating or No-Load Sequence
    ,                        !- Zone Equipment 1 Sequential Cooling Fraction
Schedule Name
    ;                        !- Zone Equipment 1 Sequential Heating Fraction
Schedule Name

ZoneHVAC:IdealLoadsAirSystem,
    Thermal Zone: closed office Ideal Loads Air System,  !- Name
    ,                        !- Availability Schedule Name
    Thermal Zone: closed office Ideal Loads Supply Inlet,  !- Zone Supply Air Node
Name
    ,                        !- Zone Exhaust Air Node Name
    ,                        !- System Inlet Air Node Name
    50,                      !- Maximum Heating Supply Air Temperature {C}
    13,                      !- Minimum Cooling Supply Air Temperature {C}
```

```
    0.0156,                  !- Maximum Heating Supply Air Humidity Ratio
{kgWater/kgDryAir}
    0.0077,                  !- Minimum Cooling Supply Air Humidity Ratio
{kgWater/kgDryAir}
    NoLimit,                 !- Heating Limit
    ,                        !- Maximum Heating Air Flow Rate {m3/s}
    ,                        !- Maximum Sensible Heating Capacity {W}
    NoLimit,                 !- Cooling Limit
    ,                        !- Maximum Cooling Air Flow Rate {m3/s}
    ,                        !- Maximum Total Cooling Capacity {W}
    ,                        !- Heating Availability Schedule Name
    ,                        !- Cooling Availability Schedule Name
    ConstantSensibleHeatRatio,  !- Dehumidification Control Type
    0.7,                     !- Cooling Sensible Heat Ratio {dimensionless}
    None,                    !- Humidification Control Type
    ,                        !- Design Specification Outdoor Air Object Name
    ,                        !- Outdoor Air Inlet Node Name
    None,                    !- Demand Controlled Ventilation Type
    NoEconomizer,            !- Outdoor Air Economizer Type
    None,                    !- Heat Recovery Type
    0.7,                     !- Sensible Heat Recovery Effectiveness
{dimensionless}
    0.65;                    !- Latent Heat Recovery Effectiveness {dimensionless}
```